Dynamics of Harmful Cyanobacteria and Their Monitoring in Lake Erhai, a Chinese Plateau Lake

Dynamics of Harmful Cyanobacteria and Their Monitoring in Lake Erhai, a Chinese Plateau Lake

A Dissertation Submitted to
the Graduate School of Life and Environmental Sciences,
the University of Tsukuba
in Partial Fulfillment of the Requirements
for the Degree of Doctor of philosophy
(Doctoral Program in Integrative Environment and Biomass Sciences)

Gongliang Yu

Contents

Abstract

Global inland lakes are suffering accelerated eutrophication and water blooms. Generally, nitrogen (N) and phosphorus (P) nutrients are the important factors leading to this problem. Lower N/P (ratio nitrogen and phosphorus) favors dominance by cyanobacteria (12< N/P <23). However, even though N/P is in this range, cyanobacterial blooms may not occur in some cases, and thus microcystin (MC) concentrations do not increase. This indicates that N and P are important factors for cyanobacterial blooms, but not the only ones. With the discovery of microcystin synthetases gene (*mcy*) cluster, precise molecular detection techniques (e.g., real-time quantitative polymerase chain reaction [qPCR]) can provide insights into the dynamics of toxic cyanobacteria and environmental regulation of toxins in the field from the point of cyanobacterium itself (e.g., genotypes diversity and regulation of gene expression). Besides the commonly *Microcysits* blooms, some rare cyanobacterial taxa are also known to massively grow into bloom occurrence in certain waterbodies, e.g., *Tychonema bourrellyi*. Furthermore, it can produce geosmin or β-Ionone and is thereby listed as the potential harmful cyanobacteria influencing the drinking water safety. However, the taxonomic of this genus *Tychonema* is still unresolved. The other biological and ecological features of *T. bourrellyi* are also well unrevealed. On the other hand, satellite remote sensing is a very useful tool for monitoring dynamics of harmful cyanobacteria blooms (HCBs) through the Chlorophyll-*a* (Chl-*a*) index with high spatial and temporal resolution in a larger scale. A proper remote algorithm for Lake Erhai should be selected. In this study, the objectives are: 1) to reveal the variation of *Microcystis* and MCs coupling with N and P nutrients; 2) to focus on the dynamics and biological characteristics of odor-producing cyanobacteria *Tychonema bourrellyi* in Lake Erhai; and 3) to discuss the application of remote sensing algorithm for monitoring HCBs of Lake Erhai.

Lake Erhai is located in Yunnan Province, China, and is the second largest lake in southwestern China with water surface area of 249 km^2 and mean depth. It plays an important

role as a drinking water source for the local people. In recent decades, Lake Erhai has got into the trouble of eutrophication and cyanobacterial blooms. The lake is currently defined as the preliminary stage of eutrophic states. Due to the sensitive variation in water quality, and the extensive representative data, Lake Erhai is regarded as a representative case for researching eutrophication progress and occurrence of HCBs.

The present study examined the dynamics of *Microcystis* blooms and toxic *Microcystis* in Lake Erhai during 2010, based on quantitative real-time PCR method using 16S rRNA sequence and *mcy* gene, and chemical analysis for MC concentrations. Total *Microcystis* cell abundance was shown as an average of 1.7×10^7 cells L^{-1}. MC-LR and MC-RR were main variants. The MC concentrations, cell abundance of total *Microsytis* and toxic *Microsystis* showed to be positively correlated with water temperature and TP, and negatively correlated with TN and NO_3-N. When 20< TN/TP <40, *Microcystis* tended to dominate and MC concentrations tended to increase. Further analysis showed that genotypes diversity of *mcy* and gene expression of NtcA coupling with N and P nutrients affect MC concentrations and toxigenicity of *Microcystis* in Lake Erhai.

The rare cyanobacterial taxa *T. bourrellyi* has been found firstly in Lake Erhai. Several strains of *T. bourrellyi* have been successfully isolated from the lake. It was only found in several lake of Europe before then. Although some intermediate characters in morphological and physiological characters, the comparative analysis, such as morphological features, 16S rDNA sequences, and planktonic habitat of these strains, helped us to identify them as *Tychonema bourrellyi* under subfamily Phormidioideae. Three strains of *T. bourrellyi* could produce both geosmin and β-Ionone volatile substances. It was confirmed by the HPLC and *mcy* gene approach that no strain produced MCs. Furthermore, the dynamics of cell abundance at 12 sampling sites of Lake Erhai with an average of 3×10^4 cells L^{-1} were shown from 2009 to 2010 using qPCR. The obvious peaks occurred in July and August every year. Furthermore, the cell abundance of *Tychonema* was far inferior to *Microcystis* due to its low anoxygenic photosynthetic capacity and its relative weak strategy for uptake of P under lower P concentrations in Lake Erhai.

Satellite remote sensing is a highly useful tool for monitoring Chl-*a* concentration of HCBs in water bodies. Remote sensing algorithms based on near-infrared-red (NIR-red) wavelengths have demonstrated great potential for retrieving Chl-*a* in inland waters. This study tested the performance of a recently developed NIR-red based algorithm, SAMO-LUT (Semi-Analytical Model Optimizing and Look-Up Tables), using an extensive dataset collected from five Asian lakes. Results demonstrated that Chl-*a* retrieved by the SAMO-LUT algorithm was strongly correlated with measured Chl-*a* (R^2 = 0.94), and the root-mean-square error (RMSE) and normalized root-mean-square error (NRMS) were 8.9 mg·m^{-3} and 72.6%, respectively. However, the SAMO-LUT algorithm yielded large errors for several sites where Chl-*a* was less than 10 mg m^{-3} (RMSE = 1.8 mg m^{-3} and NRMS = 217.9%). This was because differences in water-leaving radiances at the NIR-red wavelengths (i.e., 665 nm, 705 nm and 754 nm) used in the SAMO-LUT were too small due to low concentrations of water constituents. Using a blue-green algorithm (OC4E) instead of the SAMO-LUT for the waters with low constituent concentrations would have reduced the RMSE and NRMS to 1.0 mg m^{-3} and 16.0%, respectively. This indicates (1) the NIR-red algorithm does not work well when water constituent concentrations are relatively low; (2) different algorithms should be used in light of water constituent concentration; and thus (3) it is necessary to develop a classification method for selecting the appropriate algorithm.

Overall, this study attempts to use a combined examination method to investigate dynamics, biological and ecological features of HCBs in the lake from different perspectives. The above results only presented the partial contents on HCBs. Other contents of HCBs still need to be further studied in the future. A comprehensive study for HCBs needs to combine all kinds of analysis methods and monitoring tools.

Keywords:

Cyanobacterial blooms, Dynamics, Lake Erhai, Microcystin, *Microcystis*, Remote sensing, *Tychonema bourrellyi*.

List of Tables

List of Figures

Acknowledgements

I would like to acknowledge my academic advisor, Professor Takehiko FUKUSHIMA for his excellent guidance, inspiration and support throughout this research. His proofreading and the detailed commitment on every aspect of my research were indeed remarkably helpful.

I also would like to sincerely thank Associate Professor Bunkei MATSUSHITA. I am greatly thankful for the many stimulating discussions and the encouragement that he provided throughout my study. This research would not be accomplished without his considerable guidance, support and encouragement.

Associate Professor Motoo UTSUMI and Associate Professor Yuuhiko TANABE pleasantly agreed to become the referees of my thesis. I would like to sincerely express my appreciation to them for their detailed comments and correction for desertification and presentation. I need to sincerely thank Miss Akiko Sato for her help during my desertation defence.

Special thanks should be expressed to Professor Renhui Li of Institute of hydrobiology, Chinese Academy of Sciences, China, as my mentor during the work at the institute, he gave me the foremost knowledge of harmful cyanobacteria, and provided well laboratory condition and enough research funds for my reseach.

This research would not have been possible without the experimental skills and the field datasets. For this reason, I would like to express my special thanks to Dr. Wei YANG and Dr. Kazuya YOSHIMURA of Tsukuba University, for their kind help in filed work and laboratory analysis. They taught me the experimental skills for water quality analysis and filed data measurements.

I thank every member of lab for his/her direct and indirect contribution to the partial research, the field sampling and laborary analysis. I would like to express my sincere thanks to Dr. Fan YANG, Dr. Hiroyuki ARAI, Dr. Youichi OYAMA, Ms. Shimako KAWAMURA, and Ms. Rie IGUCHI of Tsukuba University in Japan. I would like to express my sincere thanks to

Dr. Yongguang JIANG, Dr. Jihai SHAO, Dr. Gaofei SONG, Dr. Zhongjie WANG, Dr. Xingqiang WU, Dr. Peng XIAO, Dr. Menglin ZHU, Dr. Hua LI, Ms. Wenhua TAN, Ms. Qianqian PAN, Ms. Yichao LU, Wenbo CHAI, and Youxin CHEN of Harmful algae biology group of Institute of Hydrobiology, Chinese Academy of Sciences, China.

My gratitude is extended to Professor Yongding LIU for provided well laboratory condition and enough research funds for my reseach, and the members of his group, Dr. Zheng WANG and Dr. Fengyi CHANG, Dr. Yingcai WANG for his direct and indirect contribution to the partial research and the sampling.

This acknowledgement would be incomplete if I did not mention senior engineer Zhihong WEI and Miss Xingju Lv, Liang MENG of Research Center of Lake Erhai in Dali city of China for providing the sampling boat in Lake Erhai, and analysising the water quality.

This work was supported by JSPS RONPAKU (Dissertation PhD) Program, and was also supported by the National Water Science and Technology Projects (2012ZX07105-004, 2008ZX07105-006) and National Natural Science Foundation of China (No. 30970185).

Finally, I would like to express my special deep gratitude to my wife Dr. Xianfen XIANG, my parents, and my close friends for their enormous forbearance, encouragement and supportment throughout the research period.

Chapter 1 General introduction

1.1 Cyanobacteria and harmful cyanobacterial blooms

Cyanobacteria are ancient prokaryotic organisms with fossil remains dating back 3.5 billion years (Schopf 2000, Schopf et al. 2007, Wu et al. 2014), which can be found in almost every terrestrial and aquatic habitats, such as oceans, fresh waters, damp soil, temporarily moistened rocks in deserts, bare rocks and soil, and even Antarctic rocks (Schopf and Packer 1987). Cyanobacteria show considerable morphological diversity. They are unicells (e.g., *Chroococcus*) or filaments (e.g., *Anabaena* and *Oscillatoria*) and they may occur singly or grouped into colonies. Cyanobacteria get their color from the bluish pigment phycocyanin, which they use to capture the energy of sunlight for photosynthesis. In general, photosynthesis of cyanobacteria is an important microbiological conduit of solar energy into the biosphere.

However, some cyanobacteria are known as harmful cyanobacteria due to the ecological (creation of bottom water hypoxia, disruption of food webs), economical (impact recreational, fishing, and drinking waters), and health repercussions (human and animal intoxication). Their toxins (e.g., cyclic peptides and alkaloids) have caused serious and occasionally poisoning events to mammals, including humans around the world (Falconer et al. 1983, Runnegar et al. 1993, Carmichael 2001, 2008), such as *Microcystis* produce microcystins (MCs). Some harmful cyanobacteria can release odor substances (i.e., *Pseudanabaena* and *Tychonema* can release gesomin or 2-methylisoborneol [2-MIB]) influencing the quality of water supplies, so far as to lead to the closure of recreational waters when it is serious (Yang 2007, Wang et al. 2011c, Shao et al. 2013). Several aquatic cyanobacteria are known for their extensive and highly visible blooms as harmful cyanobacteria blooms (HCBs), which can form in both freshwater and marine environments. A mass of HCBs can induce oxygen deficiency in deep waters to cause mass

mortality of benthic animals and fish (Granéli et al. 1989), and also affect the aquatic landscape (Pearl and Huisman 2008).

Harmful cyanobacteria only comprise a small proportion of all cyanobacterial species. Of the known 5,000 named living phytoplankton species (Sournia et al. 1991), about 300 HCBs species can cause water discoloration and only some 80 of which produce toxins that can cause shellfish and human poisoning (Hallegraeff 2003). *Microcystis*, *Anabaena*, *Aphanizomenon*, which have relatively large colony/filament sizes and can float on water surface through their gas vesicles, were main components of HCBs in some freshwater and have extensive effects (Yu et al. 2015). But some tiny or no gas vesicles cyanobacteria species can also form blooms in some waterbodies sometimes, e.g., *Tychonema bourrellyi* (Revaclier 1978, Berglind et al. 1983, Ganf et al. 1991).

1.2 The occurrence of HCBs

HCBs are frequently occurring in waterbodies around the world (Paerl and Huisman 2008, Yang et al. 2008, Yang et al. 2011b). Although many factors could influence cyanobacterial status in different phases (Kong and Gao, 2005), its occurrence process is a result of the combined effects of different environmental factors including physical, chemical, biological factors and cyanobacterium itself (Paerl et al. 2001, Kong and Gao 2005, Zhou et al. 2014). Generally, anthropogenic nutrient over-enrichment (mainly Nitrogen and Phosphorus nutrients) by urbanization, agricultural, and industrial development is the important factor leading to the eutrophication process (Wang et al. 2010, Wu et al. 2006). The occurrence of HCBs is the response to eutrophication of water bodies (Paerl and Huisman 2008, Xie et al. 2003).

Otherwise, climate change is a potent catalyst for the further expansion of these blooms (Paerl and Huisman 2008). Cyanobacteria favor hot environment (Paerl and Huisman 2008). Global warming causes water temperatures raise, thereby lengthens optimal growth periods for cyanobacteria. Droughts increase residence time of water in lakes or reservoirs. These changes in

the hydrological cycle could further enhance cyanobacterial dominance in many aquatic ecosystems.

1.3 Nitrogen and Phosphorus affect the occurrence of HCBs

Usually, nutrients are considered the cause of increased or reduced growth of phytoplankton in natural environments and an important driver of competition that determines community composition. Considerable attention have been focused on nutrient limitation by phosphorus (P) versus that by nitrogen (N), and the ratios of these nutrients have been used at whole lake scales to predict the relative abundance of cyanobacteria amongst phytoplankton of lakes (Oliver et al. 2012).

1.3.1 Nitrogen

N is an essential component in the synthesis of gas vesicles, and N limitation may have an impact on cell buoyancy (Šejnohová and Maršálek 2012). Cyanobacteria are able to utilize a range of N sources including ammonium, nitrate, nitrite, and urea (Flores and Herrero 2005). Some genera of heterocystous cyanobacteria (e.g., *Anabaena*) can fix N_2. Non-heterocystous cyanobacteria *Microcystis* can acquire N as NO_3^-, NO_2^- or NH_4^+, but not as N_2, because of the absence of nitrogenase (Oliver et al. 2012). *Microcystis* abundance increased in response to all forms of N (Moisander et al. 2009). Higher NO_3-N levels are beneficial for the increase of *Microcystis* abundance (Lehman et al. 2009). Generally, the order of the preference for cyanobacteria is NH_4-N > NO_3-N > N_2 (Tandeau de Marsac and Houmard 1993) and the impact of NH_4-N on *Microcystis* physiology is ten times more than that of NO_3-N. In the presence of NH_4-N, the growth rate could be 4.6 times higher than for that of NO_3-N (Sirenko 1972).

Xu et al. (2010) suggested that N was the primary limiting nutrient for *Microcystis*, with P being a secondarily limiting nutrient. Therefore, although reducing the P load is important, reducing the N load is essential for controlling the magnitude and duration of *Microcystis* blooms.

1.3.2 Phosphorus

P has long been identified as the most common limiting nutrient in freshwater ecosystems (Schindler 1977, Oliver et al. 2012), and is widely accepted as the main nutrient controlling the development of natural populations of cyanobacteria in many freshwater environments (Wu et al. 2010, Oliver et al. 2012). The main sources of P for cyanobacterial species are orthophosphates, but they can also use organic forms. Moreover, the growth rate correlates with the availability of P (Reynolds et al. 1981). Usually it requires less than 0.03 mg L^{-1} P to be sufficient to permit cyanobacteria mass development (Šejnohová and Maršálek 2012).

Cyanobacteria can accumulate P in polyphosphate bodies (Jacobson and Halmann 1982, Allen 1984). This strategy, the polyphosphate "overplus" phenomenon, provides cyanobacteria with a competitive advantage over many microalgae (Sommer 1985). For example, colony-forming *Microcystis* accumulated P better than *Oscillatoria* and *Pseudomonas* from P-containing organic sources (Yuan et al. 2009). This ability can help *Microcystis* to form the dominant mass, especially if phosphate concentrations in the water are low during bloom periods (Šejnohová and Maršálek 2012).

1.3.3 The ratio of nitrogen and phosphorus

The ratio of nitrogen and phosphorus (N/P) has been recognized as the most prevalent factor related to the dominance of bloom forming cyanobacteria. Smith (1983) proposed "TN/TP rule" that lower TN/TP (ratio of total nitrogen and total phosphorus, e.g., <29) favor dominance by cyanobacteria. The maximum growth rates of *M. flos-aquae* from Lake Taihu in China appear when the PO_4^{3-} concentration reach 1.7mg L^{-1} and TDN concentration reached 17 mg L^{-1} (Chen et al. 1999). But Scott et al. (2013) proposed a new viewpoint that the MC was the highest at intermediate TN/TP (e. g., 12 < TN/TP < 23) in Canadian lakes.

However, the "TN/TP rule" is also the most disputed (Šejnohová and Maršálek 2012). Paerl et al. (2001) indicated that this rule was less applicable to highly eutrophic waters when both N and P nutrients were very high, based on the divergent results in two subtropical lakes. In Lake Okeechobee in Florida, USA, cyanobacteria decreased with the increasing of TN/TP (McCarthy

et al. 2009). In Lake Tai in China, the cyanobacterial proportion increased with the increasing of TN/TP (Paerl et al. 2001).

Xie et al. (2003) suggested that TN/TP ratio was not the factor of *Microcystis* blooms at least in highly eutrophic Lake Donghu in Wuhan, China, because *Microcystis* bloomed in experiment enclosures either in an initial TN/TP <29 or TN/TP >29. Wu et al. (2010) suggested that water temperature was the most important correlative factor influencing the seasonal succession of *M. aeruginosa*, while TP, total TN and transparency were the second most ones.

1.4 MCs, microcystin synthetase gene and their influence factors

1.4.1 MCs and microcystin synthetase gene

MCs are a group of cyclic polypeptides of varying potency (Rinehart et al. 1994). To date, over 90 structural variants of MCs have been identified (Rinehart et al. 1994, Sivonen 1996, Kaya and Sano 2005). The general structure is cyclo (-D-Ala-L-X-D-erythro-β-methylAsp(iso-linkage)-L-Y-Adda-D-Glu(iso-linkage)-*N*-methyldehydro-Ala), in which X and Z are variable amino acids, Adda is (2S, 3S, 8S, 9S) 3-amino-9-methoxy-2,6,8-trimethyl-10- phenyldeca-4,6-dienoic acid, and Mdha is N-methyldehydroalanine (Sivonen 1996, Carmichael et al. 1988, Dittmann et al. 2013). Generally, MCs are confined within cyanobacterial intra-cellula, and also easily enter the surrounding water after the death and lysis of cyanobacterial cells (Watanabe et al. 1992) or release via an active metabolic process (Kaebernick et al. 2000, Wu et al. 2011). MCs can accumulate in multiple organs and tissues in fish and mammals: heart, liver, gonad, lung, brain and kidney with consequent physiological, tissue and cell damage (Wang et al. 2008, Zhao et al. 2009), thereby MCs can cross the blood-brainbarrier and blood-cerebrospinal fluid-barrier and thus account for neurological symptoms of toxicity in mammals (Metcalf and Codd 2012). MCs act as potent liver and colon tumour promoters in animal models (Li et al. 2009). MCs are also potent inhibitors of eukaryotic protein phosphatases including PP1, PP2A (Mackintosh et al. 1990, Honkanen et al. 1991) and phosphoprotein phosphatases PPP4 and PPP5 (Hastie et al. 2005).

MCs are a family of toxins produced by different species of cyanobacterial taxa from freshwater and marine waters, and terrestrial environments including free-living and symbiotic cyanobacteria (Codd et al. 2012, Metcalf and Codd 2012, Dittmann et al. 2013). For example, Chroococcales: *M. aeruginosa*, *M. viridis*, Oscillatoriales: *Planktothrix agardhii*, *Plectonema boryanum*, *Phormidium corium*, *P. splendidum*, *Arthrospira fusiformis*, Nostocales: *Anabaena flos-aquae*, *A. subcylindrica*, *A. variabilis*, *Nostoc spongiaeforme*, *Anabaenopsis* sp., *Gloeotrichia echinulata*, *Rivularia biasolettiana*, *R. haematites*, *Tolypothrix distorta*, Stigonematales: *Hapalosiphon* sp., etc. (Metcalf and Codd 2012, Dittmann et al. 2013).

MCs synthesized by peptide synthetases through nonribosomal pathways (Marahiel 1992). A series of studies verified that the *mcy* gene encoded the multifunctional peptide synthetase necessary for microcystin biosynthesis (Dittmann et al. 1997, 2013). The *mcy* gene cluster contains 55 kb of DNA encoding 10 ORFs, *mcyA-mcyJ*, which have been correlated with microcystin formation by gene disruption and mutant analysis (Tillett et al. 2000, Dittmann et al. 2013).

The bulk of chemical variants have a genetic basis and a number of genetic diversification mechanisms have been linked with the chemical variety of microcystins (Dittmann et al. 2013). For example, the *mcyB* and *mcyC* modules are responsible for the incorporation of L-Leu and L-Arg into MCs (Mikalsen et al. 2003, Fewer et al. 2007). Gene *mcyBA*1, described as the first module of *mcyB* gene (Kurmayer et al. 2002), contributed concentrations of MC-LR and MC-RR in the water bodies (Mikalsen et al. 2003). High diversity of genotypes within *mcyBA*1 genes was found in Lake Erhai (Jiang et al. 2013). Among the genotypes, Group 1B genotypes of *mcyBA*1 gene were dominant within the population of toxic *Microcystis* in August and November and contributed the predominance of MC-LR and MC-RR (Jiang et al. 2013).

1.4.2 Detection of MCs and MC-producing *Microcystis*

Chemical detection of MCs is mostly carried out using HPLC (high performance liquid chromatography) or LC-MS (liquid chromatography-mass spectrometry) based on quantitative standards, using ELISA (Enzyme-linked immunosorbant assay) based on sensitive antibodies

against MC or through bioassays such as protein phosphatase inhibition assays (Song et al. 1998, Li et al. 2009, Wu et al. 2011). The PCR (polymerase chain reaction)molecular techniques based on the genetic difference between different genera of toxin-producing cyanobacteria were established for detecting toxigenicity of cyanobacteria (Xu et al. 2008), and for quantitative enumerating the cell abundance of toxic cyanobacteria through the realtime PCR protocols (Kurmayer and Kutzenberger 2003, Vaitomaa et al. 2003). The qPCR (real-time quantitative polymerase chain reaction) analysis can complement the detection of toxins by chemical and immunological analyses, in particular in field samples containing different potential toxic cyanobacteria. It allows for an assignment of the actual producer of toxins and provides insights into the dynamics of toxic cyanobacteria and environmental regulation of toxins in the field (Lin et al. 2010, Xu et al., 2010). However, Real-time PCR analysis can not substitute the chemical and immunological methods that directly quantify toxins (Kurmayer et al. 2002, Via-Ordorika et al. 2004).

1.4.3 Factors controlling toxigenicity and yield

Numerous studies based on field survey and *in situ* or laboratory experiment often focused on the relationships between MCs production and environmental factors, including nutrient elements (Song et al. 1998, Wu et al. 2006, Jiang et al. 2008), temperature (Sivonen et al. 1996), pH (Song et al. 1998), and light intensity (Sivonen 1990, Rapala et al. 1993). However, N, P and N/P were regarded as the most important factors for *Microcystis* blooms and MC production (Chorus et al. 2001, Gupta et al. 2001, Gobler et al. 2007, Jiang et al. 2008, Joo et al. 2009), i.e., N and P source could increase cyanobacterial intracellular MC levels (Watanabe and Oishi 1985, Sivonen 1990). But, there were conflicting conclusions on whether the increase of nitrogen and phosphorus concentrations may trigger the increase of the MC production and *Microcystis* blooms (Watanabe and Oishi 1985, Sivonen 1990, Xu et al. 2010, Otten et al. 2012, Scott et al. 2013). Cellular MC quotas of *M. aeruginosa* showed a significant positive relationship with both nitrate uptake and cellular N content and a negative relationship with CO_2 fixation, P uptake, and cellular P content (Downing et al. 2005). Thus, the ratio of nitrate uptake to phosphate uptake,

cellular N to cellular P, and nitrate uptake to CO_2 fixation were positively correlated to cellular microcystin. An increase in ambient NO_2-N up to 10 mg L^{-1} promoted MC (-LR) production by *M. aeruginosa* PCC7806. When NO_3-N was more than 0.2 mg L^{-1}, MC increased (Kameyama et al. 2002, Wu et al. 2006).

Otherwise, low light promoted the microcystin synthesis of *Microcystis viridis* and *M. aeruginosa* from Lake Dianchi, but this effect was regulated by temperature (Song et al. 1999). Low iron concentrations had been correlated with increased toxin production (Lukac and Aegerter 1993, Nagai et al. 2006). Long et al. (2001) suggested a positive linear relationship between the MC content of cells and their specific growth rate.

NtcA is a global transcription regulator for nitrogen control in cyanobacteria (Ginn et al. 2010). While TN increases, NtcA down-regulate expression of *mcy* gene to cause the decrease of MC concentrations and *Microcytis* abundance. Under nitrogen stress conditions, NtcA is overexpressed to cause the increase of MC concentrations and *Microcytis* abundance.

1.5 Methods for monitoring dynamics of cyanobacterial blooms

More detailed studies of the population dynamics and biological characteristics in HCBs are needed. For example, competition between toxic and nontoxic strains affects the toxicity of HCBs. Development and succession of HCBs is affected by nutrients and other environmental factors. Furthermore, how to monitor the occurrence and distribution of HCBs is another problem. This kind of knowledge is important for water management in their strategies to combat the expansion of HCBs.

To achieve sustainable management of water resources, routine monitoring of water quality is critically required by scientists and governments. Conventionally, the monitoring on ecosystem of lakes has been undertaken by periodical field investigation using boats. Traditional field methods include water quality survey, phytoplankton survey and counting. Through phytoplankton survey, we can get the composition and abundance of species, but it can not distinguish between toxic and non-toxic algae.

The qPCR techniques based on the genetic difference between different genera/species of cyanobacteria or toxic cyanobacteria were widely used to quantitative enumerate the cell abundance of toxic and non-toxic cyanobacteria in field samples (Kurmayer et al. 2002, Kurmayer and Kutzenberger 2003, Vaitomaa et al. 2003, Lin et al. 2010, Xu et al. 2010). Some studies verified that the *mcy* cluster contains *mcyA-mcyJ* have been correlated with microcystin formation (Dittmann et al. 1997, Tillett et al. 2000). Therefore, it is possible to distinguish toxic and non-toxic cyanobacterial cells by detecting the *mcy* gene present or absent (Xu et al. 2008). The potential yield of the actual MC-producing cyanobacteria would be quantitative analysis by the real-time PCR method. Real-time PCR techniques provide insights into the dynamics of toxic cyanobacteria and environmental regulation of toxins in the field (Lin et al. 2010, Xu et al. 2010).

Otherwise, due to the spatial and temporal heterogeneity of water bodies and the fact that water sampling work is time consuming and laborious, conventional water quality monitoring methods frequently fail to adequately represent the actual conditions of water bodies (Khorram et al. 1991, Liu et al. 2003, Oyama et al. 2009, Matsushita et al. 2009). Since the early 1970s, satellite remote sensing has become a good option for effective monitoring of water quality and HCBs because it can provide the information spatially and temporally in a larger scale (Dekker et al. 1992, Kahru et al. 1993, Kutser 2004, Ma et al. 2009, Wang et al. 2011a). With the developments in remote sensing techniques and the increase of satellite number, the analysis methods combining multiple satellites remote sensing images are widespread used to monitor the aquatic environments (Bresciani et al. 2013, Bresciani et al. 2014).

As above, the different research purposes need to use different research methods and techniques, e.g., the constituent concentrations of phytoplankton can get by traditional survey and counting; detecting quantitatively the cell abundance of cyanobacteria and toxic cyanobacteria need to use the real-time quantitative polymerase chain reaction (qPCR); and measuring the microcystin concentrations and nutrients need to use the chemical methods. Satellite remote sensing is a highly useful tool for monitoring chlorophyll-*a* (Chl-*a)* concentration of phytoplankton in water bodies. So it can be used to monitor the occurrence and scale of cyanobacteria blooms, in spite of that it can not distinguish the toxic and non-toxic algae

in current levels. If the constituent concentrations of phytoplankton and Chl-*a* concentrations in a lake are known through the representative samples, in whole lake will be retrieved. Actually, these comprehensive studies are already focused recently, i.e., a remote sensing algorithm for counting cyanobacteria cell in the freshwater lakes across the eastern US from MERIS imagery is proposed (Lunetta et al. 2015).

Overall, the current studies for HCBs need the comprehensive and extensive researches from different scales and perspectives. Consequently, it needs to combine further all kinds of analysis methods and monitoring tools in the future.

1.6 Review of remote monitoring cyanobacterial blooms

1.6.1 Case I and case II waters

From the perspective of remote sensing, global waters can generally be divided into two classes: case I and case II waters (Morel and Prieur 1977, Oyama et al. 2007). Case I waters are those dominated by phytoplankton (e.g. open oceans), whereas case II waters contain not only phytoplankton but also tripton (the nonliving component of the total suspended matter) and dissolved organic matter (DOM). The concentrations of total suspended solids (TSS) and organic matter are not necessarily correlated with chlorophyll a concentration (IOCCG report 2000). It has been shown that many coastal and inland waters belong to case II (Nichol 1993, Gin et al. 2003).

In case I waters, Chl-*a* can generally be accurately estimated with satellite images (Gordon and Morel 1983, Oyama et al. 2007). A blue-green band-ratio algorithm (e.g. OC4E algorithm) has been proved to work well for instruments like Coastal Zone Color Scanner (CZCS) (Gordon and Morel 1983, O'Reilly et al. 1998), Sea-viewing Wide Field-of-view Sensor (SeaWiFS), Moderate resolution Imaging Spectroradiometer (MODIS), and Polarization and Directionality of the Earth's Reflectances-2 (POLDER-2) (Kishino et al 1997, O'Reilly et al 2000). However, remote sensing technique for case II waters has been far less successful, mainly due to the complex interactions of the four optically active substances (OASs) in case II waters, such as

phytoplankton, tripton, colored dissolved organic matter (CDOM) and pure water (Goodin et al. 1993, Doxaran et al. 2002, Gin et al. 2002).

To address the mentioned difficulties for monitoring case II waters, researchers have made substantial efforts to estimate accurately water quality parameters (WQPs) including concentrations of chlorophyll a, tripton, and the absorption of CDOM at 440 nm. Previous methods for case II waters can be mainly classified into three categories (Morel and Gordon 1980): (1) empirical algorithms, (2) semi-analytical algorithms, and (3) analytical algorithms. Principles and typical examples of these methods are introduced in the following sections.

1.6.2 Empirical algorithms

These empirical algorithms were developed based on the bi-variate or multivariate regression analysis between remotely sensed data (usually spectral reflectance values at the sensor or spectrometer) and *in situ* measured concentrations of water constituents, which usually collected in coincidence of the sensor overpass. These empirical algorithms included the single-band algorithm (Galat and Verding 1989, Kahru et al. 2000) and the band-ratio algorithm (e.g. NIR/RED and TM4/TM1+TM2+TM4) (Han et al. 1994, Lindell et al. 1999). All the empirical methods are simple to be performed, but the mechanisms of the methods are usually unclear. Moreover, the estimation models are derived from the simultaneous measurements of remote sensing data and *in situ* WQPs, and thereby the models are generally site- and time-specific. The *in situ* sampling must acquire within 2-3 hours of an image acquisition because water components at a point are easily changed with the times (Liu et al. 2003). In fact, it is particularly difficult in extensive waters to collect a good number of *in situ* samples within a few hours.

1.6.3 Semi-analytical algorithms

The wavelengths of remote sensing electromagnetic radiation extend from the ultraviolet, through the visible and infrared, thermal and microwave, and into the long radiowave region. For monitoring of water quality, the useful range of wavelengths is usually in the range of visible and

near infrared (400–900 nm) because of the strong absorption of water body in wavelengths larger than 900 nm.

The semi-analytical algorithms were proposed by analyzing the spectral characteristics of the water constituent of interest. The knowledge of spectral characteristics is included in the statistical analysis by focusing on well-chosen spectral areas and appropriate wavebands used as correlates. The spectral radiance values are first recalculated to the reflectance and then, through regression techniques, related to the water constituents. This method is relatively stable under varying solar angle atmospheric condition and states of the water surface (Dekker et al. 1996), and commonly used.

Three-band index is a commonly used algorithm for retrieving Chl-*a* from case II water (Dall'Olmo et al. 2003). Three-band index was denoted as NIR-red algorithms to use reflectance in the near-infrared (NIR) and red spectral regions. Gitelson et al. (2008) theoretically explained the mechanism of the three-band index and the selection of the three bands around 660, 700 and 750 nm. These bands are available in the MERIS data. The NIR-red algorithms are proposed based on the fact that the NIR and red reflectances are less affected by the presence of tripton and CDOM, compared with phytoplankton and pure water. In recent decades, a number of NIR-red algorithms have been presented and shown to accurately estimate Chl-*a* for turbid productive coastal and inland waters (Gitelson l992, Dekker and Peters 1993, Gons 1999, Dall'Olmo and Gitelson 2005, Gitelson et al. 2009, Moses et al. 2009, Yang et al. 2010, Gurlin et al. 2011). All the studies demonstrated the effectiveness of the three-band index for in situ collected data sets.

The parameters for most of these NIR-red algorithms were determined through regression analysis using remote sensing data and in situ data collected from specific regions and/or seasons. And often the validity is implemented restrictively in those regions and/or seasons. Therefore, re-parameterization of an algorithm would be needed for distinct water bodies.

A novel algorithm, semi-analytical model-optimizing and look-up-table (SAMO-LUT) method based on three wavelengths (665 nm, 708 nm and 753 nm) was proposed for Chl-*a* estimation by Yang et al. (2011a). Chl-*a* estimation models were prepared in advance for various combinations of non-algal particles (NAP) and CDOM, which were increased in small

increments, and saved in a look-up-table (LUT). An iterative search strategy was used to obtain the most appropriate Chl-*a* estimation model for a given pixel. Because a comprehensive synthetic dataset of reflectance spectra related to various combinations of water constituents with a wide dynamic range was used to calibrate the Chl-*a* estimation model, instead of an *in situ* dataset, the SAMO-LUT is capable of retrieving Chl-*a* values in wide range of inland waters, especially in more turbid waters. In addition, a different assumption, i.e., concentrations of NAP and CDOM are constants, was adopted to further minimize the effects due to the previous assumptions. Furthermore, it is possible to select the most appropriate Chl-*a* estimation model pixel by pixel rather than using only one Chl-*a* estimation model for all pixels of a lake. Otherwise, the SAMO-LUT can simultaneously retrieve three water quality parameters (i.e., the concentrations of Chl-*a*, NAP and CDOM). The applicability of the model may not only be valid in real waters, but also can be valid in simulated cases. The SAMO-LUT algorithm has been validated in Lake Dianchi and Lake Erhai in China, and Lake Kasumigaura in Japan (Yang et al. 2011a).

Further, Le et al. (2009) proposed a four-band index to improve the three-band index for extremely turbid waters. Although it is effective for the case of Lake Tai, the prerequisite of four fine bands largely limits its application in the present satellite sensors.

Another idea, such as spectral mixture analysis (SMA, Oyama et al. 2007) and spectral decomposition algorithm (SDA) were also proposed for Chl-*a* retrieval. Oyama et al. (2007) successfully applied the SDA in mapping water quality in Lake Kasumigaura from Landsat TM data. The average Chl-*a* estimation error was 9.9%, which indicated the potential robustness of the SDA-based estimation model.

1.6.4 Analytical algorithms

The analytical algorithms are based on the use of the Inherent Optical Properties (IOPs) to model the reflectance and *vice versa*. IOPs of the water column are related to the absorption coefficient a the scattering coefficients b, and the volume scattering function β (θ). Physical relationships are derived between the water constituents and spectral radiance or the reflectance.

The analytical algorithm involves inverting all above relations to determine the WQPs from remote sensing data.

A key point of the analytical methods is on how to invert the above relations. Non-linear optimization is a commonly used technique for this problem (van der Woerd and Pasterkamp 2008, Santini et al. 2010). Furthermore, the other optimization methods were proposed, such as, the so-called spectral optimization algorithm (SOA, Chomko and Gordon 1998, Kuchinke et al. 2009a, 2009b), Artificial Neural network (ANN, Doerffer and Schiller 2007), the concept of look-up-table (LUT, Mobley et al. 2005), the matrix inversion method (MIM, Hoge and Lyon 1996, Hoogenboom et al. 1998, Brando and Dekker 2003, Giardino et al. 2007, Campell and Phinn 2010).

1.7 Introduction of study area: Lake Erhai

Lake Erhai is located between 25.6°–25.9°N to 100.1°–100.3°E in Yunnan Province, Southwest China, and is the second largest lakes of Southwest China, with total water surface area of 249 km^2 and a watershed area of 1,656 km^2. The lake is 42.58 km long and 4.8 km wide, with a mean depth of 10.2 m, a maximum depth of 20.7 m and a water volume of 2.53 $\times 10^9$ m^3. Lake Erhai can be geographically divided into three parts: the northern, central and southern part, because the shape of the Plateau Lake likes a human ear, it gets the Chinese name "Ear-shaped Sea". It is an alpine fault tectonic lake, with 1,973.7 m altitude. The lake is located in the subtropical monsoon climate zone with an annual average temperature of 15.1^{o}C, the annual sunlight of 2,280.6 hours, and the percentage sunlight of 52%. The surface water is characterized by a slightly alkaline pH (8.0–8.5) and a low salinity (Du 1992, Wang and Dou 1998).

After the Neolithic Period, Lake Erhai is an important food source for the local people, who catch fish by their famous fishing methods and culture rice around the lake. It also holds a high diversity of typical carps (*Cyprinus*), for example the endemic species (*C. barbatus*, *C. daliensis* and the Spring Fish *C. longipectoralis*) being found here. Many macrophyte species could be food (Li et al. 2011a), such as *Ouelia acuminate* (the endemic species), water caltrop (*Trapa*

bispinosa), lotus (*Nelunbo nucefera*), and Cane Shoots (*Zizania caducifora*). The lake is an important drinking water source for the local people. In recent years, the lake water was used 6×10^8 m^3 to generate electricity, 1.62×10^8 m^3 to irrigate for agriculture, 0.05×10^8 m^3 for aquaculture, 0.23×10^8 m^3 for people life and others. It had six water supply stations around the lake to supply directly drinking water of 8.3×10^4 m^3 every day. Lake Erhai was a royal deer ranch for the Nanzhao Kingdom 1300 years ago, and became a famous tourist attraction to world people. In the all, Lake Erhai is the source water for industries, irrigation, and domestic water of coastal area and plays a significant role for the local people.

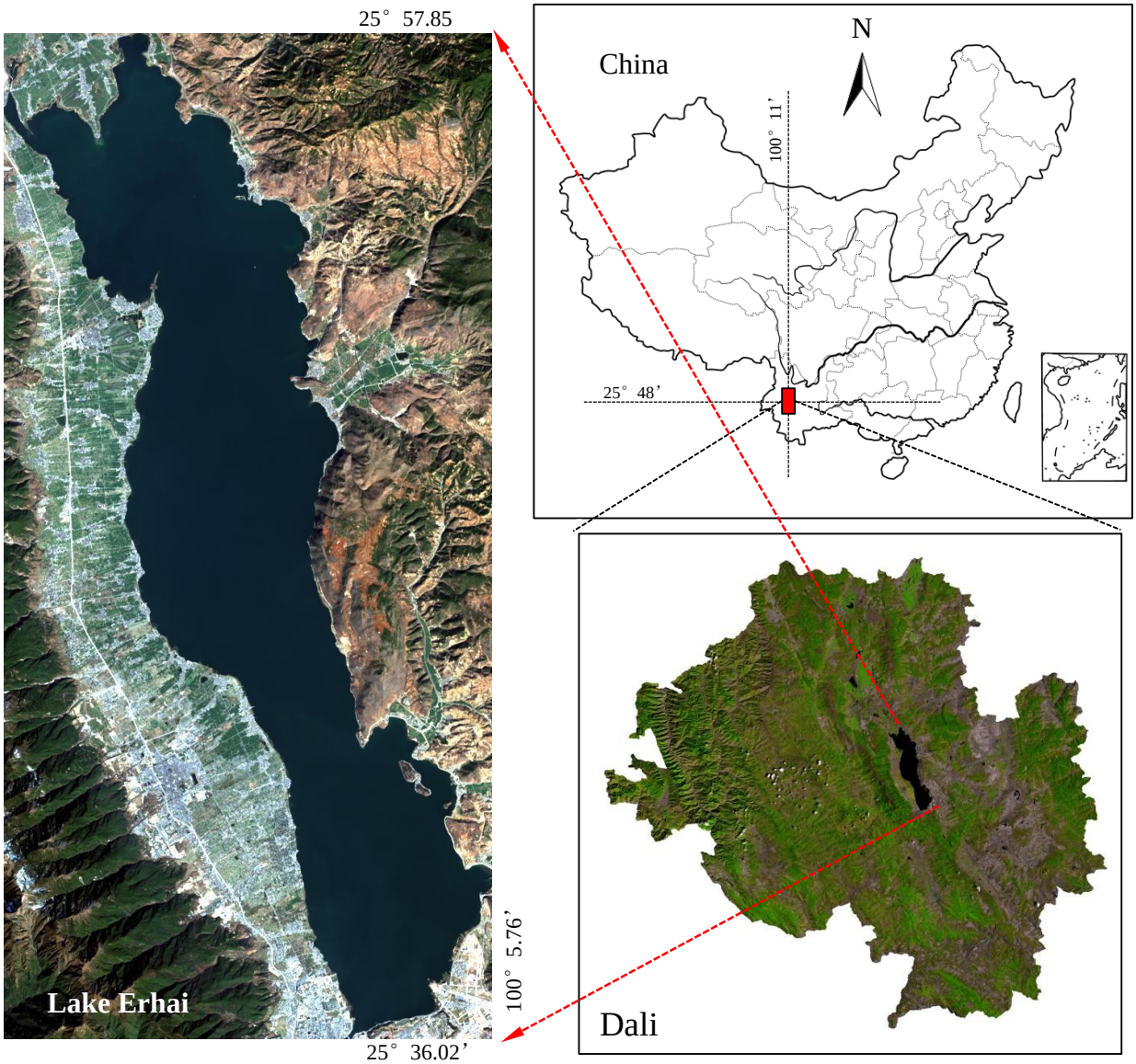

Fig. 1.1. Geographical location of Lake Erhai.

Before the 1970s, water in Lake Erhai was abundant, the water quality was very good, and the ecosystem was healthy (Du 1992, Wang and Dou 1998, Dong 2003). However, during the past 30 years, with rapid economic development and a rapid increase in population, Lake Erhai is facing a serious threat of intensive eutrophication due to the increase in anthropogenic inputs and the over-utilization of water resource (Wang and Du 1998, Dong 2003, Wang et al. 2011b, Zheng et al. 2004, Li et al. 2011a, 2011b). Water quality status was already at an initial beginning stage of eutrophication (Wang et al. 2011b). Organic matters and phytoplankton biomass increased rapidly. Cyanobaterial blooms break out in the part area of lake and bay, and the biodiversity decreased and fishery resources degenerated (Dong 2003). The biomass and coverage of submerged macrophyte have reduced rapidly (Li et al. 2011a).

Long-time field monitoring data showed that water quality of Lake Erhai was in mesotrophic state in winter and spring, but often changed to eutrophic state in summer and autumn. So its trophic state is described to be in a preliminary stage of eutrophic state. Due to the sensitive variation in water quality, and the extensive representative data, Lake Erhai is regarded as a representative case for researching eutrophication progress and the occurrence of water blooms. Furthermore, high diversity of cyanobacteria community is found in the lake, especially some harmful cyanobacteria (i.e., *Microcystis*, *Anabaena*, *Aphanizomenon*, and *Tychonema*). Their interspecific competition and relationship with the environmental factors should be further revealed. Lake Erhai is an appropriate area for researching it.

Otherwise, previous researches on the relationship between environmental factors and MC production and *Microcystis* blooms, are usually performed by multi-lakes sampling to reveal a general pattern (Smith 1983, Wu et al. 2006). However, these samplings were often limited to 1 or 2 sampling sites in each lake or only focused on the main period of cyanobacterial bloom (usually from June to October). Thus, the integrated information for a whole lake, such as the data from different regions of lake and different seasons, was lacking.

1.8 Originality of the research

Eutrophication and cyanobacterial blooms occurred widely in water bodies around the world. Generally, N and P nutrients are the important factors leading to the eutrophication and occurrence of cyanobacterial blooms in lakes. Smith (1983) proposed the "TN/TP rule" that low TN/TP favor dominance by cyanobacteria. However, the "TN/TP rule" is also the most disputed due to the divergent results (Paerl et al. 2001, Xie et al. 2003, McCarthy et al. 2009, Xu et al. 2010, Šejnohová and Maršálek 2012). With the discovery of the microcystin synthetase gene cluster (Tillett et al. 2000, Dittmann et al. 2013), precise molecular detection techniques (e.g. real-time PCR) provide insights into the dynamics of toxic cyanobacteria and environmental regulation of toxins in the field (Kurmayer et al. 2002). Therefore, the dynamics of cell abundance for total *Microcystis* and toxic *Microcystis* in Lake Erhai can be revealed by specific primers and PCR reaction. Furthermore, the correlation among TN/TP, microcystin concentrations, the genotypes diversity of *mcy* gene, and the dynamics of total *Microcystis* and toxic *Microcystis* was analyzed. Those results will provide further insights into the "TN/TP rule" from the point of cyanobacterium itself (e.g. genotypes diversity and regulation of gene expression).

Besides those commonly reported bloom forming species (e.g., *Microcystis*), some rare cyanobacterial taxa were also known to grow massively into blooms in certain waterbodies. *Tychonema bourrellyi* can form exceptional *Oscillatoria*-like blooms (Revaclier 1978, Berglind et al. 1983, Ganf et al. 1991), and produce geosmin or β-Ionone (Berglind et al. 1983, Jüttner and Watson 2007, Shao et al. 2013). Although morphological features of several species in genus *Tychonema* were researched in previous studies, comparison of genotypic features between species of this genus have not been performed, e.g. 16S rDNA sequence (Wei et al. 2012). Hence, the taxonomic of this genus is still unresolved, furthermore, the other biological and ecological features of *T. bourrellyi* is also well unrevealed. The strain *Tychonema bourrellyi* CHAB663 outside Europe were firstly isolated from Lake Erhai in China. Therefore, the characterization of *Tychonema* strains can be detected using the polyphasic approach including morphological

examination by light microscope, transmission electron microscopy (TEM) and 16S rDNA based on phylogenetic analyses. Spatial and temporal distribution of the *Tychonema* populations in Lake Erhai was investigated by the real-time quantitative polymerase chain reaction (qPCR) with specific molecular markers. Pigments, toxigenicity and volatile compounds of all strains were also examined, and the results obtained in this study will provide further insights into the taxonomy, biology and ecology of *Tychonema*.

Chl-*a* concentration is an important index to reflect the concentration of the harmful algae and trophic state. Accurate estimation of Chl-*a* from remote sensing data is a challenging in turbid waters. The SAMO-LUT algorithm significantly outperformed other indices due to the very well estimation accuracy only requires a minimum *in situ* dataset for the algorithm calibration process (Yang et al. 2011a). However, it has only been validated in Lake Dianchi and Lake Kasumigaura. A comprehensive evaluation need to perform in many lakes. Five Asian lakes represented different trophic states were selected as study cases. Lake Biwa, Lake Suwa and Lake Erhai were the representatives of clear water, the relatively clear water, and turbidity water between mesotrophic and eutrophic state, and differ to the above two lakes. The performance of SAMO-LUT algorithm can be evaluated comprehensively in this study.

1.9 Flow of the research

This thesis consists of five chapters as follows:

Chapter 1 provided the background information for the research.

Chapter 2 revealed the dynamics of *Microcystis* and MCs and its impact factors in Lake Erhai.

Chapter 3 focused on the dynamics and biological characteristics of odor-producing cyanobacteria *Tychonema bourrellyi*.

Chapter 4 discussed the applicability of the SAMO-LUT algorithm for monitoring of water blooms in five Asian lakes.

Chapter 5 presented a general conclusion of this thesis.

Chapter 2 Dynamics of *Microcystis* and microcystins and its impact factors in Lake Erhai, a drinking-water source in southwest plateau, China

2.1 Introduction

Eutrophication and cyanobacterial blooms occurred widely in water bodies around the world. *Microcystis* blooms was the main type of cyanobacterial blooms in freshwater. Microcystins (MCs) are mainly associated with *Microcystis* blooms (Hilborn et al. 2007) in freshwater bodies and threat the safety of water supply (Bourke et al. 1983, Jochimsen et al. 1998, Carmichael 2001). A guideline value of 1.0 μg L^{-1} for MCs in drinking water has been issued by the World Health Organization (WHO 2006).

The results based on field survey and *in situ* or laboratory experiment revealed that occurrence of *Microcystis* blooms and the yield variation of MCs were a result of the combined effects of different environmental factors including physical, chemical, biological factors and cyanobacterium itself (Paerl et al. 2001, Kong and Gao 2005, Neilan et al. 2012, Zhou et al. 2014). Nitrogen (N), phosphorous (P) and the ratio of total N and total P (TN/TP) were regarded as the most important factors for occurrence of *Microcystis* blooms and the yield variation of MCs (Song et al. 1998, Chorus et al. 2001, Gupta et al. 2001, Wu et al. 2006, Gobler et al. 2007, Jiang et al. 2008, Joo et al. 2009). Smith (1983) proposed the 'TN/TP rule' that lower TN/TP favored dominance by cyanobacteria. Scott et al. (2013) proposed that the MC was the highest at intermediate TN/TP (e. g. 12 < TN/TP < 23) based on the field data in Canadian lakes. However, the "TN/TP rule" is also the most disputed due to the divergent results (Paerl et al. 2001, Xie et al. 2003, McCarthy et al. 2009, Xu et al. 2010, Šejnohová and Maršálek 2012).

With the discovery of the microcystin synthetase gene (*mcy*) cluster (Tillett et al. 2000, Dittmann et al. 2013), toxic and non-toxic cyanobacteria can be directly distinguished by special primers and PCR reaction (Xu et al. 2008) and quantified by real-time quantitative polymerase chain reaction (qPCR, Kurmayer et al. 2002, Vaitomaa et al. 2003, Via-Ordorika et al. 2004, Lin et al. 2011). Precise molecular detection techniques provide insights into the dynamics of toxic cyanobacteria and environmental regulation of toxins in the field (Dittmann et al. 2013).

Lake Erhai is the second largest lake in southwestern China, and an important drinking water source for Dali City, Yunnan Province; it is also used for irrigation and aquaculture as well (Wang et al. 2011b). During the past decades, Lake Erhai has been experiencing a serious threat of intensive eutrophication due to increasing anthropogenic inputs of pollutants and the over-use of water resource (Du 1992, Wang et al. 2010). Organic matter and phytoplankton biomass increased. The biomass and coverage of submerged macrophytes, biodiversity and fishery resources have been shown to rapidly reduce (Wang et al. 2010, 2011b). The cyanobacterial blooms annually broke out in some regions of the lake (Du 1992, Wang et al. 2010), raising a potential threat to aquatic ecosystems and human health. However, to date, the basic information on dynamics of potential MC-producing cyanobacteria and the environmental factors controlling MC production in Lake Erhai has not yet been reported. It is not clear why the cyanobacterial bloom occurred in this lake since both concentrations of total nitrogen (TN) and total phosphorus (TP) are known to be much lower than those in the eutrophic shallow lakes. Therefore, the main purposes of the present study will focus on: (1) revealing the dynamics of *Microcystis* blooms and toxic *Microcystis* in Lake Erhai, and (2) discussing the correlations between MCs production and biotic and abiotic variables.

2.2 Materials and methods

2.2.1 Study area and sample collection

The environmental characters and limnological parameters of Lake Erhai were shown in Section 1.6 of Charpter 1.

Totally 16 sampling sites were set in this study. Among them, 12 sampling sites belonging to four sampling sections were selected as main study sites throughout the whole lake (Fig. 1). Four sampling sections were coded as N1, N2, S1 and S2 from north to south, successively. Site 285 and 288 were located in Haidong Bay and Xiahe Bay in the south part of the lake, respectively. The other sites were located in the open water zone of the lake. Furthermore, sites 1, 2, 3 and 4, located in Shaping Bay, Hongshan Bay, Aoshan Bay and Haichao Bay in the north part of the lake respectively, were chosen as accessorial study sites to collect some samples for MC analysis (Fig. 2.1).

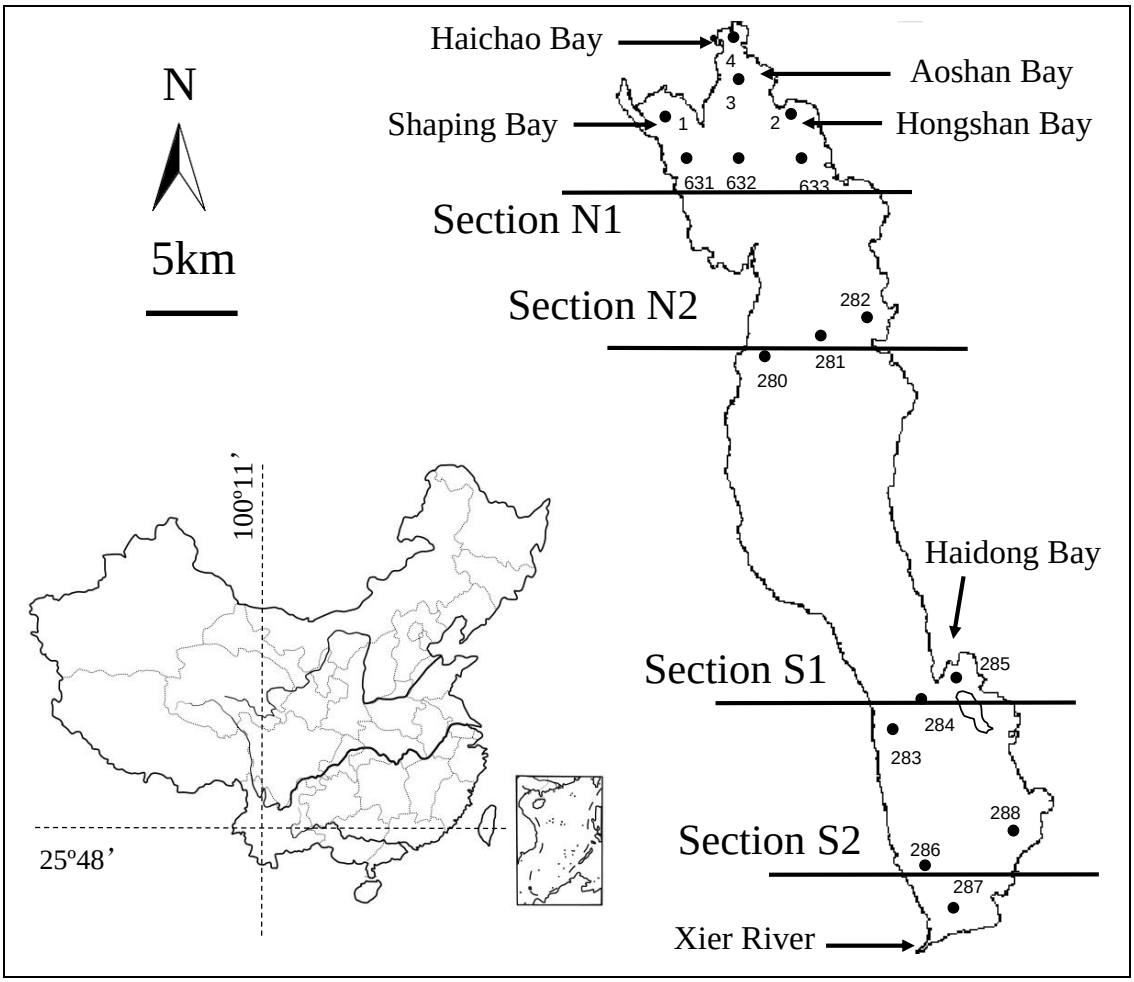

Fig. 2.1. Sampling sites in Lake Erhai in 2010.

2.2.2 Measurement of water quality parameters

Samples were collected monthly from January to December in 2010 as previously published (Jiang et al. 2013). In brief, 50−100 liters of surface water was filtrated using plankton net (mesh

size 45 μm), and concentrated algae were collected and stored at −80°C. Meanwhile, 300 mL surface water was filtrated through polycarbonate membrane filters of 0.45 μm (Millipore), then the filters were stored at −80°C until further analysis. The freeze-dried cells from the stored samples at −80°C were used to determine the concentration of MC.

Water samples for analysis of water quality parameters (WQPs) and Chl-*a* were taken from the surface layers (0−0.2 m) at each site. TN, dissolved total nitrogen (DTN), ammonia nitrogen (NH_4-N), nitrate nitrogen (NO_3-N) and TP were measured as previously described (Wu et al. 2006). Chl-*a* concentrations were measured by the ethanol method (Wang et al. 2011b). Water temperature (WT), dissolved oxygen (DO), pH and transparency (SD) were measured using YSI PRO 20, YSI PH100 meters and Secchi disk (ø 20 cm) *in situ*, respectively.

2.2.3 MCs measurement

The plankton biomass were lyophilized and weighed. The intracellular MC were extracted by 75 % methanol using 30 mg dried plankton powder and measured by HPLC (high performance liquid chromatography). The liquid extract was centrifuged (12,000 g) for 10 min and the supernatant was used for MC analysis by HPLC. The chromatographic system were consisted of a Waters Alliance HPLC equipped with a model 2695 separation module and an online degasser, a Waters model 2996 photodiode-array detector, and Waters Empower chromatography software. The elution conditions were set as reported in Jiang et al. (2013). Detection limit of the HPLC method is 0.2mg L^{-1}.

2.2.4 DNA extraction and qPCR

DNA was extracted from the frozen filters using the SDS-phenol method as described by Lin et al. (2011). Purified DNA was suspended in sterile 1× TE buffer (pH 8.0) and stored at −20°C prior to PCR analysis.

To determine the number of toxic *Microcystis*, the *mcyB* gene was quantitatively amplified using a specific primer set, 16 *mcyB*-30F (5'-CCTACCGAGCGCTTG GG-3') and 16 *mcyB*-108R (5'-GAAAATCCCCTAAAGATTCCTGAGT-3') (Kurmayer and Kutzenberger 2003, Xu et al. 2010). The total cells number of *Microcystis* was determined using the primer set, 1M-

16s209F (5'-ATGTGCCGCGAGGTGAAACCTAAT-3'), and 1M-16s409R (5'-TTACAATCCAAAGACCTTCCTCCC-3') (Neilan et al. 1997) by specifically and quantitatively amplifying the 16S rRNA gene of *Microcystis*. The specificity of primers used in this study was confirmed using the BLAST search of the GenBank databases.

The qPCR amplifications were conducted in an IQ5 Real-time PCR system (Bio-Rad) using the following parameters: 95^{o}C for 3 min, then 45 cycles of 95^{o}C for 10 s, 55^{o}C for 30 s followed by 70^{o}C for 30 s. Each reaction was performed in a 25 μL mixture with 0.5 mM of both primers, 10 μL enzyme-nucleotide-dye mix (SYBR green mixture, TOYOBO, Japan) and 0.1 μL template DNA. Each measurement was performed in triplicate. Data was analyzed using IQ5 Optical System Software, Version 2.0. Cell numbers of total *Microcystis* and toxic *Microcystis* were calculated from the mean cycle threshold value (Ct) of three replicates according to the standard curve.

2.2.5 Standard curves of cell number and gene concentrations using qPCR

The qPCR was used to enumerate the cell number of total *Microcystis* and potential toxic *Microcystis* referring to cell numbers of *M. aeruginosa* PCC 7806 based on 16S rRNA gene equivalents and *mcyB* gene equivalents, respectively. Standard curves between cell concentration and Ct were generated using strain *Microcystis aeruginosa* PCC7806 as described (Xu et al. 2010). *M. aeruginosa* PCC7806 was grown in MA media (Kasai et al. 2009) at 25^{o}C，and under 30 μmol $m^{-2}s^{-1}$ photons of cool white light with a 12:12 h light/dark cycle. The cell number of ten milliliters of this *Microcystis* culture under logarithmic phase was counted under a microscope. DNA was extracted and a tenfold dilution series of the DNA sample were prepared for qPCR amplification.

The differences between the cell number of *Microcystis* (x_1), the cell number of toxic *Microcystis* (x_2) and *Ct* (*Y*) were very significant, and the equation was $Y= -1.9309 \ln(x_1) + 41.073$, ($R^2 = 0.93$, qPCR efficiency 90.1 %, slope = −3.585), $Y= -1.4093 \ln(x_2) + 32.5.91$, ($R^2 = 0.99$, real-time PCR efficiency 91.2 %, slope = −3.553).

2.2.6 Statistical analyses

SPSS statistical software (version 13.0) was used to analyses the correlations between environmental factors and MC concentrations, dry algal biomass, Chl-*a*, and cell abundance of total *Microcystis* and toxic *Microcystis*.

2.3 Results

2.3.1 Distribution patterns of Chl-*a* concentrations and *Microcystis* abundance

Chl-*a* concentrations were shown as the average of 14.04±6.83 μg L^{-1} (2.82−32.42 μg L^{-1}), and gradually increased from the north to the south (Fig. 2.2a). The Chl-*a* concentrations have an obvious fluctuation, and the lowest and highest values occurred in April and August, respectively. The decline with an average of 9.37±2.85 μg L^{-1} (2.8−23.0 μg L^{-1}) was observed from January to April, and then the increased trend with an average of 13.60±3.50 μg L^{-1} (6.88−21.33 μg L^{-1}) occurred from May to June. The repeated fluctuation with an average of 21.65±4.71 μg L^{-1} (12.45−32.42 μg L^{-1}) occurred from July to October, and then the decline with an average of 15.41±4.80 μg L^{-1} (7.64−25.90 μg L^{-1}) was observed again from November to December.

Total *Microcystis* cell abundance ranged from 1.3×10^2 to 3.8×10^9 cells L^{-1} during 2010, with an average of 1.7×10^7 cells L^{-1}. The highest one was 3.8×10^9 cells L^{-1} at site 287 in August, indicating the occurrence of a *Microcystis* bloom around site 287. Within the four sampling sections, section N2 was higher *Microcystis* cell abundance than the other sections during the algal growth season (Fig. 2.2b). The *Microcystis* cell abundances in the northern sections (N1+N2) were higher than those in the southern sections (S1+S2) from August to November. Total *Microcystis* cells had obvious seasonal variations, falling down from winter until April as reaching the lowest average of 1000 cells L^{-1} (120−5100 cells L^{-1}), then increasing gradually to the peak in August (average 6.5×10^7 cells L^{-1}). After this, the cell abundance of total *Microcystis* kept the flat tendency as the higher level (1.1×10^7 − 2.9×10^7 cells L^{-1}).

The annual tendency on the spatial and temporal distribution of toxic *Microcystis* cells was similar to that of total *Microcystis* cells (Fig. 2.2c). And this similarity can be presented as a

significantly positive line correlation (R^2 = 0.9435, n = 144). The lowest and highest abundance of toxic *Microcystis* also occurred in April and August, respectively. Toxic *Microcystis* cell abundance ranged from 30 to 9.4×10^7 cells L^{-1} during 2010, with an average of 5.5×10^6 cells L^{-1}. The highest value was 9.4×10^7 cells L^{-1} at site 280 in August (Fig. 2.2c).

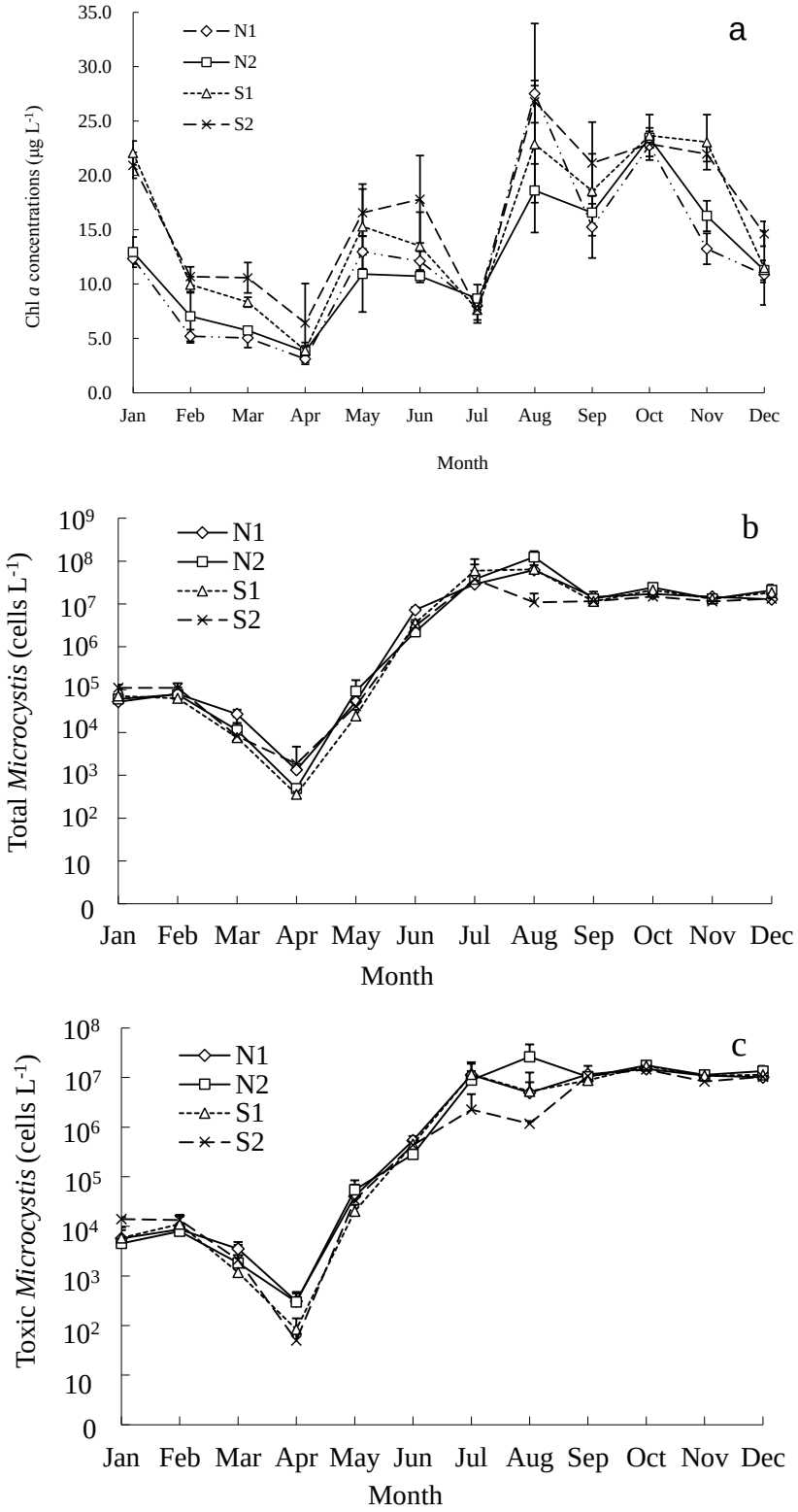

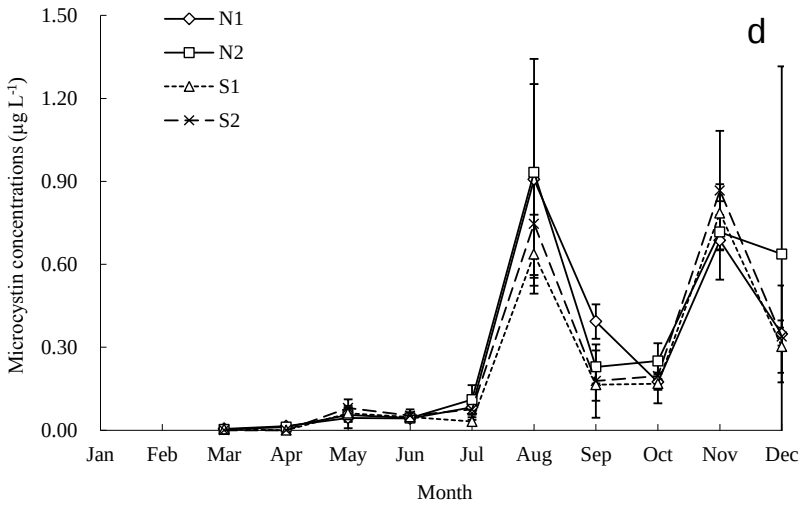

Fig. 2.2. Spatial and temporal variations of Chl-*a* concentrations (a), cell abundance of total *Microcystis* (b), cell abundance of toxic *Microcystis* (c), and MC concentrations (d) in Lake Erhai in 2010.

2.3.2 Main types and distribution patterns of MCs

Microcystin LR (MC-RR) and microcystin RR (MC-LR) were the main variants of MCs in Lake Erhai (Fig. 2.3). The average concentrations of total MC (MC-RR plus MC-LR), MC-RR and MC-LR in Lake Erhai were 0.30±0.34 μg L^{-1}, 0.26±0.63 μg L^{-1} and 0.15±0.33 μg L^{-1}, respectively. MC-RR concentrations were slightly higher than MC-LR concentrations. It was shown that total MC concentrations from nine samples exceeded 1.0 μg L^{-1}, especially site 3 and site 2 in September obtaining the highest concentration (8.95 μg L^{-1}) and second highest concentration (5.98 μg L^{-1}) respectively, and site 287 in November with a higher value (3.75 μg L^{-1}). Higher concentration values were found to usually occur during blooms (from August to December) and at the centre zone of the lake (site 281, 284 and 287) and the bays where blooms are easily gathered (Hongshan Bay and Aoshan Bay).

The concentrations of MC-RR and MC-LR in open water were less than those in the bays, and higher in the north part than that in the south one, exhibiting heterogeneity in different lake areas. The extremum usually occurred in the bays, for example, MC-RR concentrations sit 2 and site 3 in September were 3.94 μg L^{-1} and 5.89 μg L^{-1}, and meanwhile MC-LR concentrations were 2.04 μg L^{-1} and 3.06 μg L^{-1}, respectively. A few samples, such as site 281 in December and

site 287in November, showed that the concentrations of MC variants in the open water were low, but the total MC still reached up to 1.0 μg L^{-1}.

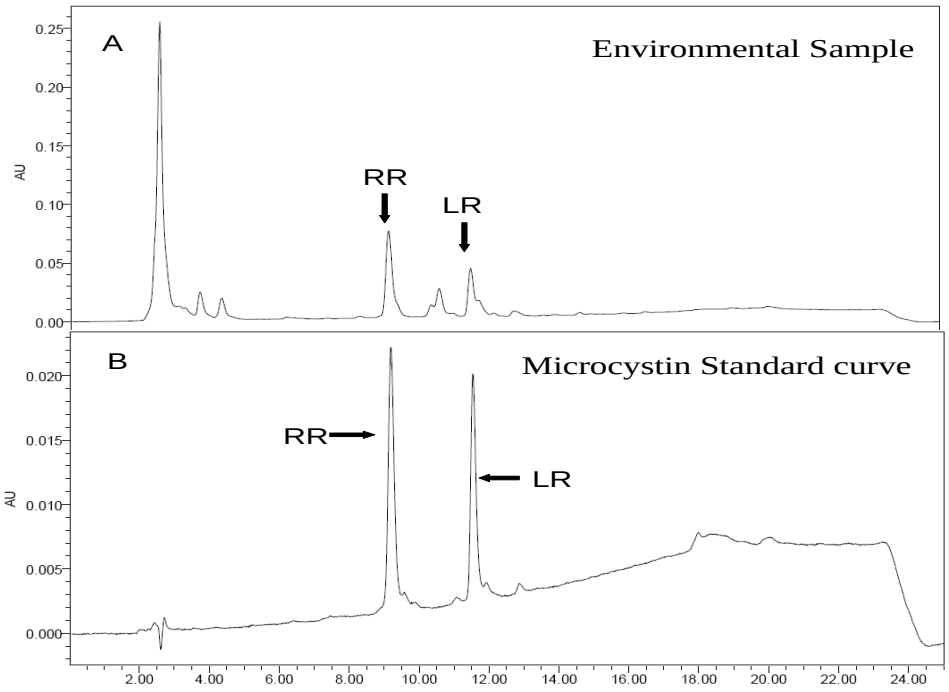

Fig. 2.3. Microcystins from Lake Erhai by HPLC.

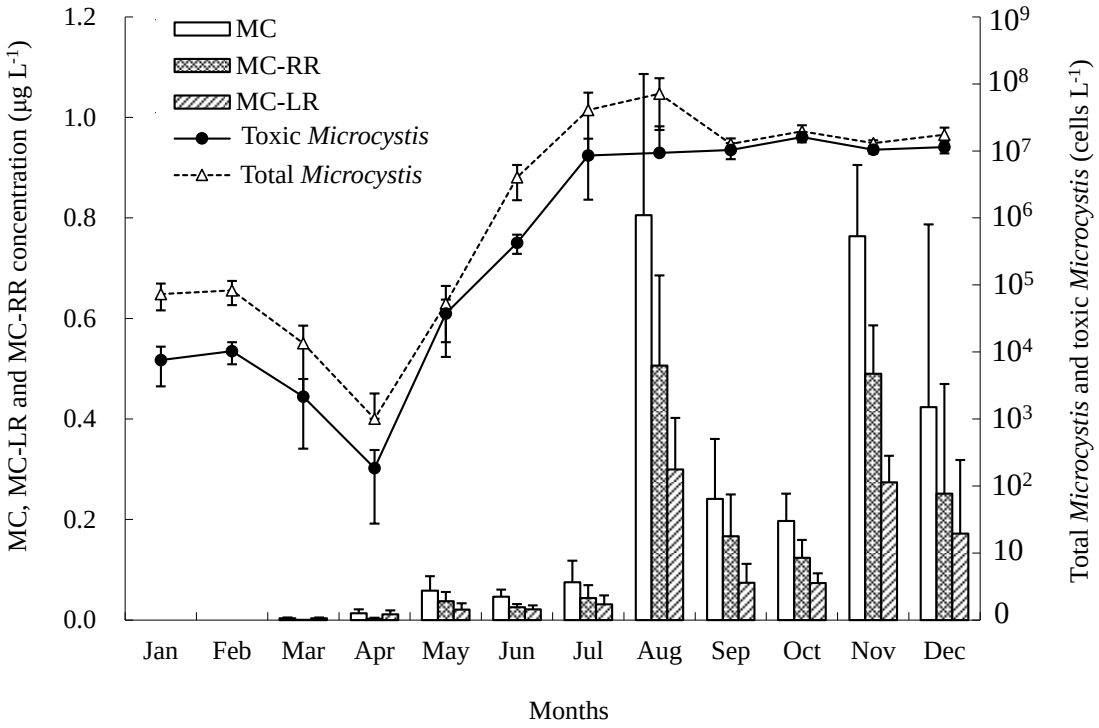

Fig. 2.4. Monthly variety of total MC, MC-LR, MC-RR, cell abundance of total *Microcystis* and toxic *Microcystis* in 2010.

The monthly variations of total MC, MC-LR and MC-RR were also shown as the four stages as described above (Fig. 2.2d and Fig. 2.4). During the lowest concentration stage (from January to April), MCs concentrations were so low that MCs could not be detected in some samples. In the second stage, in spite of the increase of MCs concentrations from May to July, the values were still very low (<0.15 μg L^{-1}). After August, MCs concentrations obviously rose up, then declined substantially in September and October, and increased again in November then declined in December (Fig. 2.4).

2.3.3 Relationship between Chl-*a*, total *Microcystis*, toxic *Microcystis* and MCs

As shown in Table 2.1, MC concentrations were positively correlated with Chl-*a*, the cell abundances of total *Microcystis* and toxic *Microcystis*, but uncorrelated with the ratio of the cell abundance of *Microcystis* and toxic *Microcystis*. Thus, the output of MC increased with the Chl-*a* concentrations. The linear equation between Chl-*a* and total MC during difference phases were: MC = 0.0042 (Chl-*a*) −0.0074 (R^2 = 0.59) from March to June, and MC = 0.0327 (Chl-*a*) − 0.1978 (R^2 = 0.62) from July to October, and MC = 0.0411 (Chl-*a*)−0.0816 (R^2 = 0.53) from Nov to Dec, respectively (Fig. 2.5). The slopes among three equations showed significantly differences in three phases. The slope (0.411) in winter was almost ten times higher than that in autumn (0.0327) and the slope in autumn as ten times higher than that in summer (0.0042).

Table 2.1. Correlation matrix between total MCs concentrations, dry algal biomass, Chl-*a*, cell abundance of *Microcystis* and toxic *Microcystis*.

Variable	Total MC (μg L^{-1})		MC-LR (μg L^{-1})		MC-RR (μg L^{-1})	
	r	n	r	n	r	n
mcyB [a] (cells L^{-1})	0.64**	81	0.64**	81	0.58**	77
Mic[b] (cells L^{-1})	0.66**	82	0.67**	82	0.60**	78
(*mcyB*)% [c]	0.11	82	0.08	82	0.08	78
Dry alga mass (μg L^{-1})	0.67**	102	0.64**	102	0.70**	98
Chl-*a* (μg L^{-1})	0.64**	102	0.61**	102	0.61**	98

[a], cell abundance of toxic *Microcystis*; [b], cell abundance of *Microcystis*; [c], the cell abundance ratio of *Microcystis* and toxic *Microcystis*; **P<0.01.

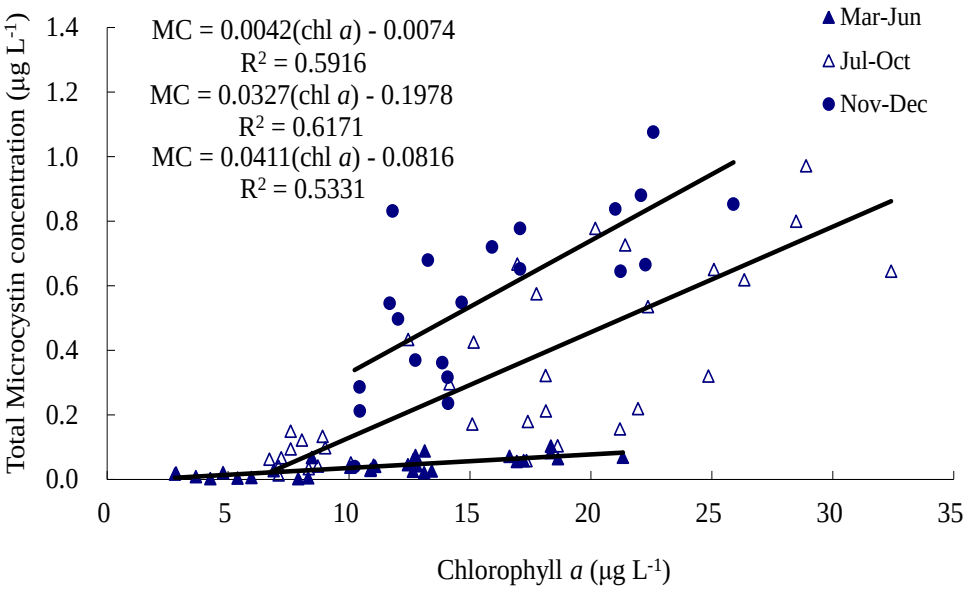

Fig. 2.5. The relationship between MC concentrations and Chl-*a* concentrations.

2.3.4 Environmental factors and trophic states

The WQPs variables were presented in Table 2.2. According to lake trophic states criteria defined by Smith et al. (1999), trophic states of Lake Erhai was described potentially mesotrophic before July (0.35 mg L^{-1}< TN <0.65 mg L^{-1}, 0.01 mg L^{-1}< TP <0.03 mg L^{-1}) and slightly eutrophic after July (TN >0.65 mg L^{-1}, TP >0.03 mg L^{-1}). According to TN/TP criteria of Forsberg and Ryding (1980), Lake Erhai was potentially P-limited (TN/TP >17). According to the concentration of Chl-*a* (Chl-*a* >9 μg L^{-1} from May), it insinuated that Lake Erhai might be in eutrophic states. Overall, the trophic state of Lake Erhai was described to be in preliminary stage of eutrophic states.

The monthly variations of TN were not significantly different (P >0.05), ranging from 0.39 to 0.60 mg/L, except for a few sites in July, September and October reached over 0.80 mg L^{-1} TN. The variations of NH_4-N, NO_3-N and DTN, were also not significantly different (P >0.05). The monthly variations of TP varied 0.004−0.028 mg/L, with a significant change in different months (P <0.05). TP increased from March to July and then decreased after July. The lowest and highest TP occurred in March and July, respectively. In the spatial variation, TP before May gradually decreased from the south to north (S2 >S1 >N2 >N1) and not significantly different

between sections after June. On the contrary, TN/TP decreased from March to June and then kept within the lower level (22−28) from September.

2.3.5 Relationship between MC concentrations, *Microcystis* and environmental factors

MC concentrations were shown to be positively correlated with pH, DO and TP, while negatively correlated with SD, NO_3-N, TN/Chl-*a* and TN/TP, but not correlated with NH_4-N, TN, DTN and WT (Table 2.3). Similarly, the cell abundance of total *Microcystis* and toxic *Microcystis* were positively correlated with TN, TP and WT, while negatively correlated with DO, SD, NO_3-N, TN/Chl-*a* and TN/TP, but not correlated with the other factors. In addition, when TN/TP was between 20 and 40, *Microcystis* cells and MC concentrations became higher (Fig. 2.6a, b, c). Whereas TN/TP was over 40, *Microcystis* cell abundance and MC concentrations fluctuated but maintained at lower levels, mostly with 2.5×10^7 cells L^{-1} and 0.2 μg L^{-1}, respectively.

Furthermore, the exponential regression model was used to detect the relationship between MC concentrations and some environmental factors, such as pH, TP and TN/TP. The exponential regression equation between MC concentrations and these factors were $MC = 0.0123e^{135.14\ (TP)}$ ($R^2 = 0.46$), $MC = 2E{-}44e^{11.323\ (pH)}$ ($R^2 = 0.73$), and $MC = 0.9069e^{-0.0499\ (TN/TP)}$ ($R^2 = 0.64$), respectively.

After analysis in details, the abundances of total *Microcystis* and toxic *Microcystis* were high in July and October, but their MC concentrations were low. In August and November, abundances of total *Microcystis* and toxic *Microcystis* at several sites were low, but the MC concentrations were high. The results demonstrated that the variation tendency of total *Microcystis*, toxic *Microcystis*, and MC coupling with TN/TP did not coincide in some months during cyanobacterial blooms.

Table 2.2. Seasonal variation of water quality parameters, cell abundance of *Microcystis* and toxic *Microcystis* in Lake Erhai in 2010.

Variable	Jan	Feb	Mar	Apr	May	Jun	Jul	Aug	Sep	Oct	Nov	Dec
TN (mg L^{-1})	0.39	0.47	0.43	0.44	0.57	0.47	0.79	0.57	0.60	0.53	0.46	0.42
NH_4-N (mg L^{-1})	0.07	0.04	0.06	0.06	0.06	0.08	0.11	0.05	0.07	0.05	0.20	0.08
NO_3-N (mg L^{-1})	0.11	0.09	0.13	0.15	0.08	0.13	0.12	0.09	0.08	0.11	0.10	0.10
DTN (mg L^{-1})	0.22	0.30	0.22	0.38	0.33	0.28	0.29	0.16	0.32	0.37	0.35	0.28
TP (mg L^{-1})	0.017	0.010	0.004	0.006	0.009	0.020	0.028	0.026	0.025	0.019	0.018	0.009
TN/TP	28	62	108	69	63	23	29	22	24	28	25	48
T (℃)	10.8	11.1	13.8	15.6	18.5	21.4	22.9	23.3	23.6	20.0	18.2	8.7
DO (mg L^{-1})	8.85	8.79	8.32	7.73	7.38	6.57	6.47	6.75	7.54	7.48	7.87	15.01
SD (m)	1.37	1.91	2.20	3.23	2.35	1.87	1.24	1.29	1.43	1.40	1.67	2.23
pH	8.55	9.02	8.39	8.49	8.63	8.45	8.73	8.75	8.84	8.74	8.68	8.75
MC (μg L^{-1})	*	*	0.004	0.011	0.070	0.047	0.099	0.608	1.136	0.211	0.988	0.353
MC-RR (μg L^{-1})	*	*	0.002	0.003	0.041	0.025	0.058	0.382	0.748	0.125	0.627	0.210
MC-LR (μg L^{-1})	*	*	0.003	0.009	0.030	0.022	0.040	0.226	0.388	0.086	0.362	0.143
Chl-*a* (μg L^{-1})	17.05	8.39	7.58	4.47	13.55	13.66	8.03	23.67	17.88	23.40	18.73	12.09
Dry algal biomass (mg L^{-1})	0.720	0.180	0.865	0.441	0.302	1.480	0.588	0.363	1.036	0.596	0.720	0.180
Total *Microcystis* (cells L^{-1})	73293	82585	13531	1008	52788	4.0×10^{6}	4.0×10^{7}	4.2×10^{8}	1.3×10^{7}	2.0×10^{7}	1.3×10^{7}	1.7×10^{7}
Toxic *Microcystis* (cells L^{-1})	7538	10277	2153	185	37311	4.2×10^{5}	8.5×10^{6}	1.8×10^{7}	1.0×10^{7}	1.6×10^{7}	1.0×10^{7}	1.1×10^{7}

* the data have not been measured successfully because they limited under the detection line of HPLC.

Table 2.3. Correlations matrix between environmental factors and MCs (-RR and -LR) concentrations, dry algal biomass, Chl-*a*, cell abundance of *Microcystis* and toxic *Microcystis* in 2010.

Variable	MCs		MC-LR		MC-RR		*mcyB*[a]		Mic[b]		(*mcy*)% [c]		Dry algal biomass		Chl-*a*	
	r	n	r	n	r	n	r	n	r	n	r	n	r	n	r	n
T	0.12	102	0.10	102	0.06	98	0.58**	121	0.56**	122	0.12	122	0.10	117	0.31**	144
DO	0.22*	102	0.23*	102	0.31**	98	-0.45**	121	-0.46**	122	0.01	122	0.06	117	-0.15	144
SD	-0.35**	102	-0.34**	102	-0.32**	98	-0.50**	121	-0.61**	122	0.14	122	-0.27**	117	-0.54**	144
pH	0.81**	102	0.82**	102	0.81**	98	0.51	121	0.55	122	0.26	122	0.43	117	0.13	144
NH_4-N	0.13	102	0.12	102	0.15	98	0.06	121	0.06	122	0.04	122	0.06	117	0.08	144
NO_3-N	-0.35**	90	-0.31**	90	-0.37**	86	-0.19*	117	-0.19*	118	-0.12	118	-0.38**	105	-0.28**	132
DTN	-0.17	102	-0.16	102	-0.21*	98	-0.02	121	-0.14	122	0.30**	122	-0.35**	117	-0.07	144
TN	-0.05	102	-0.05	102	-0.08	98	0.49**	121	0.50**	122	0.10	122	0.09	117	0.14	144
TN/Chl-*a*	-0.64**	102	-0.61**	102	-0.62**	98	-0.42**	121	-0.36**	122	-0.22**	122	-0.54**	117	-0.90**	144
TP	0.33**	102	0.30**	102	0.26**	98	0.63**	121	0.69**	122	-0.07	122	0.19*	117	0.56**	144
TP/Chl-*a*	-0.11	102	-0.10	102	-0.19	98	0.12	121	0.21*	122	-0.18*	122	-0.22*	117	-0.16	144
TN/TP	-0.37**	101	-0.35**	101	-0.34**	98	-0.45**	117	-0.51**	118	0.15	118	-0.23*	113	-0.58**	140

[a], cell abundance of toxic *Microcystis*; [b], cell abundance of total *Microcystis*; [c], the cell abundance ratio of total *Microcystis* and toxic *Microcystis*; *P<0.05; **P<0.01.

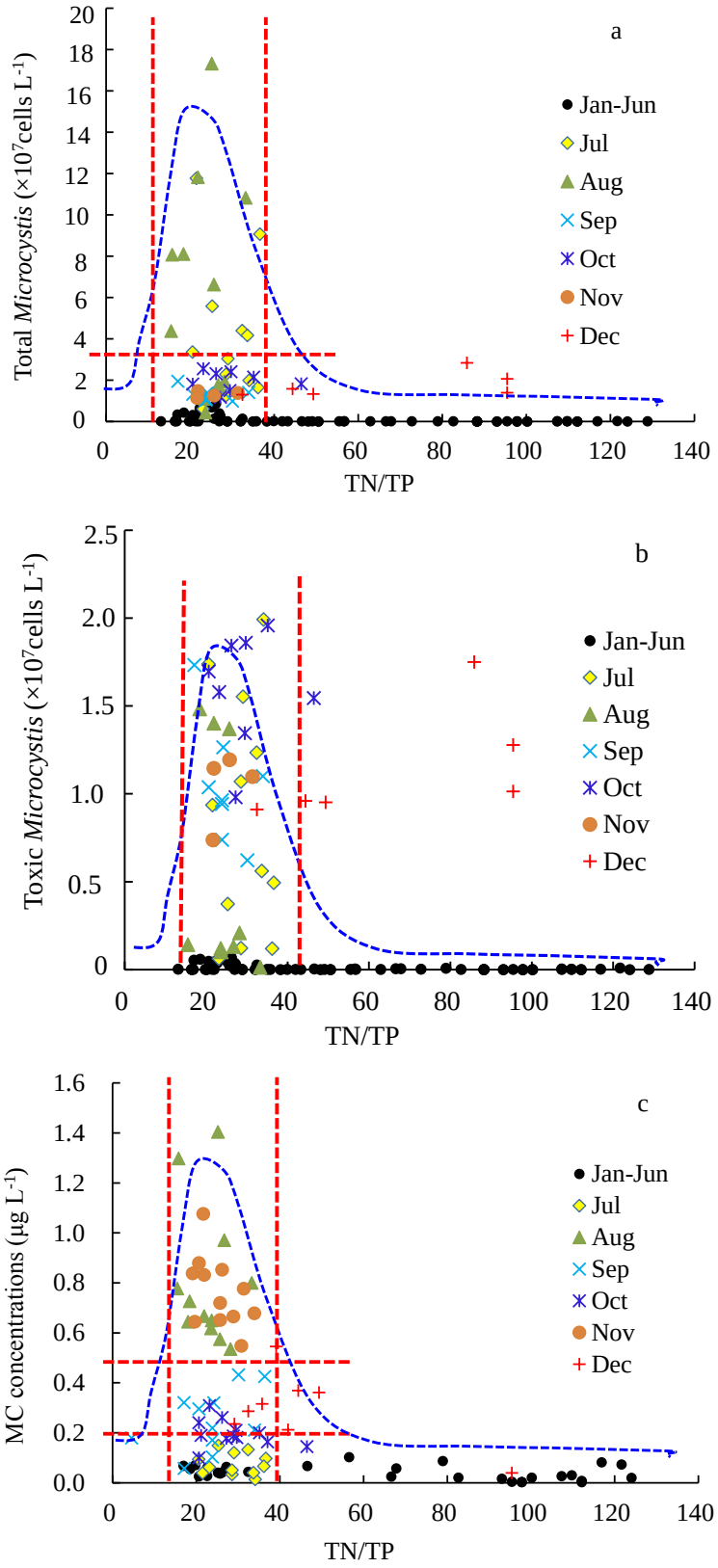

Fig. 2.6. The relationship between MC concentrations, the cell abundance of total *Microcystis* and toxic *Microcystis*, and TN/TP in 2010.

2.4 Discussion

Unlike other large shallow eutrophic lakes along the Yangtze River, Lake Erhai is characterized with its plateau geography, medium-depth water and lower nutrition loadings. Recent development of eutrophication and cyanobacterial blooms in Lake Erhai led to several studies on phytoplankton and bacterioplankton (Wang et al. 2011b, Li et al. 2011b, Hu et al. 2013). But, specific information on *Microcystis* and MC in the lake is still not available. Therefore, it is much necessary to obtain the general knowledge on the distribution and dynamics of MC caused by cyanobacterial blooms in the lake. High diversity of blooms-forming cyanobacterial groups were reported to occur in Lake Erhai, including seven species of *Microcystis* (*M. aeruginosa*, *M. wesenbergii*, *M. viridis*, *M. novacekii*, *M. smithii*, *M. ichthyoblabe*, *M. flos-aquae*), four of *Anabaena* (*An. ucrainica*, *An. spiroides*, *An. circinalis*, *An. flos-aquae*) and two of *Aphanizomenon* (*Aph. flos-aquae*, *Aph. issatschenkoi*) (Lv et al. 2010). Thus, such a diversity of cyanobacterial species provided the seed resource for the formation of water blooms. *Microcystis* species, along with some *Anabaena* ones, were found to mainly dominate in summer and autumn, while *Aph. flos-aquae* occurred in early spring. Spatially, higher *Microcystis* cells were shown to occur in the bays of the lake, such as Aoshan Bay station and Hongshan bay station.

The distribution pattern of *Microcystis* concentrations was associated with the geographical, meteorological and hydrological characteristics. Lake Erhai is located in the subtropical monsoon climate zone with strong southwestern winds, pushing the lake water toward the northeast to form anticlockwise circular flows (Wang and Dou 1998). The shape of Lake Erhai was geographically divided into three parts by two peninsulas stretching out, and three smaller anticlockwise circular flows among whole circular flow were therefore formed in the north, central and south part, respectively (Du 1992, Wang and Dou 1998). *Microcystis* dominated blooms were driven by those anticlockwise circular flows and strong southwestern winds and subsequently gathered into Hongshan bay and Aoshan bay along the central axis of lake from the south to the north leading to

higher Chl-*a* concentration (20.55 mg L^{-1} and 19.09 mg L^{-1}) and MC concentrations (5.2 μg L^{-1} and 8.95μg L^{-1}) in this area.

MC-RR and MC-LR were the main variants of MC in Lake Erhai (Fig. 2.3). The other probable MC variant with maximum UV absorbance at 238 nm was also observed constituting a minor proportion of total MC, and hence was not discussed in this study. Potentially MC-producing cyanobacterial genera *Anabaena*, *Planktothrix* and *Phormidium* were also observed in Lake Erhai. However, a large number of strains belonging to these three groups were isolated from Lake Erhai and none of them contains *mcy* genes or MCs (data not shown). Hence, MC was predominantly produced by *Microcystis* in Lake Erhai. It was also clearly indicated by the high relationship coefficient (0.64) between MC and *Microcystis*.

Recently, the fact that a considerable portion of MC is neglected with current analysis techniques due to MC binding to the proteins was reported (Meissner et al. 2013). However, a reliable assay method for quantifying the protein-bound MC concentrations has not been established so far. The MC concentrations measured based on methanol extracts in this study was actually free MC. Nonetheless, a positive correlation between free MC and protein-bound MC was also observed in all field samples (Meissner et al. 2013). The results for the factors affecting MC production of *Microcystis* populations in lake water are still reliable in the present study.

Temporally, total *Microcystis* cells and MC-producing *Microcystis* cell abundance and MC concentrations in mid-summer and autumn were higher than those in other seasons. Because abundant pollutants are subsequently brought into the lake by rainwater and river flood flow in rainy season in summer, nutritional loading increase in the whole lake. In autumn, sustaining high nutritional loads and optimal climate conditions triggered and maintained *Microcystis* blooms (Dong 2003) and further increased the MC concentrations. Afterwards, *Microcystis* blooms were succeeded by green algae and diatom in winter, and then *Aph. flos-aquae* populations dominated in next spring. Hence, during last the blooms, although Chl-*a* concentrations were relatively higher, a large portion

of *Microcystis* cells and MC concentrations already decreased. Therefore, phytoplankton community succession was also an important reason to influence the temporal distribution patterns of MC.

Microcystis blooms and the production of MC were regarded to be associated with environmental factors such as nutrients (Xie et al. 2003). P and N sources have been considered as the main factors to affect the growth of *Microcystis* cells and MC levels, and such influencing process is so complicated that the different conclusions were obtained by different investigators from different lakes (Paerl et al. 2001, Xie et al. 2003, McCarthy et al. 2009, Xu et al. 2010). The results obtained in the present study showed that TP was positively correlated with total *Microcystis*, MC-producing *Microcystis* and MC production, which agreed with the previous studies suggesting that phosphorus was the main factor leading to high *Microcystis* cell abundances and MC levels (Chorus et al. 2001).

With regard to the effect of N nutrient on MC production, TN and DTN were reported to increase MC levels in a pond of Japan (Joo et al. 2009). In the present study, TN, DTN, and NH_4-N were irrelevant with Chl-*a*, MC, total *Microcystis* and toxic *Microcystis* (Table 2.3). However, when TN were normalized with Chl-*a*, the high relationship between MC and TN per unit Chl-*a* (TN/Chl-*a*) was more clearly shown than the results without normalization (Table 2.3). Several studies indicated that high NO_3-N loading was shown as a significant factor enhancing MC concentrations and the growth of toxic *Microcystis* within the *Microcystis* community (Yoshida et al. 2007, Jiang et al. 2008, Joo et al. 2009, Xu et al. 2010). Kameyama et al. (2002) found that the growth rate of *M. viridis* NIE 102 and the yield of MC-RR favorably increased at NO_3-N concentrations ranging from 0.2 to 0.8 mg L^{-1}, and then the effect plateaued at 1.0 mg L^{-1} of NO_3-N. However, Wu et al. (2006) reported that the relationships between MC and NO_3-N were fitted well with a unimodal curve, and the maximum MC concentration easily occurred when NO_3-N concentrations ranged from 0.2 to 0.7 mg L^{-1}. The present study showed that NO_3-N was negatively related to *Microcystis* cell abundance and MC levels, and other N sources, such as TN, DTN, and NH_4-N, were irrelevant with Chl-*a*, MC, total *Microsytis* and toxic *Microsystis* (Table. 2.3). This result was similar to the study in lakes of

central Alberta, Canada, where nitrate concentrations were relatively low (almost <0.2 mg L^{-1}) (Kotak et al. 2000).

MC concentrations in the lake showed two obvious peaks in August and November in the main lake without obvious fluctuation of MCM abundance (Fig. 2.4). While MC concentrations increased sharply in August and November, TN declined obviously by 28% and 13% (Table 2.2). On the contrary, while MC concentrations declined sharply in September, TN rose obviously by 6% (Table 2.2). Consequently, variations of MC concentrations were negatively associated with TN. NtcA is a global transcription regulator for nitrogen control in cyanobacteria (Ginn et al. 2010). Nitrogen levels affect MC production rates and the expression of *mcy* gene by the NtcA approach (Ginn et al. 2010). Hence, it was guessed that NtcA coupling with nitrogen may present the expression of *mcy* gene to affect MC concentrations during cyanobacterial blooms.

*McyBA*1 was described as the first module of mcyB gene (Kurmayer et al. 2002). Genotypes of *mcyBA*1 gene contribute concentrations of MC-LR and MC-RR in the water bodies (Mikalsen et al. 2003). In Lake Erhai, there had the significant seasonal variations and the high diversity in the composition of *mcyBA*1 genotypes during the blooms (Jiang et al. 2013). The different MC production capability of toxic *Microcystis* within different *mcyBA*1 gene types may lead to variations of MC concentrations. For example, group 1B of *mcyBA*1 gene was dominant within the population of toxic *Microcystis* in August and November and contributed the predominance of MC (Jiang et al. 2013). Otherwise, genotypes of *mcyBA*1 genes could be associated with MC concentrations and cell abundance of toxic *Microcystis* in Lake Erhai.

TN/TP ratio has been recognized as the most prevalent factor related to the dominance of bloom forming cyanobacteria. “TN/TP rule” hypothesis that cyanobacteria tended to dominate in the lake when TN/TP <29, while decreased when TN/TP >29 (Smith 1983). But Scott et al. (2013) confirm the new viewpoint that the MC was highest at intermediate TN/TP (e.g. 12 < TN/TP < 23) in Canadian lakes. Paerl et al. (2001) indicated that this rule is less applicable to highly eutrophic waters when both N and P nutrients are very high. Xie et al. (2003) found that *Microcystis* bloomed

in experiment enclosures either in an initial TN/TP <29 or TN/TP >29, suggesting that TN/TP ratio is not the factor bursting of blooms of *Microcystis* at least in highly eutrophic Lake Donghu. In the present study, trends of both *Microcystis* abundance and MC production in Lake Erhai showed visually that *Microcystis* tended to dominate and MC concentrations tended to increase when TN/TP decrease (Fig. 2.6). The correlation coefficient (R^2) of the exponential regression equation between MC concentrations and TN/TP was 0.64. This obtained result suggested that the "TN/TP rule" may be applied into the case in Lake Erhai. This lake is characterized by its deeper water but lower N and P loadings, compared to those hypereutrophic lakes mentioned above, and such characteristics may partially explain why the *Microcystis* blooms and MC production corresponded to the "TN/TP rule", implying that Lake Erhai can be a good model for study on the correlation between TN/TP and cyanobacterial blooms and MC production in the future.

From the superficial meaning of the TN/TP formula, increasing TN level in the lake may change TN/TP ratio, thus be able to control cyanobacterial blooms (Smith 1983). But it is clear that the increase of TN level will easily cause eutrophication and subsequent cyanobacterial blooms for lakes. On the other hand, high N/P ratios (20–50:1) lead to a community dominated by green algae (Bulgakov and Levich 1999) or diatoms (McCarthy et al. 2009). That is why the "TN/TP rule" was also not likely to be applied in many lakes with higher nutrient concentrations, which often have lower TN/TP (Xie et al. 2003, Scott et al. 2013). Therefore, the rule could be partially applied to explain the correlation between the cyanobacterial blooms with nutrients N and P only within a certain nutrient level.

Chapter 3 Dynamics and polyphasic characterization of odor-producing cyanobacteria *Tychonema bourrellyi* from Lake Erhai, China

3.1 Introduction

Harmful cyanobacterial blooms frequently occur in eutrophic lakes, reservoirs and ponds, around the world (WHO 2006, Kameyama et al. 2002, Otten et al. 2012). Many cyanobacterial genera, such as *Microcystis*, *Anabaena*, and *Aphanizomenon*, are associated with bloom formation (Hu and Wei 2006, Lin et al. 2010). Some species of these genera produce potent toxins or taste and odor substances (Wang et al. 2011), which allow them to threat human health safety through the drinking water path (Jochimsen et al. 1998, Carmichael 2001).

Aside from the above commonly reported bloom forming species, several rare cyanobacterial taxa are also known to massively grow into bloom in certain water bodies. *Tychonema bourrellyi* (Lund) Anagnostidis et Komárek is originally distributed in colder lakes of Northern Europe with slight eutrophication (Anagnostidis and Komárek 1988, Komárek and Anagnostidis 2005). This species form exceptional *Oscillatoria*-like blooms (Revaclier 1978, Berglind et al. 1983, Ganf et al. 1991). Furthermore, *T. bourrellyi* also produce geosmin or β-Ionone (Berglind et al. 1983, Jüttner and Watson 2007, Shao et al. 2013), exhibiting potential harmful impact. *T. bourrellyi* is one of three formally accepted species of the genus *Tychonema* in latest edition of Oscillatoriales taxonomy by Komárek and Anagnostidis (2005). Comparing the phenotypic features (i.e., cells size, cellular ultrastructure structure, and pigment) among the three *Tychonema* species, namely, *T. bourrellyi*, *T. bornetii* (Zukal) Anagnostidis et Komárek (originally *O. bornetii*, Lund 1955), and *T. tenue* (Skuja)

Anagnostidis et Komárek (originally *O. tenue*, Lund 1955), Skulberg and Skulgerg 1991, Komárek 1994) reveals that the combined characters of *T. bourrellyi* (i.e., having a smaller cell width and reddish pigment, as well as being planktonic in freshwater) could distinguish *T. bourrellyi* from the other two species (Komárek and Anagnostidis 2005). However, a comparison of the genotypic features between the species of genus *Tychonema* has not been performed, and the taxonomy inside the genus still remains unresolved. Furthermore, the relationships between *Tychonema* and other cyanobacteria genera or families are not clearly understood (Komárek and Albertano 1994). Except for some morphological descriptions, the other biological and ecological features of *T. bourrellyi* are also unclear. Thus, studies based on more strains from wider global regions are necessary to solve those problems.

Recently, *T. bourrellyi* has been found in Lake Erhai, a plateau lake in Yunnan Province, and taxonomically described as a new record in China (Wei et al. 2012). Several strains of *T. bourrellyi* have been successfully isolated from the lake. The present study attempts to characterize *Tychonema* strains using the polyphasic approach, including morphological examination by light microscope, transmission electron microscopy (TEM), and 16S rDNA based on phylogenetic analyses. The spatial and temporal distributions of the *Tychonema* populations in Lake Erhai are investigated using real-time quantitative polymerase chain reaction (qPCR) with specific molecular markers. The pigments, toxigenicity, and volatile compounds of all strains are also examined. The obtained results could provide further insights into the taxonomy, biology, and ecology of *Tychonema*.

3.2 Materials and methods

3.2.1 Sample collection and measurement of water quality parameters

Water samples were collected monthly from 12 sites in Lake Erhai from January 2009 to August 2010 (Fig. 2.1, except for sites 1, 2, 3, and 4 north of the lake). Water quality parameters, including TN, DTN, NH_4-N, NO_3-N, TP, Chl-*a*, WT, DO, pH, and SD, were measured according to

the methods described in Section 2.2.2 of Chapter 2 (Wu et al. 2006, Wang et al. 2010). Approximately 300 mL surface water (0−0.2 m) for environmental DNA was filtrated through 0.45 μm polycarbonate membrane filters (Millipore), and the filters were then stored at −80 °C until DNA extraction.

3.2.2 Isolation and cultivation of strains

Tychonema strains were isolated using the Pasteur micropipette method (Rippka 1988) from water samples of Lake Erhai in 2009. Five uni-algal strains were successfully obtained and cultured in liquid MA medium (Kasai et al. 2009) at 25 ± 1 °C under a constant white light intensity of 25 μmol photons m^{-2} s^{-1} on a 12 h:12 h light/dark cycle. These strains were named CHAB1238, CHAB1264, CHAB1271, CHAB1274, and CHAB1282 and stored at the Institute of Hydrobiology, Chinese Academy of Sciences.

3.2.3 Morphological examination

The above five strains were morphologically identified according to the description of Anagnostidis and Komárek (1988) and Komárek and Anagnostidis (2005). Morphological studies were performed on the specimens collected from cultures on the exponential growth phase. The cell densities were approximately 1×10^5 cells mL^{-1}. The morphologies of cells and trichomes were observed using an Olympus BX51 light microscope with a digital camera (Qimaging Micropublish 5.0 RTV, USA). Cell sizes were measured from at least 100 trichomes per strain were analyzed using the Image-pro Express (Media Cybernetics, Inc., USA).

The ultrastructural features of the strains were studied using TEM. The strains during the exponential growth phase were fixed following a procedure similar to that described by Shao et al. (2011). Briefly, the strains in the exponential growth phase were fixed at room temperature for 2 h in 2.5% glutaraldehyde buffered with phosphate buffer (pH 7.0), then post-fixed in 1% osmium tetraoxide, dehydrated, and embedded in Spurr's resin (Yu et al. 2015). The fixed samples were observed under a TEM (Philips TECNAI G2) at an accelerating voltage of 80 kV.

Microphotographs were generated with a MegaView II digital camera using the Mega Vision software (Soft Imaging System GmbH, Germany).

3.2.4 Pigment analysis

The absorption spectra of the strains were measured by dual beam spectrophotometer using the filter membrane methods. The procedure is described as follows. Approximately 20 mL samples of every strain were filtered using the Whatman GF/F filter, and the filter samples were then measured by the spectrophotometer (SHIMADZU, UV2550) from 300 nm to 800 nm. Finally, the absorption coefficients were converted into chlorophyll-specific absorption coefficients (a^*) by normalizing to the Chl-*a* concentrations to remove the effect of pigment concentrations.

3.2.5 DNA extraction and qPCR amplification

Total genomic DNA and environmental samples were extracted from the culture strains according to the SDS-phenol method (Lin et al. 2011). Purified DNA was suspended in sterile 1×TE buffer (pH 8.0) and stored at −20 °C prior to PCR analysis.

The 16S rRNA gene sequences were amplified from the genomic DNA using the PCR primers F106: 5'-CGGACGGGTGAGTAACGCGTGA-3' (Nübel et al. 1997) and R4: 5'-TACGGCTACCTTGTTACGAC-3' (Neilan et al. 1997). PCR was performed in a reaction volume of 50 μL, similar to the description by Lin et al. (2010), which contains 5 ng to 10 ng of total genomic DNA, 1 U Taq DNA polymerase (Takara, Japan), 1× PCR reaction buffer with 1.5 mM $MgCl_2$, 10 pmol of each primer, and 200 mM concentrations of each deoxyribonucleoside triphosphate. The amplification program was set at 94 °C for 5 min, followed by 40 cycles of 94 °C for 40 s, 55 °C for 50 s, 72 °C for 2 min, and a final extension at 72 °C for 5 min. PCR products were examined on 1% (w/v) agarose gels dyed with ethidiumbromide and purified by the PCR purification kit (Omega, USA). Then the purified PCR products were then directly sequenced by Invitrogen Biotechnology Co. Ltd. (Shanghai, China).

The qPCR was used to enumerate the total cell numbers of *Tychonema*. The qPCR primers set were used as follows: TychoF (5-CCCACGATGTGACAGAGTTT-3) and TychoR (5-TTTCAGGATTGCTGGTAGCC-3). The specificity of the primers for *Tychonema* was checked in the preliminary experiment. The qPCR amplifications were conducted in an IQ5 Real-Time PCR system (Bio-Rad) with the following parameters: 95 °C for 3 min, then 45 cycles at 95 °C for 10 s, 55 °C for 30 s, and 70 °C for 30 s. Each reaction was performed in a 25 μL mixture with 0.5 mM of both primers, 10 μL enzyme-nucleotide-dye mix (SYBR green mixture, TOYOBO, Japan) and template DNA. Each measurement was performed in triplicate. Data were analyzed using the IQ5 Optical System Software Version 2.0. The cell numbers of *Tychonema* were calculated from the mean cycle threshold (*Ct*) value of three replicates according to the standard curve. Standard curves between cell concentration and *Ct* were created similar to the description in Section 2.2.5 of Chapter 2. The *Tychonema* culture under the logarithmic phase was subpackaged as six concentration gradients. Their DNA products were extracted and then amplified using the qPCR method to calculate the *Ct* values. The *Ct* values reflected the cell numbers of *Tychonema* using the linear regression equation.

3.2.6 Phylogenetic analysis

The 16S rDNA sequences of *Tychonema* strains obtained in this study, together with the other sequences from the GenBank, were aligned using CLUSTAL X integrated into the BioEdit package (Hall 1999). *Microcystis aeruginosa* PCC 7806 (AF139299) was selected as the outgroup. Phylogenetic trees were constructed with the MEGA 6.0 program package (Tamura et al. 2013) using a neighbor-joining (NJ) tree based on Kimura's two-parameter model of approximately 1,000 bootstraps. A maximum likelihood (ML) tree was constructed using PHYML version 3.5c (Guindon and Gascuel 2003); 100 bootstrap replicates were analyzed. Clade support was estimated using the general time-reversible (GTR) model. The parameters of the ts/tv ratio and p-invar were set to correspond to the outputs from the test model (Posada and Crandall 1998). Bayesian phylogenetic

analysis was performed by the MrBayes program with 5×10^6 generations, 5×10^4 trees, sampling at every 100^{th} generation, using the DNA substitution (HKY) model, Nst = 6, and rates = gamma. Given that all the methods yielded similar results, only the bootstrap values above 50% for ML and Bayes analyses were indicated at the NJ tree nodes.

3.2.7 Identification of odorous and volatile compounds

Volatile compounds of *T. bourrellyi* were extracted using headspace solid phase micro-extraction according to Shao et al. (2011, 2013). Gas chromatography–mass spectrometry (GC-MS, HP6890GC-5973MSD, Hewlett-Packard, USA) was used to separate and identify volatile compounds. Separation of extracted compounds was conducted on a capillary column (TC series, WondaCap 5, 0.25 mm × 30 m × 0.25 μm, Shimadzu, Japan). The injector temperature was set at 250 °C. The oven temperature program was as follows: initial temperature was set at 60 °C for 2 min, increased to 200 °C at a rate of 5 °C min^{-1}, maintained at this temperature for 2 min, followed by 250 °C at 20 °C min^{-1} that was held for 2 min. High purity N_2 ($\geq$ 99.99%) was used as the carrier gas under a pressure of 150 Kpa. Mass analysis was performed in the electron ionization mode at 70 eV and mass range at m/z 50 to 500. The quadrupole and ion source temperatures were set at 150 °C and 230 °C, respectively.

3.2.8 Statistical analyses

SPSS statistical software (version 13.0) for Canonical Correspondence Analysis (CCA) was used to analyze the correlations between the environmental factors and abundance of *Tychonema* cells.

3.3 Results

3.3.1 Morphological characterization

Five strains from Lake Erhai were examined for their morphological characteristics. These strains have the following characteristics. The trichomes were solitary in plankton or sometimes in mats attached to the wall of the culture tubes. The trichomes were reddish brown (Fig. 3.1) or blue-green, usually straight, unconstricted crosswall, wide toward the end, with thin sheath, and usually invisible in light microscopy. The cells were 7.2 µm to 10.7 µm wide (average of 9.1 µm) and 3.8 µm to 7.2 µm long (average of 5.4 µm) with clear keritomized content (Fig. 3.1b). The reticular pattern called "keritomy" by Komárek and Albertano (1994) was clearly observed in light microscopy. Apical cells were wide round with narrow calyptra. The large "vacuoles" were often visible within older cultures in light microscopy (Figs. 3.1d and 3.1e, indicated by the arrow).

The fine ultrastructure of *T. bourrellyi* demonstrates that the thylakoid organization were partly fasciculated and radially orientated, lengthwise or sometimes crosswise, and characteristically widen as "vacuoles" to form intrathylakoids spaces (Figs. 3.2a and 3.2b, indicated by the blue arrows). A pair or multiple twin unclosed septa were often observed within a cell in the light microscope and TEM (Figs. 3.1a and 3.2a, indicated by the green arrows). Cells with clear polyphosphate particles are shown in Figs. 3.2d (indicated by the white arrows).

Five strains were identified as *Tychonema bourrellyi* (Lund) Anagnostidis et Komárek in the morphology on the basis of the taxonomic criteria of the genus *Tychonema* (Anagnostidis and Komárek 1988, Komárek and Anagnostidis 2005).

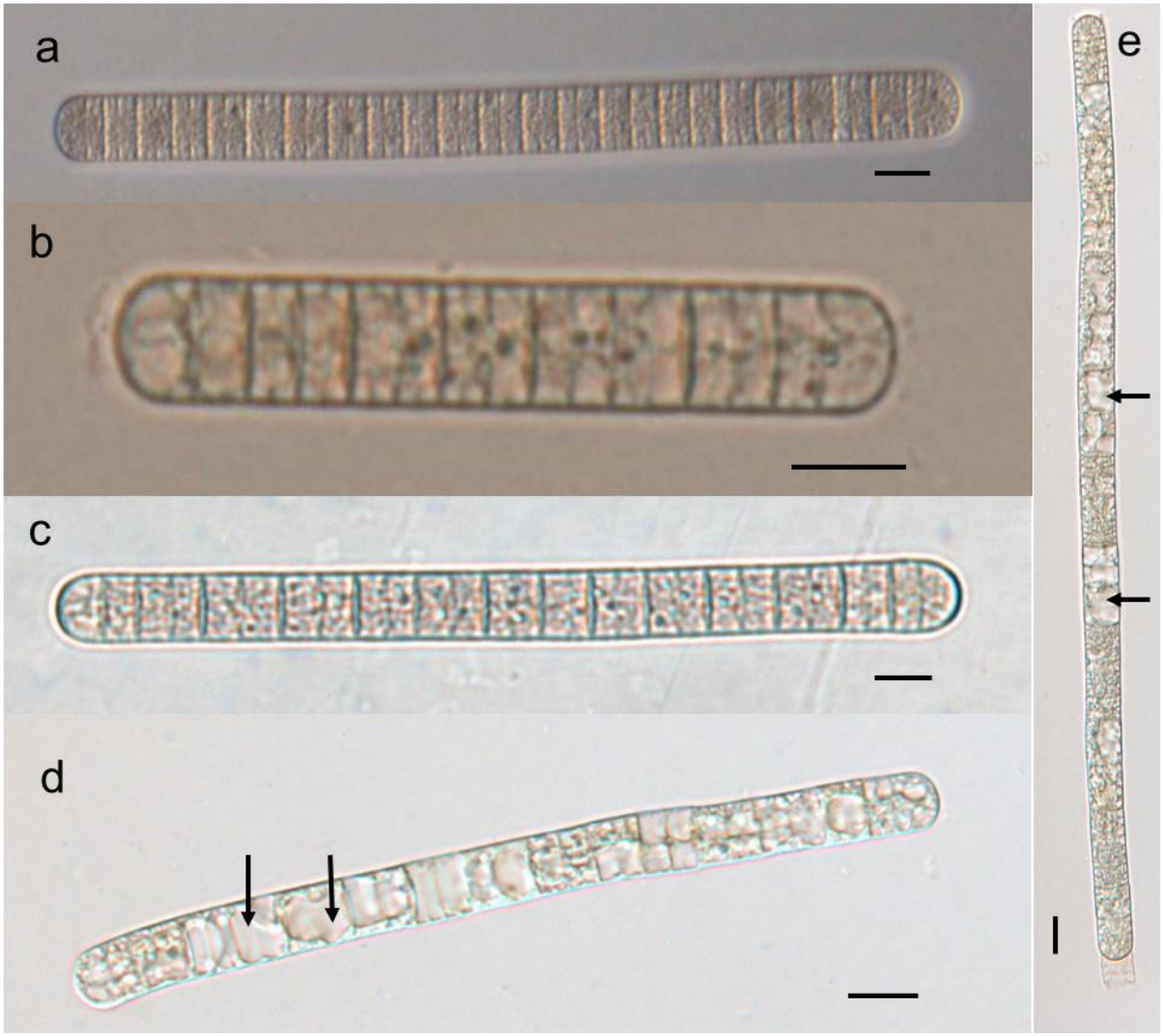

Fig. 3.1. Micrograph of *T. bourrellyi* in light microscopy. (a), (b) Field samples. (c) to (e) Isolated strain. (d) to (e) Older trichomas with the “vacuoles”. These “vacuoles” are indicated by the arrows. Bars = 10 µm.

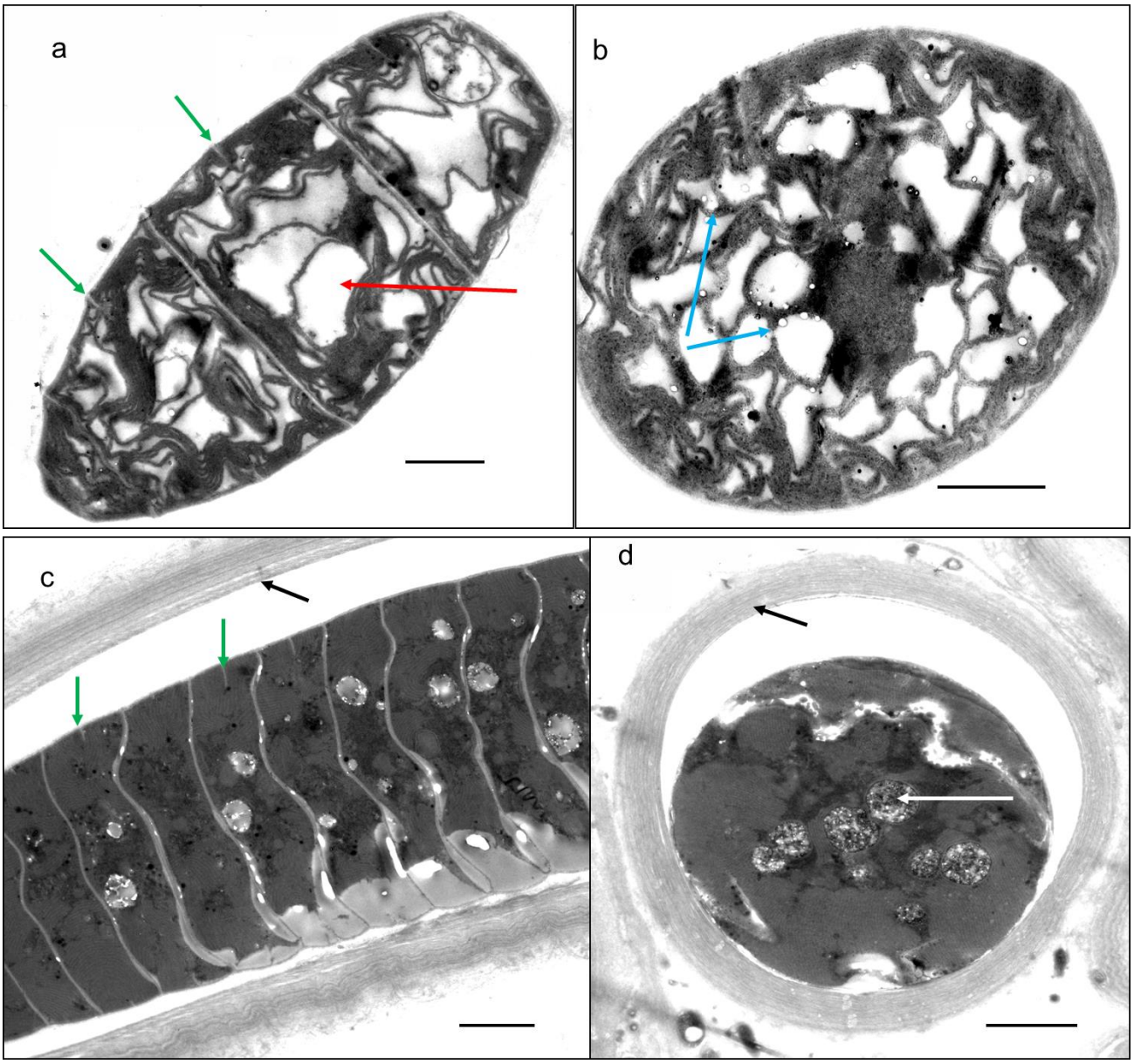

Fig. 3.2. TEM micrograph of *T. bourrellyi* during the exponential growth phase. Bars = 2 µm. The "vacuoles" are indicated by the red arrows, unclosed septa by the green arrows, sheaths by the black arrows, and polyphosphate by the white arrows.

3.3.2 Phylogenetic analysis based on 16S rRNA gene sequences

The 16S rDNA sequences of five strains with a size of 1384 bp were amplified with primers F106 and R4. The BLAST results show that 16S rDNA sequences within five strains isolated from Lake Erhai have 100% similarity and have high similarity (99%) to *T. bourrellyi* HAB663 (FJ184385), a strain found in the same lake (Wei et al. 2012). Furthermore, these sequences also have 99% similarity with *T. tenue* SAG4.82 (GQ324973) and *T. bourrellyi* CCAP1459/11B (AB045897) from Europe. However, a 98% similarity was also observed between two strains of *Microcoleus* (AF218377 and AF218373) and five strains of *T. bourrellyi* in the present study.

Five sequences in this study and 65 sequences of the 16S rDNA sequences cited from the GenBank Database, including three sequences of *Tychonema* and sequences of other cyanobacterial genera, were used to construct the phylogenetic trees (i.e., NJ, ML, and Bayesian trees). All sequences used to construct the phylogenetic trees were 1063 bp long. The phylogenetic trees reveal that the strain of the subfamily Phormidioideae are divided into five large clusters that support the current taxonomic system of Komárek and Anagnostidis (2005, Fig. 3.3). Given that all the trees yielded similar results, only the NJ tree is shown. However, bootstrap values of > 50% are shown. A comparison of the phylogenetic relationship between cyanobacteria shows that all *Tychonema* strains, including those newly isolated in this study, gathered tightly in a cluster in the NJ, ML, and Bayesian trees (Fig. 3.3). The cluster in the NJ, ML, and Bayesian trees were supported by high bootstrap values of 87%, 78%, and 92%, respectively.

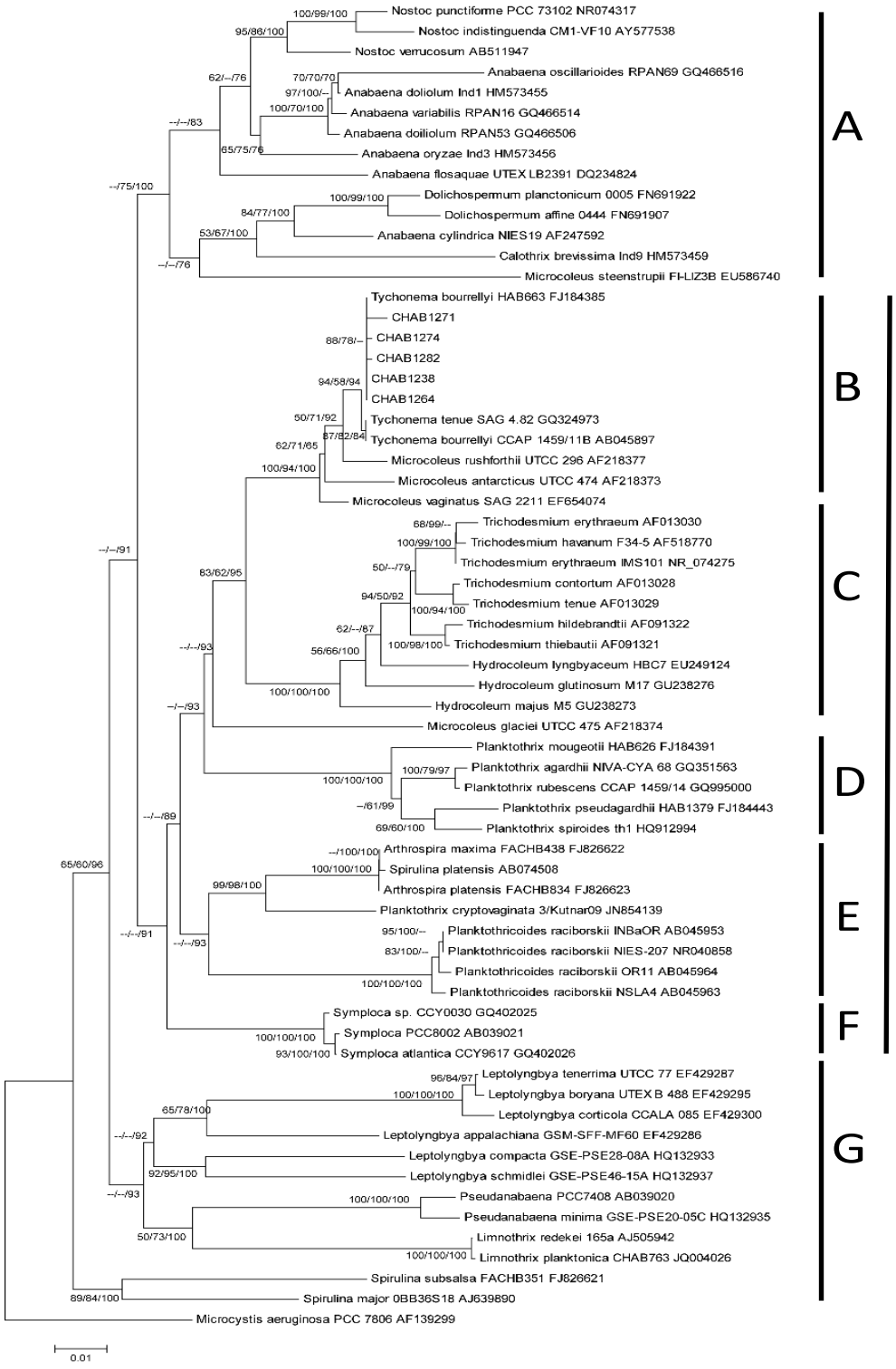

Fig. 3.3. NJ tree that shows the phylogenetic relationships between *Tychonema* and other cyanobacteria based on the 16S rDNA gene sequences of 60 strains of 1063 bp nucleotides. Bootstrap values larger than 50% with the NJ, ML, and Bayesian methods are shown on the tree. *M. aeruginosa* PCC 7806 was used as the outgroup.

3.3.3 Pigment composition

The absorption spectra show four clear peaks from 300 nm to 750 nm. Pigment composition is comprised of xanthophyll (474–480 nm), phycocyanin (PC, 615–622 nm), and Chl-*a* (432–436 nm and 663–667 nm, Fig. 3.4). In addition, a weak absorption peak at 560 nm to 590 nm indicates that phycoerythrin (PE) was present in the *Tychonema* strains.

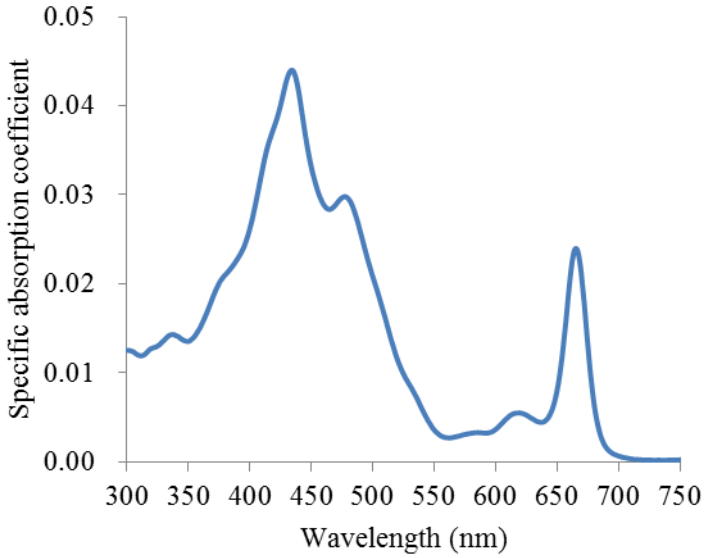

Fig. 3.4. Absorption spectra of *T. bourrellyi* strain pigments.

3.3.4 Identification of odorous and volatile compounds

As soon as the sample bottles were opened, the odorous earth-musty odor from the three stains (i.e., CHAB1238, CHAB 1264, and CHAB663) among the five *T. bourrellyi* strains can be obtained directly. The GC–MS analysis identified geosmin and β-Ionone as the major ingredients in the volatile substances. The total ion chromatography and MS reveal that the compound peak with a retention time of 17.60 min and m/z 112 was the main odorous component, which corresponds to geosmin (Fig. 3.5a). In addition, the other compound peak with a retention time of 19.57 min and m/z 177 was the main odorous component, which corresponded to β-Ionone (Fig. 3.5b).

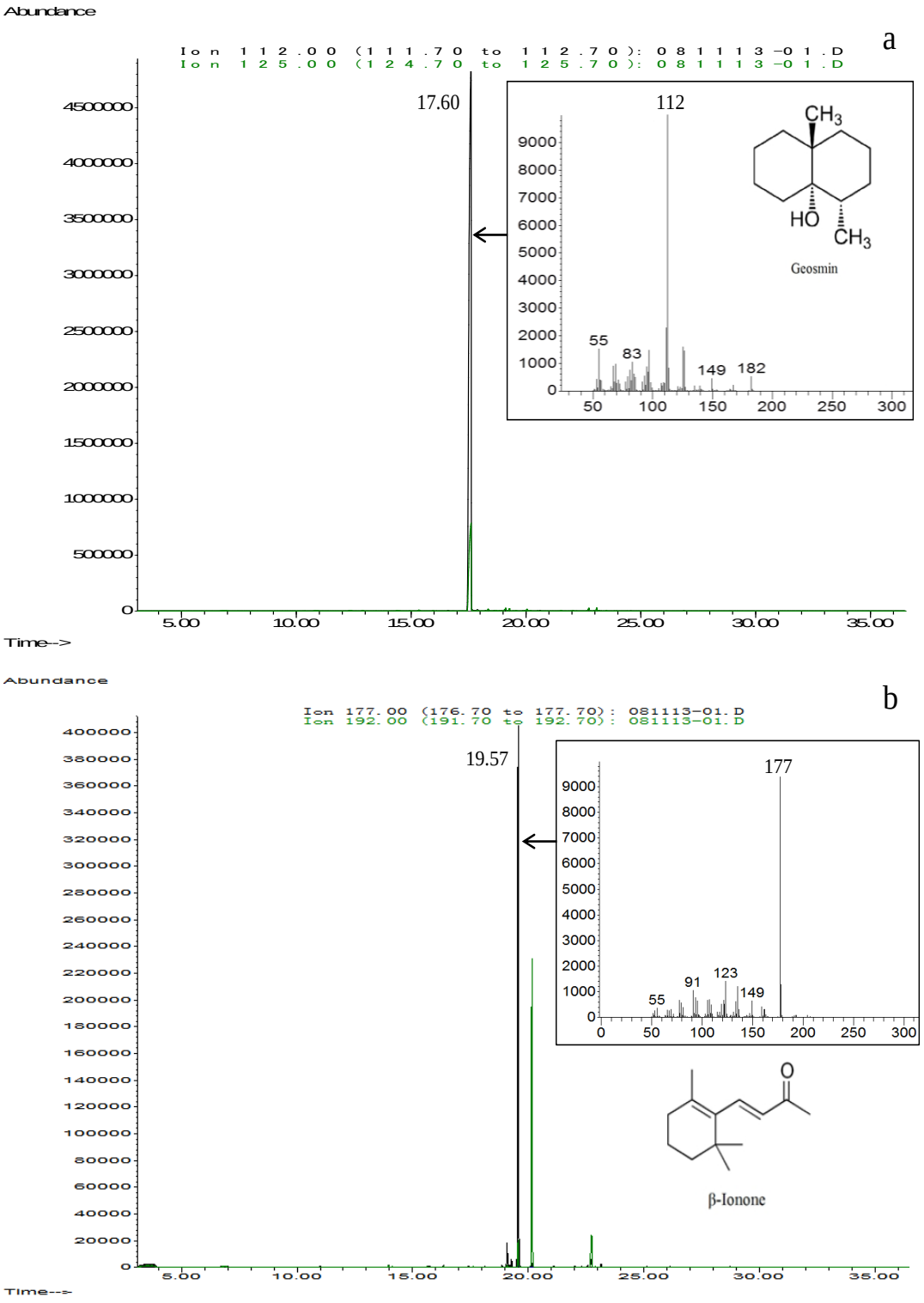

Fig. 3.5. GC–MS analysis of volatile substances obtained from the gaseous phase of the *T. bourrellyi* strains. MS reveals that the main volatile compounds were (a) Geosmin (retention time of 17.6 min, m/z 112) and (b) β-Ionone (retention time of 19.57 min, m/z 177).

3.3.5 Toxigenicity measurement

The toxigenicity of the strains was examined by the HPLC method and *mcy* gene (both *mcyA* and *mcyB*) approach. However, it was checked that no *T. bourrellyi* strains produced MCs. Results demonstrate that all *T. bourrellyi* strains did not produce microcystins.

3.3.6 Distribution of *T. bourrellyi* populations in Lake Erhai

The total *T. bourrellyi* cell abundance ranged from 104 cells L^{-1} to 9.9 $\times 10^5$ cells L^{-1} from 2009 to 2010, with an average of 3.0 $\times$ 10^4 cells L^{-1}. The annual tendency of the temporal distribution shows that a peak occurred both in July 2009 and July 2010 (Fig. 3.6). The cell abundances of *T. bourrellyi* around the central and southern parts were higher than those in other zones in other months within the four sampling sections. These results indicate that a clear seasonal variation occurred in July and August of every year.

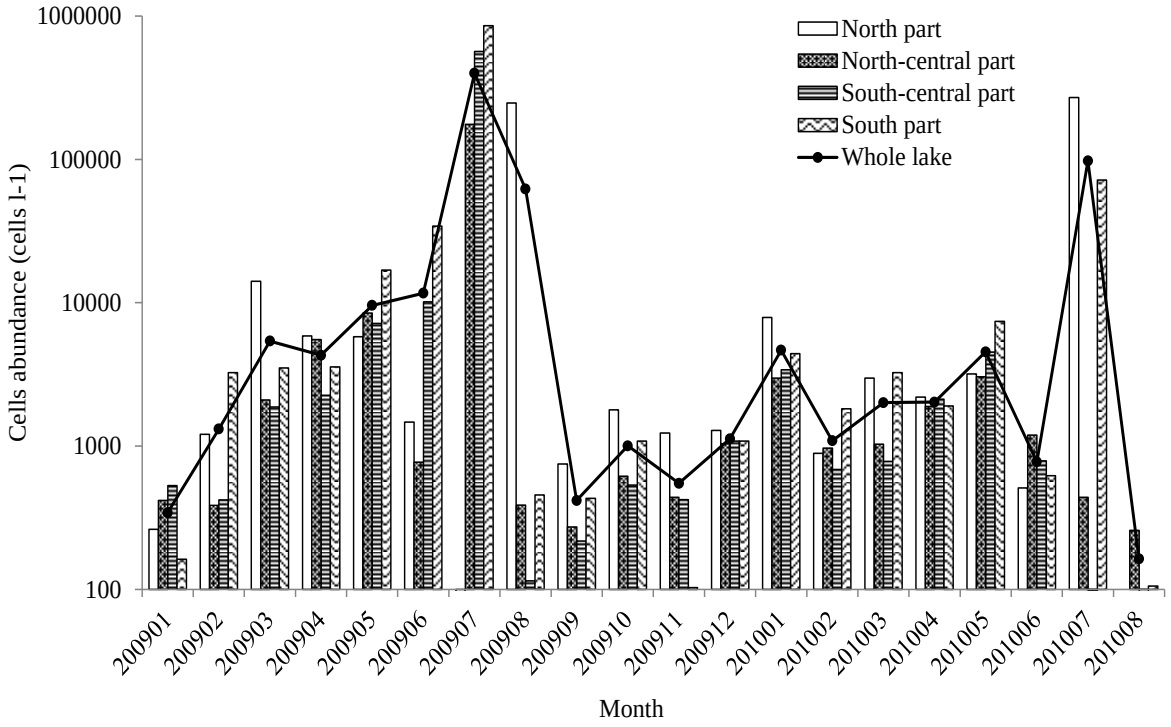

Fig. 3.6. Cell abundance of *T. bourrellyi* in Lake Erhai from January 2009 to August 2010.

3.3.7 Relationship between the *T. bourrellyi* population and environmental factors

The monthly variations of TN, TP, NH_4-N, NO_3-N, and DTN were 0.39 mg L^{-1} to 0.81 mg L^{-1}, 0.004 mg L^{-1} to 0.039 mg L^{-1}, 0.03 mg L^{-1} to 0.28 mg L^{-1}, 0.03 mg L^{-1} to 0.21 mg L^{-1}, and 0.13 mg L^{-1} to 0.53 mg L^{-1}, respectively. Their mean values were 0.57, 0.002, 0.12, 0.09, and 0.29 mg L^{-1}, respectively. The lowest values occurred in March or April, whereas the highest values occurred from July to September. The monthly variations imply that Lake Erhai can be in eutrophic states from July to September. The trophic state of Lake Erhai was generally described to be in a preliminary stage of eutrophic states.

The cell abundance of *T. bourrellyi* was positively correlated with WT, TN, TP, and Chl-*a*. However, the result based on the CCA analysis indicates that the cell abundance of *T. bourrellyi* was weakly correlated with WT, TN, TP, and Chl-*a* (Fig. 3.7).

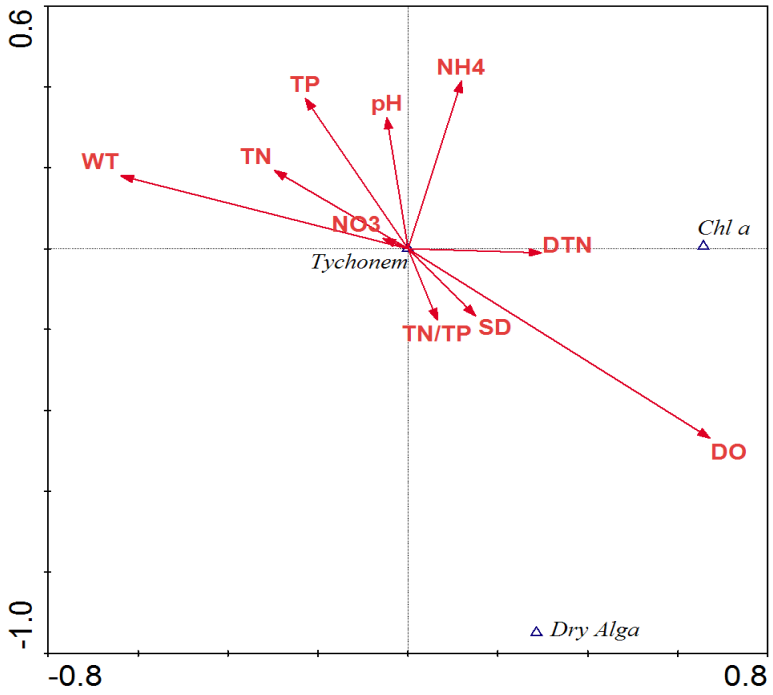

Fig. 3.7 Ordination biplot between the cell abundance of *T. bourrellyi* and environmental variables according to the CCA analysis.

3.4 Discussion

Anagnostidis and Komárek (1988) established the new genus *Tychonema* with the species *T. tenue* as a member of the family Phormidiaceae, order Oscillatoriales, and mainly based on the peculiar keritomized content of cells. This genus is generally characterized by solitary non-heterocystous filamentous trichomes without gas vesicles and cells with peculiar keritomized chromatoplasma (Anagnostidis and Komárek 1988, Komárek and Anagnostidis 2005). Ten species was listed within this genus by transferring from the genera *Oscillatoria* and *Lyngbya* when the genus *Tychonema* was initially established (Anagnostidis and Komárek 1988). However, only three species (i.e., *T. tenue*, *T. bourrellyi*, and *T. bornetii*) were formally accepted in the later edition of Oscillatoriales taxonomy by Komárek and Anagnostidis (2005). Skulberg and Skulberg (1991) argued that *T. tenue* and *T. bornetii* f. *tenue* were synonyms of *T. bourrellyi* based on the evidence of comparative experiments, but Komárek and Anagnostidis (2005) disagreed with this opinion. The *Tychonema* strains from Lake Erhai were planktonic and have large "vacuoles" in the cells, which could be distinguished them from the epiphytic species *T. tenue* and *T. bornetii* (Geitler 1932, Skulberg and Skulgerg 1991, Komárek 1994, Komárek and Anagnostidis 2005).

Several aspects of the intermediate characters were found in the *Tychonema* strains from Lake Erhai by comparing them with the strains of other species within this genus reported in previous studies (Table 3.1). The cell widths in this study (7–10.7 µm) were morphologically larger than those of *T. bourrellyi* (4–6.3 µm) and *T. tenue* (5.5–8 µm), but less than the sizes of *T. bornetii* (12–16 µm). These characters were similar to those of *Oscillatoria bornetii* var. *intermedia* Voronichin 1930, whereas the latter can be but has not formally been classified into the genus *Tychonema* (Geitler 1932, Komárek and Anagnostidis 2005). The strains examined in the present study have both reddish- and blue-green-colored trichomes, which are similar to *T. bornetii* (Geitler 1932, Komárek and Anagnostidis 2005) rather than *T. bourrellyi* that was never blue green (Lund 1955, Komárek and Anagnostidis 2005). These findings indicate that the *Tychonema* strains isolated from

Lake Erhai cannot be exactly classified into certain species identified in previous studies based only on their morphological and physiological characters because of intermediate characters. Genetic proof is expected to provide new evidence to solve this problem. A comparative result of the 16S rDNA gene sequences shows that the *Tychonema* strains isolated from Lake Erhai have more than 99% similarities to all the strains in the genus *Tychonema*, especially 100% with *T. bourrellyi* HAB663 (Wei et al. 2012). The phylogenetic trees based on the 16S rDNA gene sequences also show that the five strains in the present study formed a tight cluster with all *Tychonema* strains and supported by the NJ, ML, and Bayesian methods.

Komárek and Anagnostidis (2005) mentioned that a row of transient morphological forms existed between the narrowest and widest species, as well as emphasized that the interspecific limits must be revised. Although intermediate characters existed in these *Tychonema* strains, the variations in these characters (i.e., cell size and trichome color under PE/PC) were usually found in many cyanobacterial strains at culture conditions. No significant divergence in 16S rDNA gene sequences was also observed between the examined strains and those of the *Tychonema* species, so the emphasis on planktonic habitat of these strains helped us to identify them as *T. bourrellyi*. The final solution to the taxonomic system within the genus *Tychonema* is expected to rely on examining more genetic regions within the genomes of these *Tychonema* species.

Table 3.1. Feature comparison between the strains in the present study and other strains from previous studies within the genus *Tychonema*.

Species	Width	Color	Style	Reference
T. bourrellyi	7–10.7 μm	reddish or blue green	planktonic	In the present study
T. bourrellyi	4–6.3 μm	never blue green	planktonic	Komárek and Anagnostidis, 2005
T. tenus	5.5–8 μm		epiphytic	Geitler, 1932
T. bornetii	12–16 μm	reddish or blue green	epiphytic	Geitler, 1932
T. bornetii var. *intermedia*	7–11 μm		epiphytic	Komárek and Anagnostidis, 2005

The phylogenetic trees can effectively reveal the relationship between the genera of subfamily Phormidioideae to support the current taxonomic system of Komárek and Anagnostidis (2005) from the perspective of higher taxonomic ranks. Both *Tychonema* and *Microcoleus* genera without gas vesicles from freshwater clearly gathered into cluster B (Fig. 3.3). Genera from marine water, such as *Trichodesmium* and *Blennothrix*, gathered into cluster C. Freshwater genera, including *Planktothricoides*, *Arthrospira*, and *Plantothrix* with a gas vesicle group gathered into clusters D and E. These results suggest that the ecological features, such as habitats and gas vesicle structures that represent planktonic life style, should be considered as the taxonomic criteria in the subfamily Phormidioideae.

The qPCR results indicate that the cell abundance of *T. bourrellyi* in the surface water of Lake Erhai were low (usually less than 1×10^4 cells L^{-1}) and can reach 10^5 cells L^{-1} only in July. The CCA analysis indicates that cell abundance was only slightly correlated with WT, TN, TP, and Chl-*a* (Fig. 3.7). Skulberg and Skulberg (1991) demonstrated that *Tychonema* are abundant in plankton and benthos in boreal inland waters that range from oligotrophic to eutrophic conditions. The trophic state of Lake Erhai is described to be at a preliminary stage of eutrophic state (Wang et al. 2011b). The water temperature of Lake Erahi ranged from 8.7°C to 23.3°C with an annual average of 15.1°C, which is similar to the temperate lakes from Europe (Revaclier 1978, Berglind et al. 1983, Ganf et al. 1991, Skulberg and Skulberg 1991, Komárek and Anagnostidis 2005). Thus, the environmental and trophic conditions of Lake Erhai can meet the requirement for growth of *Tychonema*, but *T. bourrellyi* in Lake Erhai did not form a large biomass, which indicates that the influence factors that inhibit its growth in the lake can exist. More data is required to reveal the physio-ecological feature of *T. bourrellyi* in the future studies, such as the effects of the light and photosynthetic pigments (PC and PE) on the growth of *T. bourrellyi*. The abundant contents of PC and PE play important roles in both the chromatic adaptation and photosynthesis of cyanobacteria, as well as help them to adapt to the deep water conditions (Ojala 1993).

However, compared with the cell abundance of *Tychonema* at the same time during 2010, total *Microcystis* from same sites of Lake Erhai have higher cell abundance with an average of 1.7×10^7 cells L^{-1} (see the results of section 2.3.1). The nutrients concentrations during 2010 showed that N concentrations reached to mesotrophic and eutrophic level (0.39–0.81 mg L^{-1}), and P concentrations reached to oligotrophic and mesotrophic level (0.004−0.039 mg L^{-1}). P was limiting nutrient (usually <0.03 mg L^{-1}) in Lake Erhai. The results indicated that *Microcystis* have an advantage over *Tychonema* under relative lower P nutrients concentrations (an average of 0.02 mg L^{-1}). Cyanobacteria can accumulate P in polyphosphate bodies (Jacobson and Halmann 1982, Allen 1984). *Microcystis* adapt to P limitation with a fluctuating P-supply of water bodies by increasing its P uptake capacity and decreasing its light harvesting capacity (Brookes and Ganf 2001). These storage attributes of *Microcystis* can form new cells six times more than *Oscillatoria* (Brookes and Ganf 2001). Colony-forming *Microcystis* accumulated P better than *Oscillatoria* and *Pseudomonas* from P-containing organic sources (Yuan et al. 2009). This strategy, the polyphosphate "overplus" phenomenon, provides *Microcystis* with a competitive advantage over many microalgae (Sommer 1985). This ability is very useful, especially if phosphate concentrations in the water are low during bloom periods. Therefore, under lower P concentrations in Lake Erhai, the cell abundance of *Microcystis* outcompeted *Tychonema* due to its relative strong strategy for uptake of P. Otherwise, comparison experiment indicated that *Tychonema* (*O*. cf. *tenuis*) would not be a good competitor in environments such as the hypolimnion of Lake Arcas, due to its low anoxygenic photosynthetic capacity and to the low tolerance of oxygenic photosynthesis to sulfide (Camacho et al. 1996).

T. bornetii can produce geosmin (Berglind et al. 1983). Shao et al. (2013) indicated that *T. bourrellyi* CHAB663 isolated from Lake Erahi was a producer of β-Ionone. Three strains of *T. bourrellyi* isolated from Lake Erhai can produce both β-Ionone and geosmin in the present study, but the yield of these odor substances and influence factors, as well as their association, still need to be further examined in the future.

Chapter 4 Monitoring of water blooms in Lake Erhai, a drinking-water source in southwest plateau, China: Based on remote sensing

4.1 Introduction

With satellite remote sensing, the state of inland waters can be monitored through synoptic observations collected at frequent intervals. Generally, remote sensing of inland waters is much more difficult than that of open oceans. This is because the optical properties of inland waters are not determined only by phytoplankton (like open oceans), but are also strongly influenced by other constituents (i.e., non-algal particles (NAP) and colored dissolved organic matter (CDOM). As a result, inland waters have more complex optical properties. Both NAP and CDOM have larger absorptions at the blue and green spectral regions, and thus make these bands inappropriate for retrieving chlorophyll-*a* concentration (Chl-*a*) in many inland waters (Gilerson et al. 2010, Gitelson et al. 2008, Gitelson et al. 2009, Gons 1999, Moses et al. 2012, EI-Alem et al. 2012).

To address this problem, several indices have been proposed to remove or minimize the effects of NAP and CDOM based on use of remote sensing reflectance at the red and near infrared (NIR) spectral regions (NIR-red algorithms, Gilerson et al. 2010, Gitelson et al. 2008, Dall'Olmo et al. 2003, Gurlin et al. 2011, Moses et al. 2009). However, two challenges remain. First, although the design of these indices was based on theoretical studies of the inherent optical properties (IOP) of inland and coastal waters, Chl-*a* estimation models were still empirically calibrated through regression analyses of the proposed indices and measured Chl-*a*. Therefore, the developed Chl-*a* estimation models strongly depend on the calibration dataset used. Ideally, the calibration dataset

used does not have a sampling bias. Practically, however, it is difficult to collect enough water samples to represent all the water conditions in the world, and thus the applicability of the models will be limited. Second, the proposed indices were developed based on several specific assumptions, some of which may not be valid in highly turbid lakes such as Lake Taihu and Lake Dianchi in China and Lake Kasumigaura in Japan (Le et al. 2009, Yang et al. 2010, 2011a).

Recently, a semi-analytical model-optimizing and look-up-table (SAMO-LUT) method was proposed (Yang et al. 2011a), which can potentially estimate Chl-*a* in wide range of inland waters. Since the SAMO-LUT was proposed based on three wavelengths (665 nm, 708 nm and 753 nm) for Chl-*a* estimation, it is a NIR-red algorithm. In the SAMO-LUT algorithm, a comprehensive synthetic dataset of reflectance spectra related to various combinations of water constituents with a wide dynamic range was used to calibrate the Chl-*a* estimation model, instead of an *in situ* dataset. It thus improved the applicability of the model. In addition, a different assumption, i.e., concentrations of NAP and CDOM are constants, was adopted to further minimize the effects due to the previous assumptions. The new assumption may not be valid in real waters, but can be valid in simulated cases. Chl-*a* estimation models were then prepared in advance for various combinations of NAP and CDOM, which were increased in small increments, and saved in a look-up-table (LUT). An iterative search strategy was used to obtain the most appropriate Chl-*a* estimation model for a given pixel. A more detailed description of the SAMO-LUT algorithm can be found in Section 3 and in the previous study (Yang et al. 2011a).

Although the SAMO-LUT algorithm has been validated in Lake Dianchi, China, and Lake Kasumigaura, Japan, further validation is necessary to determine both the advantages and potential limitations of the algorithm. The present study had three objectives: (1) to evaluate the performance of the SAMO-LUT algorithm using a more extensive dataset collected from five Asian lakes (three in Japan and two in China); (2) to determine whether the fixed Specific Inherent Optical Properties (SIOPs, collected from Lake Dianchi) affected the accuracy of the SAMO-LUT algorithm in Chl-*a*

estimation for other lakes; and (3) to provide recommendations for the operational application of the SAMO-LUT algorithm for remote monitoring of Chl-*a* in inland waters.

4.2 Materials and methods

4.2.1 Study areas

The data used in this study were collected from five Asian lakes, which cover trophic categories from oligotrophic to hypertrophic. The first is Lake Biwa, which is located in the western part of Japan (35.33°N, 136.17°E, Shiga Prefecture). It is the largest freshwater lake in Japan with a surface area of 670 km^2, a maximum depth of 104 m, and an average depth of 41 m. Lake Biwa serves as reservoir for the cities of Kyoto and Ōtsu, and provides drinking water for about 15 million people in the Kansai region. It is also a valuable water resource for many kinds of nearby textile industries. Water quality in the lake is currently good, and it belongs to the oligotrophic category.

The second is Lake Suwa, which is located in the central part of Japan (36.05°N, 138.08°E, Nagano Prefecture). It has a surface area of 13.3 km^2, an average depth of 4.7 m, and a maximum depth of 7.2 m. In the 1960s, the lake underwent a very rapid hypertrophication. This was caused by the spectacular growth of industrial activity around the lake, and is indicated by heavy blooms of blue-green algae. Water quality has been remarkably improved since the end of 1990s, thanks to effective management. Therefore, the current trophic status of the lake is close to the boundary between mesotrophic and eutrophic.

The third lake is Lake Kasumigarua, situated in the eastern part of Japan's Kanto plain (36.03°N, 140.40E, Ibaraki Prefecture). It is Japan's second largest lake, with a surface area of 171 km^2, an average depth of 4 m, and a maximum depth of 7.3 m (only for Nishiura). This lake is considered hypertrophic because of its high loads of nutrients and shallow depth (Fukushima et al. 1996). Although average Chl-*a* has decreased from 87 to 61 mg m^{-3} during the past three decades, the mean total phosphorus concentration increased from 116 to 138 mg m^{-3}. Secchi disk depth

decreased from 70 to 52 cm in the last twenty years (CGER 2010). Total suspended sediment (TSS) concentrations increased from 14.1 to 26.4 g m^{-3} during the last decade, due mainly to the resuspension of bottom sediments (Fukushima et al. 2005). Diatoms (e.g., *Cyclotella* sp. or *Synedra* sp.) are generally observed during winter, spring, and autumn, while harmful blooms (blue green algae, e.g., *Microcystis* sp. or *Anabaena* sp.) are sometime observed during summer. The concentration of dissolved organic carbon (DOC), which is often correlated with CDOM concentration, is always low (2.9–4.2 g m^{-3}; Fukushima et al. 1996, Imai et al. 2003) compared to lakes such as Lake Taihu (8.8–20.2 g m^{-3} in Zhang et al. 2005) and Finnish lakes (6.0–12.3 g m^{-3} in Kutser et al. 2005). The absorption coefficients of CDOM at 420 nm ranged from 0.5 to 0.6 m^{-1} when DOC concentrations ranged from 1.9 to 2.7 g m^{-3} (CGER 2010), which was lower than the absorption coefficients of CDOM at 420 nm in Finnish lakes (1.7–7.7m^{-1} in Kutser et al. 2005).

The fourth lake in our database is Lake Dianchi, located in a plateau area of the southwestern part of China (24.83°N, 102.72°E). It has a surface area of 300 km^2 and is the largest lake in Yunnan Province, with an average depth of 4.3 m, and a maximum depth of 11.3 m. Eutrophication has become more and more serious in the lake over the past 20 years due to the large quantities of industrial wastewater and municipal sewage discharged into it. Algal blooms occur frequently from April to November each year (Gao et al. 2005). The trophic status of Lake Dianchi also belongs to the hypertrophic category.

The final lake is Lake Erhai (25.82°N, 100.18°E), which is the second largest lake in the Yunnan Province of China. It has a surface area of 249 km^2, an average depth of 10.2 m, and a maximum depth of 20.7 m. Lake Erhai is an important drinking water resource for the local people, supplying drinking water of 8.3×10^4 m^3 per day. It is also utilized for local industries, irrigation, and domestic water in the coastal area. During the past 30 years of rapid economic development and increasing population, Lake Erhai has faced a serious threat of intensive eutrophication due to anthropogenic inputs and overuse (Zheng et al. 2004). The water quality status of Lake Erhai is already at the initial stage of eutrophication, with organic matter and phytoplankton biomass

increasing rapidly, and cyanobacteria blooms breaking out in the embayment and some parts of the lake.

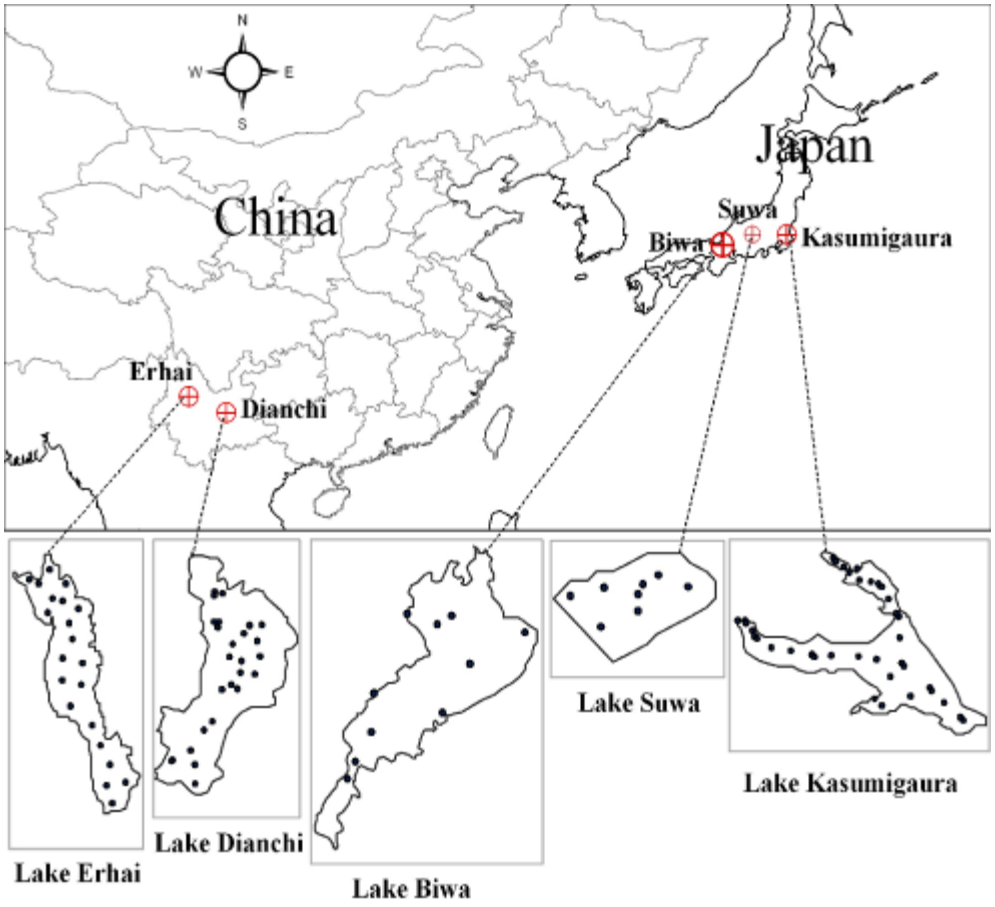

Fig. 4.1 Distribution of sampling sites in Lakes Erhai and Dianchi of China, and Lakes Biwa, Suwa and Kasumigaura of Japan.

4.2.2 Data collection

Water samples and corresponding reflectance spectra were collected from Lake Biwa in a campaign undertaken in October 2011 (10 sites available); from Lake Suwa in a campaign in July 2010 (8 sites); from Lake Kasumigaura in February 2006, August 2008, and May 2010 (46 sites). Data collection was also carried out in Lake Dianchi in October 2007, July 2008, and July 2009 (28

sites). In Lake Erhai, there were two field campaign—one in September 2011 and the other in July 2012. In each field campaign, the investigation was performed at 21 sites (42 sites in total).

Reflectance was measured between 10:00 and 14:00 local time. All measurements were taken over optically deep water with depths larger than Secchi disk depth; floating scum was not found at these sampling sites. The water-leaving radiance ($L_u(\lambda)$), the downward irradiance ($E_d(\lambda)$), and the downward radiance of skylight ($L_{sky}(\lambda)$) were measured at each site using a FieldSpec HandHeld spectroradiometer (Analytical Spectral Devices, Inc., Boulder, CO) in the range of 325 to 1075 nm at 1-nm intervals. The above-water remote-sensing reflectance ($R_{rs}(\lambda)$) was calculated approximately using the following equation (Mobley 1999):

$$R_{rs} \approx \left(\frac{L_u(\lambda)}{E_d(\lambda)} - \frac{rL_{sky}(\lambda)}{E_d(\lambda)}\right) \times Cal(\lambda) \times 100, \quad (1)$$

where $Cal(\lambda)$ is the spectral reflectance calibration factor for the Spectralon reflectance panel, and r is the reflectance of skylight determined as a function of wind speed (SCOR-UNESCO 1966).

Water samples were collected at each site, and taken to laboratory within approximately 0.5-1.5 h after the field investigation. Chl-*a* was extracted using methanol (100%) at 4^{o}C for 24 h under dark conditions. The absorbance of the extracted Chl-*a* was measured at four wavelengths (750, 663, 645 and 630 nm), and the concentrations were calculated according to SCOR-UNESCO equations (SCOR-UNESCO 1966). The concentrations of total suspended solids (TSS), organic suspended solids (OSS), and inorganic suspended solids (ISS) were determined gravimetrically. Samples were filtered through pre-combusted Whatman GF/F filters at 500^{o}C for 4 h to remove dissolved organic matter in suspension, and then dried at 105^{o}C for 4 h and weighed to obtain TSS. The filters were re-combusted at 500^{o}C for 4 h and then weighed again to obtain ISS. OSS was derived by subtracting ISS from TSS. The absorption coefficient of CDOM was measured using a Shimadzu UV-2450 spectrophotometer after the water sample was filtered. The absorption coefficients of phytoplankton (a_{ph}) were measured according to the quantitative filter technique (Mitchell 1990). The a_{ph} data were available only for the stations collected after 2009.

4.2.3 SAMO-LUT method

The basic idea of the SAMO-LUT involves the use of an imaginary case II body of water, in which only one constituent changes while the other two are controlled as constants (Yang et al. 2011a). A comprehensive synthetic dataset was used for model calibration, rather than in situ data. In this way, we hoped to obtain not only a large number of samples without a sampling bias for model calibration, but also a series of special cases to avoid effects from other constituents and thus improve model performance (e.g., a dataset only with various Chl-*a* while concentrations of NAP and CDOM are constants).

The procedures of the SAMO-LUT are summarized as follows:

Step 1: Generation of simulation dataset. The R_{rs} spectra were generated based on the SIOPs from target water and a bio-optical model. In the present study, only the SIOPs collected from Lake Dianchi were used due to the lack of complete SIOPs data for other lakes. I felt it would be worthwhile to examine how the SIOPs affected the accuracy of the SAMO-LUT algorithm. The concentrations of Chl-*a* and NAP (i.e., tripton in the original paper), as well as the absorption coefficient of CDOM at 440 nm were varied in a wide range of 1–300 mg m^{-3} (31 values), 1–250 g m^{-3} (28 values) and 0.1–10 m^{-1} (23 values), respectively. In all, 19,964 sample spectra were generated (Yang et al. 2011a).

Step 2: Computation of selected semi-analytical indices. Three semi-analytical indices were selected for the estimation of Chl-*a*, NAP and CDOM, based on their reasonableness and performance. The selected indices were: A three-band index ($[1/R_{rs}(665)-1/R_{rs}(708)]*R_{rs}(753)$) for Chl-*a*, remote-sensing reflectance for the band centered 753 nm, $R_{rs}(753)$, for NAP, and the band-ratio $R_{rs}(560)/R_{rs}(665)$ for CDOM (Gitelson et al. 2008, Ammenberg et al. 2002). The synthetic reflectances were resampled to the bandwidths of the MERIS (Medium Resolution Imaging Spectrometer) sensor based on its spectral response function, and then calculated as the selected indices.

Step 3: Construction of look-up tables. I constructed three 2-dimensional look-up tables containing the coefficients of the estimation model for one constituent of interest, determined by the concentrations of the other two constituents. For instance, for the estimation of Chl-*a*, increments of 1 mg m^{-3} for NAP and of 0.1 m^{-1} for CDOM were respectively used in the ranges of 1-250 mg m^{-3} and 0.1–10 m^{-1}, and the regression coefficients corresponding to different combinations of NAP and CDOM were stored in the LUT.

Step 4: Initial estimations of Chl-*a* and NAP. I derived initial values of Chl-*a* and NAP using two general estimation models obtained through regression analysis between the simulated reflectance and corresponding Chl-*a* and NAP. The two general estimation models were:

$$\text{Chl}^{-}a = 223.86(R_{\text{rs},665}^{-1} - R_{\text{rs},708}^{-1}) \times R_{\text{rs},753} + 23.95 \quad (2)$$

$$NAP = 49909 R_{\text{rs},753}^{2} - 61.38 R_{\text{rs},753} + 4.74 \quad (3)$$

The calculated initial Chl-*a* and NAP were then used to estimate initial CDOM through a prepared LUT in step 3.

Step 5: Iteration to select more appropriate model coefficients. The estimation models were improved according to the initial Chl-*a*, NAP, and CDOM. After that, the refined Chl-*a*, NAP, and CDOM were obtained by using the improved estimation models.

Step 6: End of iteration. I found a more appropriate estimation model from the LUTs for each water constituent through the iterative use of the newly obtained Chl-*a*, NAP and CDOM. The iteration was stopped when the difference between the current and last output was sufficiently small. Generally, the differences become stable after the 10^{th} iteration.

4.2.4 Conventional 3-band index-based estimation model

For comparison analysis, a conventional 3-band index-based linear model (Simple 3-band Model), calibrated by the same simulated dataset used in the SAMO-LUT, was also applied to the validation datasets (Yang et al. 2011a). This model was used as the initial estimation of Chl-*a* in the SAMO-LUT method (i.e., Equation 2). The comparison between this method and the SAMO-LUT

can demonstrate how the iteration process in the SAMO-LUT method influences the estimation of Chl-*a*. In addition, it is worth noting that the slope and intercept of this linear model were close to those of the models proposed by the previous studies (e.g. 232.29 for slope and 23.174 for intercept in Moses et al. 2009).

4.2.5 Accuracy assessment

Four indices (i.e., the root mean square error [RMSE], normalized root mean square error [NRMS], mean normalized bias [MNB], and normalized mean absolute error [NMAE]) were used in accuracy assessment (Gitelson et al. 2008, Gurlin et al. 2011) These indices are defined as follows:

$$\mathrm{RMSE} = \sqrt{\frac{\sum_{i=1}^{N}\left(X_{esti,i} - X_{meas,i}\right)^2}{N-1}} \quad (5)$$

$$\mathrm{NRMS} = \mathrm{stdev}(\varepsilon_i)\% \quad (6)$$

and

$$\mathrm{MNB} = \mathrm{mean}(\varepsilon_i)\% \quad (7)$$

$$\mathrm{NMAE} = \mathrm{mean}(|\ \varepsilon_i\ |)\% \quad (8)$$

where $X_{esti,i}$ and $X_{meas,i}$ are the estimated and measured Chl-*a*, respectively; N is the number of samples; and $\varepsilon_i = 100\times(X_{esti,i}-X_{meas,i})/X_{meas,i}$ is the percent difference between the estimated and measured Chl-*a*. The NRMS denotes the relative random uncertainty of the results, the MNB denotes the average bias in the estimation, and the NMAE denotes the average relative error in the estimation. The correlation between the measured and estimated values was also calculated.

4.3 Results

4.3.1 Water constituent concentrations and spectral reflectance properties

Table 4.1 contains descriptive statistics of the water constituent concentrations for the five lakes. Lake Biwa was the clearest, with mean Chl-*a* and TSS concentrations of 2.2 mg m^{-3} and 1.0 g m^{-3}, respectively, followed by Lake Suwa (mean Chl-*a* of 11.4 mg m^{-3} and mean TSS of 5.4 g m^{-3}),

Lake Erhai (mean Chl-*a* of 19.6 mg m^{-3} and mean TSS of 5.8 g m^{-3}), and Lake Kasumigaura (mean Chl-*a* of 66.5 mg m^{-3} and mean TSS of 24.5 g m^{-3}). Lake Dianchi had the highest turbidity, with mean Chl-*a* and TSS concentrations of 87.7 mg m^{-3} and 37.4 g m^{-3}, respectively. All five lakes showed low absorption coefficients of CDOM at 440 nm, with measures ranging from 0.15–3.98 m^{-1} (most were less than 1 m^{-1}). The overall Chl-*a* of the five lakes varied by two orders of magnitude in the range of 1.8–153.9 mg m^{-3}. Except for Lake Suwa, each lake showed larger spatial heterogeneity for Chl-*a* (coefficient of variation larger than 19.3%). These datasets encompassed varying optical conditions and trophic statuses (from oligotrophic to hypertrophic), and thus can provide a thorough assessment of the SAMO-LUT method.

The reflectance spectra collected from the five lakes are shown in Fig. 4.2. The reflectance spectra of Lake Biwa were similar to those collected from European lakes with low Chl-*a* and TSS (Odermatt et al. 2010), showing a unique peak in the green wavelength range (500–600 nm) and low magnitudes of the remote sensing reflectances along the visible and NIR spectral ranges (below 0.007 sr^{-1}). For the other four lakes, reflectance in the blue wavelength range (400–500 nm) was remarkably lower than in the green wavelength range (500–600) due to the high absorptions of phytoplankton, NAP, and CDOM in the shorter wavelengths (Gitelson et al. 2009, Gons 1999, Gulin et al. 2011). Reflectance troughs around 620 nm can be seen in the reflectance spectra of Lakes Erhai, Kasumigaura and Dianchi, demonstrating the dominance of cyanobacteria in those bodies of water (Simis et al. 2005). A second minimum was also found at around 675 nm, which corresponded to the red Chl-*a* absorption maximum. In addition to chlorophyll, the reflectance near 675 nm was also affected by absorption and scattering by other constituents. A noticeable peak between 690 and 715 nm appeared in almost all spectra of the lakes except for Lake Biwa. This peak was the result of both high backscattering and a minimum in the absorption of all water constituents, including pure water (Gitelson et al. 1985, Gitelson 1992). Finally, reflectance in the NIR region (700–750 nm) varied widely, and was consistently comparable with that in the blue region. In the NIR region of the spectrum, reflectance is mostly controlled by the scattering of particulate matters.

Table 4.1 Statistical description of water constituent concentrations for Lakes Biwa, Suwa, Erhai, Kasumigaura and Dianchi.

		Chl-*a* (mg m^{-3})	TSS (g m^{-3})	ISS (g m^{-3})	OSS (g m^{-3})	CDOM (m^{-1})
Biwa	Min	1.81	0.77	0.45	0.31	0.15
	Max	2.90	1.99	1.49	0.49	0.26
	Mean	2.21	1.01	0.64	0.38	0.21
	Median	2.02	0.87	0.55	0.34	0.20
	Stdev	0.43	0.37	0.31	0.07	0.03
	CV	19.33	36.61	49.24	19.33	15.64
Suwa	Min	9.79	4.81	1.21	3.30	0.41
	Max	11.37	6.06	2.19	4.79	0.48
	Mean	10.72	5.37	1.65	3.72	0.44
	Median	10.86	5.42	1.56	3.59	0.44
	Stdev	0.63	0.43	0.40	0.45	0.02
	CV	5.87	8.02	24.37	12.12	5.38
Erhai	Min	9.68	3.54	0.17	2.87	0.33
	Max	36.08	11.29	1.62	10.63	0.56
	Mean	19.58	5.75	0.78	4.98	0.41
	Median	18.73	5.64	0.83	5.08	0.40
	Stdev	5.92	1.70	0.40	1.61	0.06
	CV	30.20	29.45	51.51	32.30	13.49
Kasumigaura	Min	36.60	11.65	3.10	4.39	0.51
	Max	95.02	47.90	37.30	11.70	1.78
	Mean	66.47	24.45	16.31	8.13	0.90
	Median	67.88	21.92	14.50	8.42	0.92
	Stdev	19.48	8.24	7.28	2.36	0.29
	CV	29.30	33.70	44.65	29.03	32.04
Dianchi	Min	30.21	24.50	0.50	4.47	0.41
	Max	153.92	55.00	42.27	46.50	3.98
	Mean	87.74	37.38	12.39	24.98	1.25
	Median	84.56	37.42	6.50	27.00	0.96
	Stdev	29.16	7.80	11.79	11.49	0.84
	CV	33.23	20.86	95.12	46.01	66.87

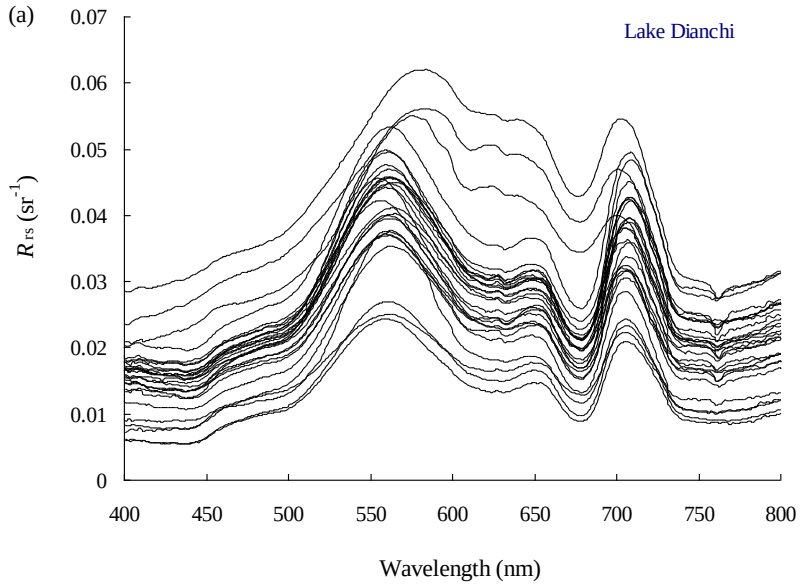
(a)
Lake Dianchi
R_{rs} (sr^{-1})
0.07
0.06
0.05
0.04
0.03
0.02
0.01
0
400
450
500
550
600
650
700
750
800
Wavelength (nm)

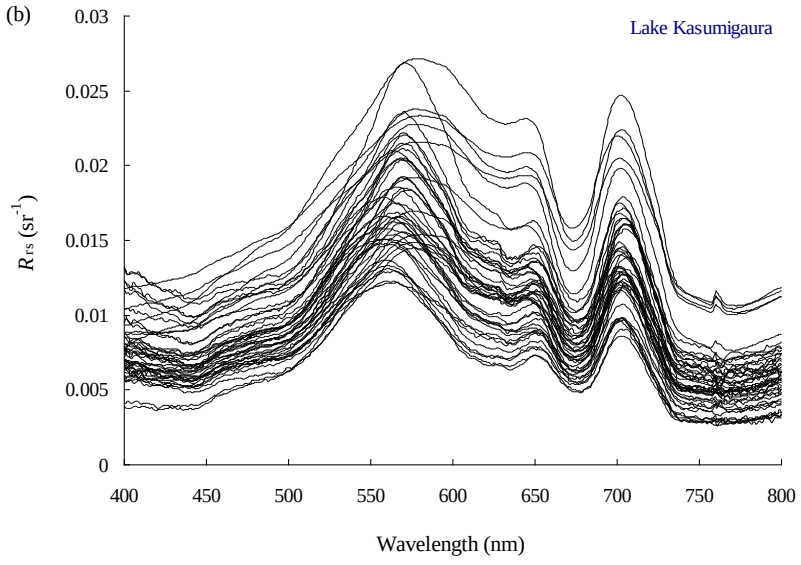
(b)
Lake Kasumigaura
R_{rs} (sr^{-1})
0.03
0.025
0.02
0.015
0.01
0.005
0
400
450
500
550
600
650
700
750
800
Wavelength (nm)

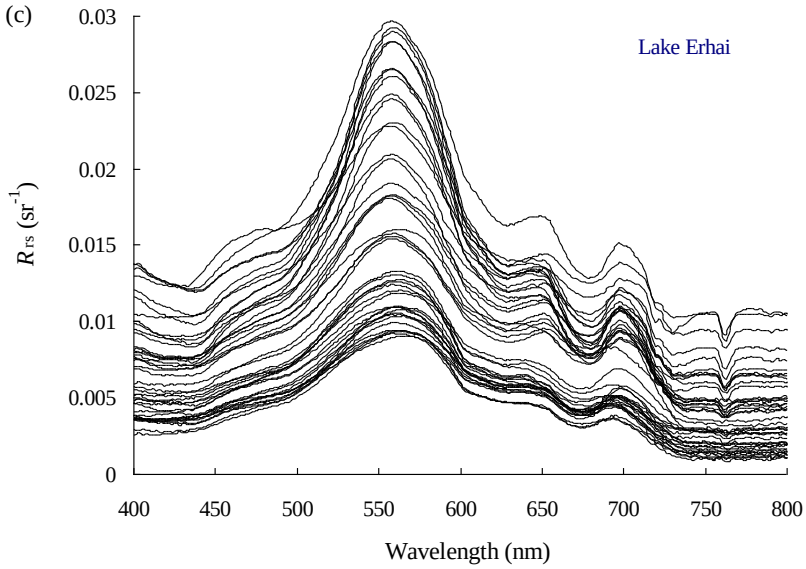
(c)
Lake Erhai
R_{rs} (sr^{-1})
0.03
0.025
0.02
0.015
0.01
0.005
0
400
450
500
550
600
650
700
750
800
Wavelength (nm)

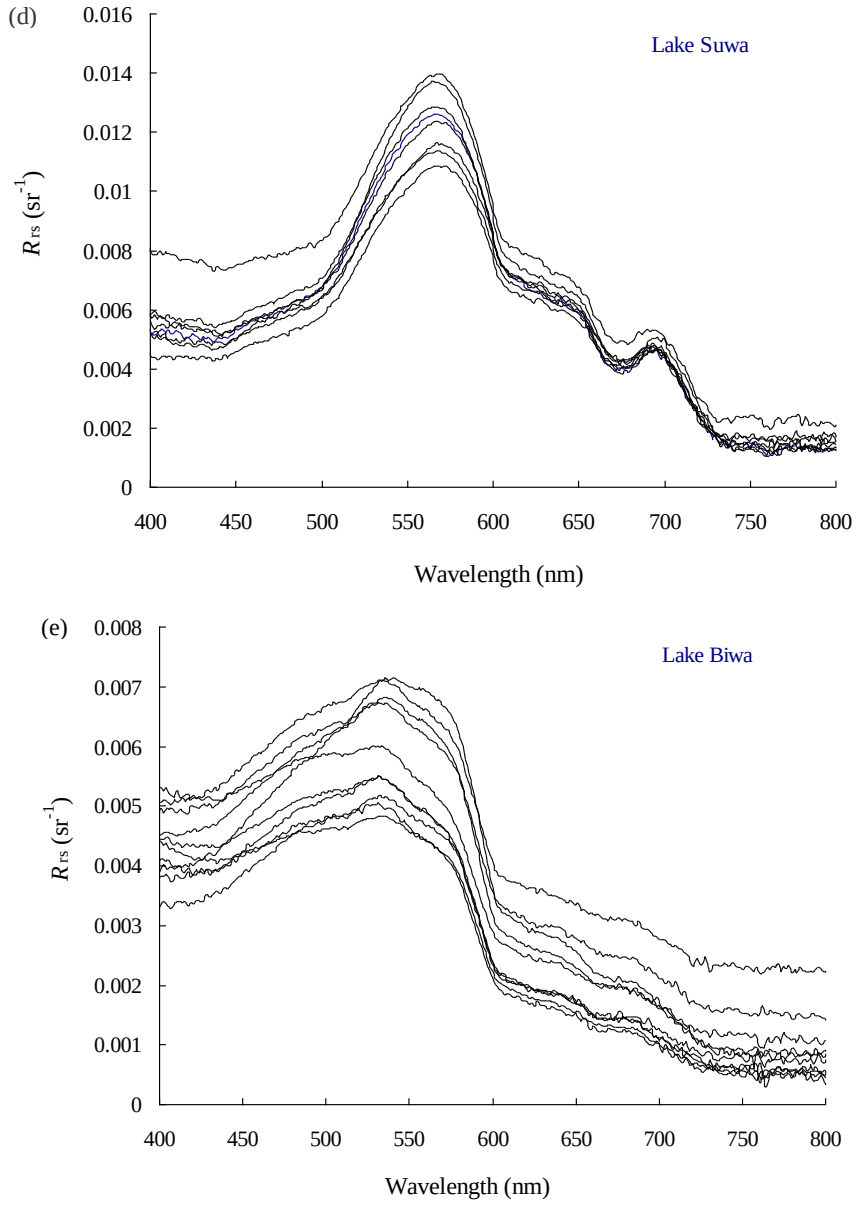

Fig. 4.2 Remote-sensing reflectance collected from Lakes Biwa, Erhai, Suwa, Kasumigaura and Dianchi.

4.3.2 Performance of the SAMO-LUT algorithm for each lake

Figure 4.3 shows the comparison between the measured Chl-*a* and that estimated by the SAMO-LUT method for Lake Dianchi, China. The SAMO-LUT yielded an estimation of very high accuracy, with RMSE, NRMS, MNB and NMAE of 7.39 mg m^{-3}, 11.3%, 1.3% and 6.9%, respectively (Table 4.2). It is worth noting that the dataset for Dianchi was collected over three years,

and that the accuracy for each year was comparable with the data points distributed around the 1:1 line (Fig. 4.3).

Table 4.2 Performance of the SAMO-LUT, Simple 3-band Model and OC4E for the estimation of Chl-*a* in Lake Dianchi, China.

	RMSE (mg m^{-3})	NRMS(%)	MNB(%)	NMAE(%)	R^2	Slope
Lake Dianchi, China (N=28)						
SAMO-LUT	7.39	11.3	1.3	6.9	0.94	0.998
Simple 3-band model	8.81	13.73	3.08	8.04	0.91	0.931
OC4E	79.14	8.7	-81.3	81.3	0.05	0.049

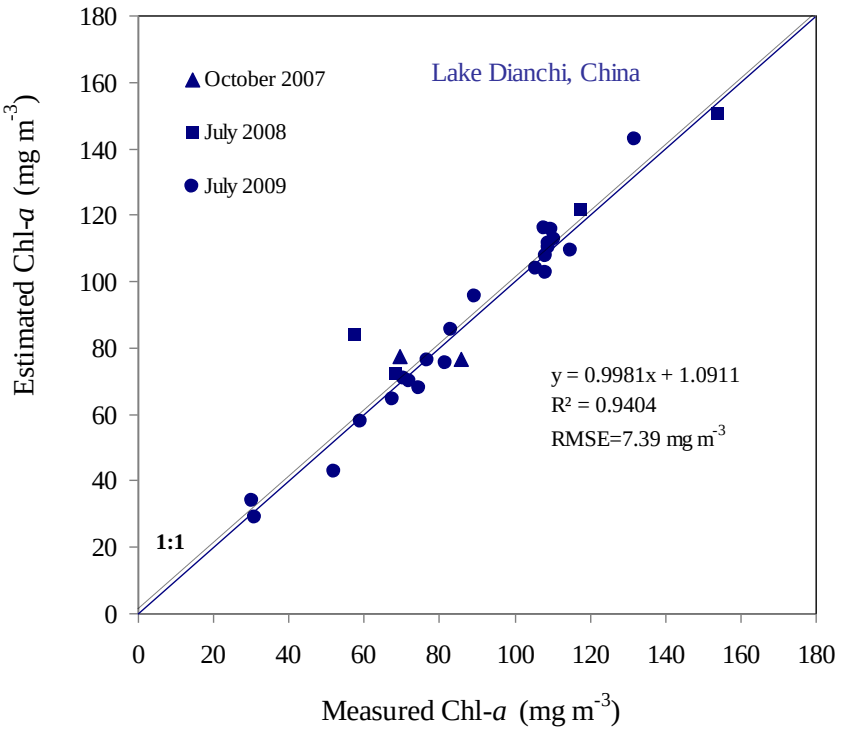

Fig. 4.3 Comparison of the measured and estimated Chl-*a* by the SAMO-LUT for Lake Dianchi, China.

As for Lake Kasumigaura, Japan, and Lake Erhai, China, the SAMO-LUT was able to estimate the Chl-*a* with acceptable accuracy (Figs 4.4 and 4.5); NRMS, MNB and NMAE were lower than 22%, 4% and 18%, respectively (Tables 4.3 and 4.4). The high turbidity of the two lakes guaranteed

that the SAMO-LUT method would be applicable to the reflectance at NIR-red wavelength. However, the accuracy of the estimates for these two lakes was noticeably lower than that for Lake Dianchi. This was because the SAMO-LUT was calibrated by the SIOPs of lake Dianchi, which likely differed from those for lakes Kasumigaura and Erhai.

Table 4.3 Performance of the SAMO-LUT, Simple 3-band Model and OC4E for the estimation of Chl-*a* in Lake Kasumigaura, Japan.

	RMSE (mg m^{-3})	NRMS(%)	MNB(%)	NMAE(%)	R^2	Slope
Lake Kasumigaura, Japan (N=46)						
SAMO-LUT	13.26	18.4	-3.9	16.2	0.64	0.511
Simple 3-band model	14.51	23.0	18.4	23.3	0.63	0.551
OC4E	59.60	13.1	-78.8	78.8	0.50	-0.143

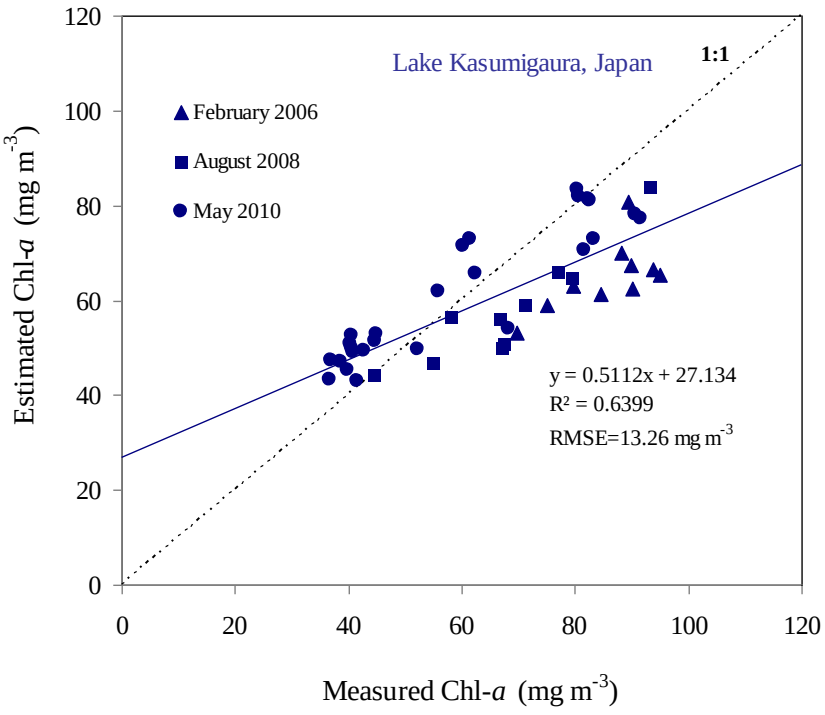

Fig. 4.4 Comparison of the measured and estimated Chl-*a* by the SAMO-LUT for Lake Kasumigaura, Japan.

Table 4.4 Performance of the SAMO-LUT, Simple 3-band Model and OC4E for the estimation of Chl-*a* in Lake Erhai, China.

	RMSE (mg m^{-3})	NRMS(%)	MNB(%)	NMAE(%)	R^2	Slope
Lake Erhai, China (N=42)						
SAMO-LUT	3.88	21.2	-2.8	17.1	0.71	1.025
Simple 3-band model	5.67	30.3	-19.4	26.6	0.74	1.306
OC4E	12.28	18.4	-50.1	50.3	0.01	0.047

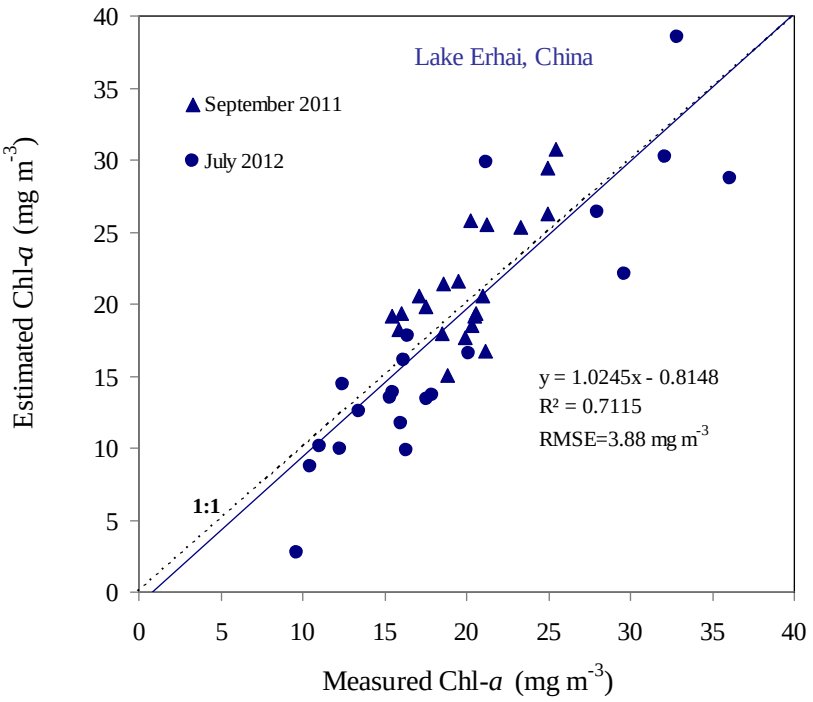

Fig. 4.5 Comparison of the measured and estimated Chl-*a* by the SAMO-LUT for Lake Erhai, China.

Fig. 4.6 shows the comparison between the measured and estimated Chl-*a* by SAMO-LUT for Lake Suwa. Compared with Lakes Kasumigaura and Erhai, the accuracy of SAMO-LUT was further reduced, with increasing NRMS, MNB and NMAE values of 23.9%, 8.3% and 19.8%, respectively (Table 4.5). Moreover, the correlation between measured and estimated Chl-*a* was statistically insignificant with very low R^2, which was probably due to the small dynamic range of Chl-*a*. It should be noted that the R^2 is shown here just for reference, but not for accuracy assessment. The reduced performance of SAMO-LUT in Lake Suwa was due to the decreased signal-to-noise ratio

(SNR) at the NIR-red spectral regions owing to the low concentrations of phytoplankton and TSS (Table 4.1).

Table 4.5 Performance of the SAMO-LUT, Simple 3-band Model and OC4E for the estimation of Chl-*a* in Lake Suwa, Japan

	RMSE (mg m^{-3})	NRMS(%)	MNB(%)	NMAE(%)	R^2	Slope
Lake Suwa, Japan (N=8)						
SAMO-LUT	2.77	23.9	8.3	19.8	0.0004	-0.078
Simple 3-band model	4.72	32.2	-31.3	33.5	0.0007	0.147
OC4E	1.73	15.6	-1.0	12.2	0.0033	0.151

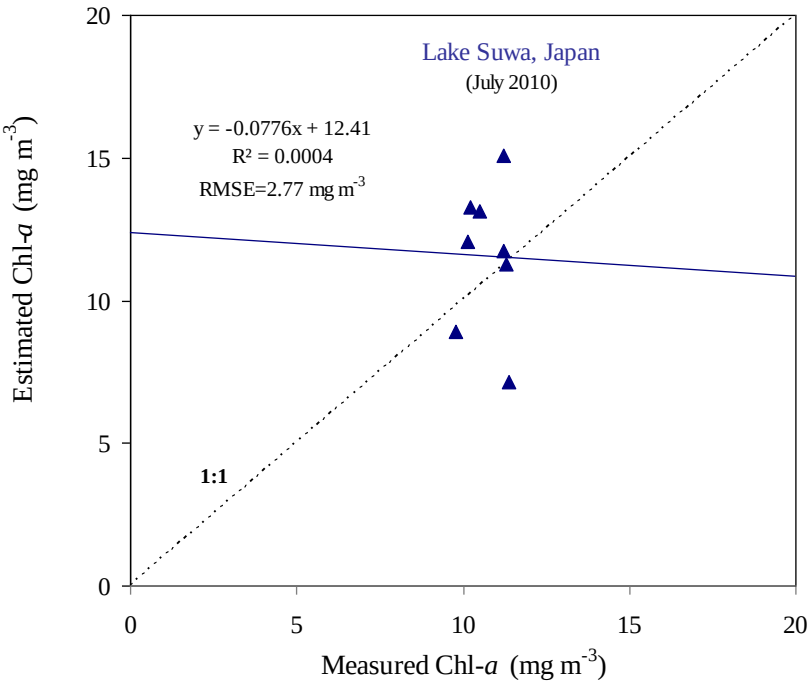

Fig. 4.6 Comparison of the measured and estimated Chl-*a* by the SAMO-LUT for Lake Suwa, Japan

Fig. 4.7 shows the comparison between the measured and estimated Chl-*a* in Lake Biwa by the SAMO-LUT method. Results showed that the SAMO-LUT yielded very large errors in this lake (see Table 4.6, RMSE=5.9 mg m^{-3}, NRMS=141.5%, and MNB=221.8%). The very weak correlation between the estimated and measured Chl-*a* (R^2=0.07) indicated that the Chl-*a* estimated by SAMO-LUT could not explain actual Chl-*a* variation in Lake Biwa. This was because the concentrations of

water constituents in the Lake Biwa were very low, and thus could not provide enough SNR for water-leaving reflectances at NIR-red spectral regions. This was despite the fact that, in theory, the SAMO-LUT can be used for such low concentrations (Yang et al. 2011a).

Table 4.6 Performance of the SAMO-LUT, Simple 3-band Model and OC4E for the estimation of Chl-*a* in Lake Suwa, Japan

	RMSE (mg m^{-3})	NRMS(%)	MNB(%)	NMAE(%)	R^2	Slope
Lake Biwa, Japan (N=10)						
SAMO-LUT	5.90	141.5	221.8	221.8	0.07	1.953
Simple 3-band model	20.84	276.83	-917.58	917.58	0.11	-4.39
OC4E	0.30	12.3	-1.1	9.4	0.54	0.592

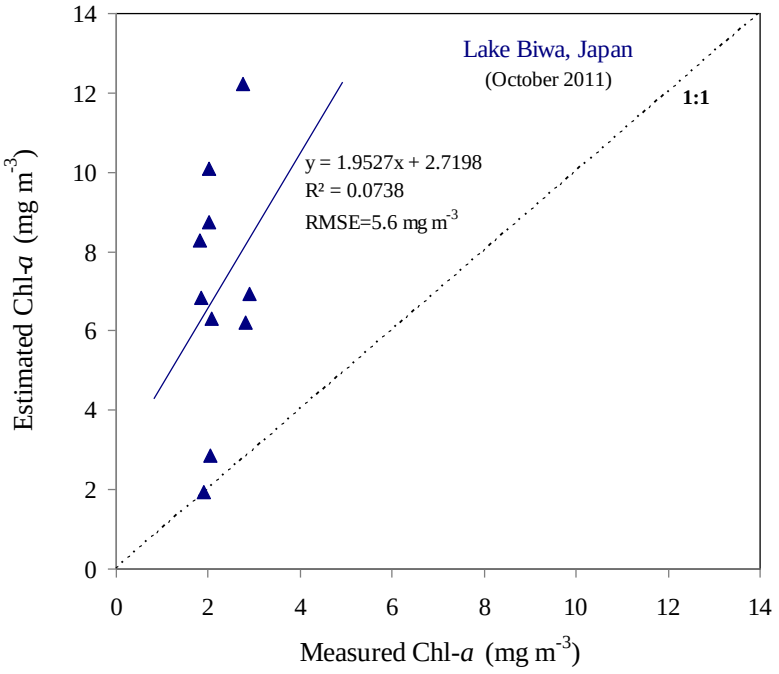

Fig. 4.7 Comparison of the measured and estimated Chl-*a* by the SAMO-LUT for Lake Biwa, Japan

4.3.3 Performances of the Simple 3-band Model

The evaluation indexes for the Chl-*a* estimations using the Simple 3-band Model are also summarized in Tables 4.2-4.6. It can be seen that the Simple 3-band Model yielded remarkably

lower accuracy for Lake Dianchi compared with the SAMO-LUT algorithm, with RMSE, NRMS, MNB and NMAE increased from 7.39 mg/m^3, 11.3%, 1.3% and 6.9% to 8.81 mg/m^3, 13.73%, 3.08% and 8.04%, respectively (Table 4.2). For the other two turbid lakes, Kasumigaura and Erhai, the SAMO-LUT also significantly outperformed the Simple 3-band Model, with much lower values of NRMS, MNB and NAME (Tables 4.3 and 4.4). These results indicate that the iteration process based on the look-up tables used in the SAMO-LUT method can effectively improve Chl-*a* estimation for turbid lakes with adequately high SNR in the NIR-red spectral regions. For Lake Suwa, a water body with relatively low turbidity, the Simple 3-band Model yielded very low accuracy, with values of NRMS, MNB and NAME larger than 30% (Table 4.5). Especially in the case of Lake Biwa, a body of water with fairly low loads of suspended solids, the Simple 3-band Model generated negative estimations for Chl-*a*, and consequently very large values of RMSE, NRMS, MNB and NMAE (over 300%, as shown in Table 4.6). It demonstrated again that the NIR-red bands-based methods do not work well for relatively clear waters.

4.3.4 Application of a Blue-Green algorithm to clear waters

Since the SAMO-LUT and the Simple 3-band Model both yielded high errors in estimating Chl-*a* in relatively clear lakes like Suwa and Biwa, we tested a blue-green algorithm (OC4E, O'Reilly et al. 1998) for these two lakes. The OC4E has been widely used for estimating Chl-*a* in case-1 waters using water-leaving reflectances at blue-green spectral regions (i.e., 443, 490, 520, and 565 nm).

Fig. 4.8 shows the comparison between the measured and estimated Chl-*a* by the OC4E for Lakes Suwa and Biwa. In the case of Lake Suwa, the OC4E performed slightly better than the SAMO-LUT (Table 4.5, RMSE: 1.7 mg m^{-3} vs. 2.8 mg m^{-3}; NRMS: 15.6% vs. 23.9%; MNB -1.0% vs. 8.3%). Neither SAMO-LUT nor OC4E showed a significant correlation between the estimated and measured Chl-*a* in the lake. This was because of the small Chl-*a* variation among the sites (Table 4.1, CV= 5.9%). In contrast, the OC4E algorithm promised an accurate Chl-*a* estimation in

Lake Biwa with an RMSE of 0.3 mg m^{-3} and NRMS of 12.3%, as well as a small bias in the estimation (MNB= -1.1%, Table 4.6). The OC4E also explained 54% of the Chl-*a* variation in Lake Biwa even though the data had a narrow dynamic range (Chl-*a* ranging from 1.81–2.90 mg m^{-3}). This was likely because the effects of NAP and CDOM at the blue-green spectral regions were negligible in Lake Biwa due to the lower concentrations of NAP and CDOM (Table 4.1). We also tested the performance of OC4E for turbid waters (i.e., Lakes Dianchi, Kasumigaura and Erhai). The accuracy evaluation indexes are summarized in Tables 4.2-4.4. The OC4E not only produced a large underestimation (MNB ranging from -50.1% to -81.3%), but also could not present Chl-*a* variation for these lakes (very low determination coefficients except for Lake Kasumigaura, which showed a higher negative correlation).

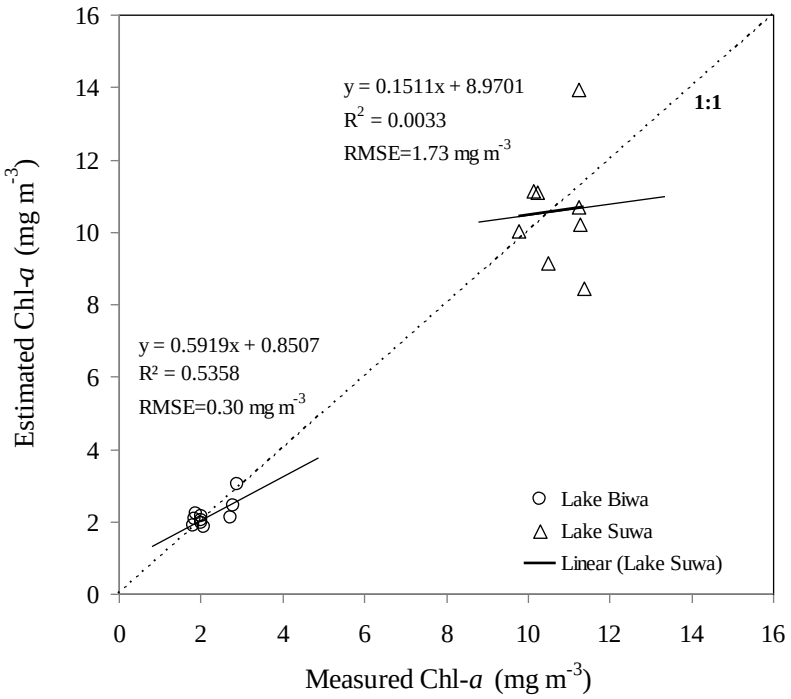

Fig. 4.8 Comparison of the measured and estimated Chl-*a* by the OC4E algorithm for Lakes Suwa and Biwa, Japan

The above results were not surprising. Previous studies have pointed out that water-leaving reflectances at blue-green spectral regions are influenced not only by phytoplankton but also by

NAP and CDOM, and thus the OC4E fails in turbid productive waters (Gilerson et al. 2010, Gitelson et al. 2008, Gurlin et al. 2011, Moses et al. 2009, Yang et al. 2011a). To reduce the effects of NAP and CDOM for Chl-*a* estimation, these previous studies suggested the use of water-leaving reflectances at the NIR-red spectral regions. The SAMO-LUT was specifically designed based on these spectral regions (Yang et al. 2011a). The high concentrations of TSS in these three lakes improved SNR in the NIR-red spectral regions, and thus promised accurate estimations for Chl-*a*.

4.4 Discussion

One advantage of the SAMO-LUT algorithm is that the model calibration process requires a minimum of field data (Yang et al. 2011). In the SAMO-LUT, only the SIOPs of water constituents must be collected from the target water. After that, a comprehensive synthetic dataset is generated based on the obtained SIOPs and a bio-optical model, and the LUTs are constructed to save the coefficients of water constituent estimation models (e.g., Chl-*a* estimation models). Yang et al. (2011a) suggested that the LUTs should be reconstructed if the SAMO-LUT algorithm was applied to a water body with different SIOPs. In practice, the SIOPs do change according to the dominant phytoplankton species in water bodies. For example, the dominant phytoplankton species changed seasonally in Lake Kasumigaura (Fukushima et al. 2010). Generally, cyanobacteria are the dominant species during the summer season, while Bacillariphyceae is dominant from autumn to spring. Therefore, the SIOPs changed accordingly (Yang et al. 2011b). The dominant phytoplankton species in Lakes Erhai and Dianchi were cyanobacteria during the field surveys (Wang et al. 2011b).

In this study, the SIOPs collected from Lake Dianchi in July 2009 were used to construct LUTs, which were then applied to other periods of Lake Dianchi and other lakes without any adjustment. The results in Section 4.2 showed that the SAMO-LUT algorithm was able to achieve acceptable accuracy for all tested cases, with NMAE less than 20%, except for Lake Biwa. These findings indicate that not only did the variation of SIOPs not affect the performance of the SAMO-LUT

dramatically, but also that the use of a comprehensive synthetic dataset for model calibration can prevent the uncertainty in estimation models caused by sampling bias. The results thus present a strong case for the use of the SAMO-LUT algorithm as an operational method for estimating Chl-*a* from remote sensing data. Moreover, the best performance of the SAMO-LUT algorithm in Lake Dianchi and its slightly degraded performance in Lake Kasumigaura in February 2006 suggest that the algorithm has the potential to provide more accurate Chl-*a* estimation if the SIOPs of the target water were available.

I do not believe, however, that the failure of the SAMO-LUT algorithm in the cases of Lakes Biwa and Suwa were caused by the differences in SIOPs between them and Lake Dianchi. In the other words, the performance of the SAMO-LUT algorithm would not have been satisfactorily improved had SIOPs been collected from these two lakes. From Fig. 4.2 it can be seen that the R_{rs} in the red-NIR spectral region of Lakes Biwa and Suwa are much lower than those of the other three lakes. Weak signals from water bodies with too low TSS will be hidden by environmental noise, and thus cannot provide enough information for estimating water constituents. Therefore, the SNR at selected red-NIR bands used in the SAMO-LUT algorithm are not applicable to relatively clear waters. Alternatively, for clear waters with negligible effects of NAP and CDOM, a blue-green algorithm (e.g., OC4E) can be used to replace the NIR-red algorithms (e.g., Lakes Biwa and Suwa) because the signals in blue-green spectral regions remain strong even for this kind of water. A classification method for selecting an appropriate algorithm in the case of different types of water is needed.

On the other hand, the SAMO-LUT algorithm was developed based on the bandwidths of MERIS. The most important prerequisite is the band around 708 nm, as used in the three-band index. Therefore, it can be directly applied to water-color sensors with configurations similar to MERIS, such as the Ocean and Land Colour Instrument (OLCI, Donlon et al. 2012), the Hyperspectral Infrared Imager (HyspIRI, Devred et al. 2013) or the Airborne Imaging Spectrometer for Applications (AISA, Moses et al. 2012). Extension of the SAMO-LUT method to more satellite

sensors without the 708 nm band, such as the Moderate Resolution Imaging Spectroradiometer (MODIS), and the Sea-viewing Wide Field-of-view Sensor (SeaWiFS), will be carried out in the future studies.

Chapter 5 General conclusions

5.1 Summary

Lake Erhai is located in Yunnan Province, China, and is the second largest lake in southwestern China with water surface area of 249 km^2, mean depth of 10.2 m, and maximum of 20.7 m. It plays an important role as a drinking water source for the local people. In recent decades, Lake Erhai has got into the trouble of eutrophication and cyanobacterial blooms. The lake is currently defined as the preliminary stage of eutrophic states. Due to the sensitive variation in water quality, and the extensive representative data, Lake Erhai is regarded as a representative case for researching eutrophication progress and occurrence of water blooms.

Generally, nitrogen and phosphorus nutrients are the important factors leading to eutrophication process and occurrence of cyanobacterial blooms. "TN/TP rule" indicates that lower TN/TP favors dominance by cyanobacteria, and it is the most disputed due to the divergent results. With the discovery of *mcy* gene cluster, precise molecular detection techniques (e.g. real-time PCR) can provide insights into the dynamics of toxic cyanobacteria and environmental regulation of toxins in the field from the point of cyanobacterium itself (e.g. genotypes diversity and regulation of gene expression). Consequently, it was proposed in this study that variation of harmful cyanobacterial abundance and MC concentrations associated with *mcyBA*1 genotypes, NtcA gene, N and P nutrients during the blooms seasons. On the other hand, dynamics and biological features of other harmful cyanobacteria were researched by polyphasic approach including phytoplankton survey and counting, real-time PCR method. Furthermore, satellite remote sensing method, which can provide the information spatially and temporally in a larger scale, was also used to monitor the dynamics of cyanobacterial blooms by Chl-*a* index.

5.1.1 Variations of *Microcystis* abundance and MC concentrations coupling with N and P nutrients, *mcyBA* and NtcA genes

Based on the investigation from the sixteen sampling sites of Lake Erhai during 2010, MC-LR and MC-RR were main variants of microcystins in the lake. The concentrations of Chl-*a* and MC and abundances of total *Microcystis* and toxic *Microcystis* were shown to be positively correlated with WT and TP, while negatively with NO_3-N, TN/Chl-*a* and TN/TP, but not correlated with NH_4-N. The relationship between cyanobacterial blooms and TN/TP shown in this study suggested that the "TN/TP rule" could be partially applied to explain the correlation between the cyanobacterial blooms with nutrients N and P only within a certain nutrient level. The further research in details indicated that variations of MC concentrations, *Microcystis* toxicity and toxic *Microcystis* abundance in Lake Erhai associated with *mcyBA*1 genotypes, NtcA gene, nitrogen, and phosphorus nutrients during the blooms seasons. So, it is speculated that N and P nutrients, genotype of *mcy* gene, and NtcA gene have together to affect the dynamics of *Microcystis* and MCs in Lake Erhai.

5.1.2 Dynamics and biological characterization of odor-producing cyanobacteria *Tychonema bourrellyi* using the polyphasic character approach

In this study, *T. bourrellyi* has been found firstly in Lake Erhai. It is only found in several lake of Europe before then. Several strains of *T. bourrellyi* have been successfully isolated from the lake. This species was listed as the potential harmful cyanobacteria influencing the drinking water safety around Lake Erhai due to its volatile substances. However, the dynamics and biological information of this species were too limited. The polyphasic approach was used to reveal those features. The morphological characters of trichomes, such as solitary, reddish-brown or blue-green, obvious keritomized content, and 7.2–10.7 μm cell width, were observed by the microscopy method. Although some intermediate characters in morphological and physiological characters, they were planktonic, and gathered tightly in a cluster in the NJ, ML, and Bayesian trees with the strains of *T. bourrellyi* and *T. tenue*. The comparative analysis on 16S rDNA sequences and planktonic habitat of

these strains helped us to identify them as *Tychonema bourrellyi* under subfamily Phormidioideae. GC-MS analysis indicated that three strains of *T. bourrellyi* isolated from Lake Erhai produced both β-Ionone and geosmin. It was confirmed by the HPLC and *mcy* gene (both *mcyA* and *mcyB*) approach that no strain produced MCs. Furthermore, the dynamics of cell abundance at 12 sampling sites of Lake Erhai were shown as an average of 3×10^4 cells L^{-1} from 2009 to 2010. The obvious peaks occurred in July and August every year. Furthermore, the cell abundance of *Tychonema* was far inferior to *Microcystis* due to its low anoxygenic photosynthetic capacity and its relative weak strategy for uptake of P concentrations in Lake Erhai.

5.1.3 Application of remote sensing algorithm for monitoring cyanobacterial blooms of Lake Erhai

The performance of the Semi-Analytical Model Optimizing and Look-Up Table (SAMO-LUT), a recently developed algorithm for estimating Chl-*a* in inland waters, was evaluated using an extensive dataset collected from five Asian lakes in which the concentrations of total suspended solids varied from 0.77 to 55.00 g m^{-3}. Results showed that the SAMO-LUT algorithm was able to provide acceptably accurate estimates for all cases but one, with normalized mean absolute error (NMAE) less than 20% (the exception was Lake Biwa). This was the case even though the SIOPs from Lake Dianchi were used for all lakes. These findings indicate that a variation in SIOPs does not significantly affect the performance of the SAMO-LUT algorithm, and thus it has the potential to be an operational method for estimating Chl-*a* from remote sensing data. The failure of the SAMO-LUT algorithm in the case of Lake Biwa (NMAE of 221.8%) was mainly to the lack of sufficient signals from water-leaving reflectances at the NIR-red spectral regions, due to very low concentrations of total suspended solids (TSS) in the water, rather than to the use of SIOPs from Lake Dianchi in the algorithm. To overcome this problem, a blue-green algorithm such as the OC4E could be used to replace the SAMO-LUT algorithm for estimating Chl-*a* concentration in Lake

Biwa, which could reduce the NMAE to 9.4%. It is therefore necessary to develop a classification method in the future for selecting the appropriate algorithm for different cases of waters.

Overall, a comprehensive study for HCBs needs to combine all kinds of analysis methods and monitoring tools. This study attempts to use a combined examination method to investigate dynamics, biological and ecological features of HCBs in the lake from different perspectives. The above results only presented the partial contents on HCBs. Other contents of HCBs still need to be further studied in the future

5.2 The following research in the future

5.2.1 NtcA coupling with genotypes of *mcyBA*1 and N nutrients affect MC concentrations and cell abundance of toxic *Microcystis* in Lake Erhai

NtcA is a global transcription regulator for nitrogen control in cyanobacteria (Ginn et al. 2010). Under nitrogen stress conditions, NtcA can overexpress to cause the increase of MC concentrations and *Microcystis* abundance. While TN increases, NtcA can down-regulate its expression to decrease MC concentrations and *Microcystis* abundance. Consequently, nitrogen levels affect MC production rates by the NtcA approach. In my dissertation, I guess that NtcA coupling with nitrogen may present the expression of *mcy* genes to affect MC concentrations during cyanobacterial blooms. However, due to the absence of the direct evidence, the more experiments and the *in situ* sampling need to be verified.

5.2.2 Monitoring the abundance of geosmin/β-Ionone-producing *T. bourrellyi* and concentrations of volatile substance in Lake Erhai

The strains of *T. bourrellyi* from Lake Erhai produce both geosmin and β-Ionone. But the abundance of odor-producing cells and the concentrations of geosmin and β-Ionone in Lake Erhai are not revealed. So research on the abundance of odor-producing cells and concentration of volatile

substance in Lake Erhai are needed. qPCR method with *geo* gene, GC-MS analysis, and the *in situ* sampling will be used.

5.2.3 A hybrid algorithm for operationally estimating the Chl-*a* concentrations in Lake Erhai

In my dissertation, the SAMO-LUT algorithm was able to provide acceptably accurate estimates for the most case, but in clear water, such as Lake Biwa and several sites with clear water in Lake Erhai and Lake Suwa, the algorithm showed poor performance. Their reflectance spectra demonstrated the water-leaving radiances at the longest wavelength of 754 nm were too small due to low concentrations of water constituents. The strongly absorption of water appeared at this wavelength. The reflectance value at the longest wavelength of 754 nm used in the SAMO-LUT algorithm is too small so that the wavelength is not used by the SAMO-LUT algorithm. However, a blue-green algorithm such as the OC4E can get well performance in this case.

The water quality in a lake is not homogeneous. In some areas, the water is very clear, while in other areas, the water is turbid. Therefore, when using a single algorithm at all areas in the lake, all samples cannot conformably have a good performance. There are always poor performances at several sites. Consequently, there is a well suggestion that the appropriate remote sensing algorithm should be chosen to evaluate water Chl-*a* concentrations based on the case of water quality condition and the optical properties at different sampling sites. For example, the OC4E algorithm, RN2-Gil10 algorithm (a two-band index-based red-near infrared algorithm), and SAMO-LUT algorithm are chosen for clear water, turbid water, and highly turbid water, respectively. So a hybrid algorithm for operationally estimating the Chl-*a* concentration is proposed in the following research.

The first, before using the algorithm, the trophic states and optical water type of the lake must be evaluated. The MCI (maximum chlorophyll index), which can be easily calculated from satellite data, is used to switch the three algorithms. Then, the suitable algorithm is selected for monitoring Chl-*a* in lakes according to the estimated results. For example, the OC4Ev4, the RN2-Gil10, and the

SAMO-LUT algorithms are selected for clear, moderate-turbidity and high-turbidity waters, respectively, to compose the hybrid algorithm. The hybrid algorithm should be superior to all of the single algorithms tested when considering the entire observed range of optical properties with widely varying trophic conditions without the requirement of reparameterization.

References

Allen M.M. (1984) Cyanobacterial cell inclusions. *Annual Review of Microbiology*, 38: 1–25.

Ammenberg P., Flink P., Lindell T. (2002) Bio-optical modelling combined with remote sensing to assess water quality. *International Journal of Remote Sensing*, 23: 1621–1638.

Anagnostidis K., Komárek J. (1988) Modern approach to the classification system of cyanophytes 3 – Oscillatoriales. *Algological Studies*, 50–53: 327–472.

Arp G., Bissett A., Brinkmann N., Cousin S., de Beer D., Friedl T., Mohr K.I.,. Neu T.R, Reimer A., Shiraishi F., Stackebrandt E., Zippel B. (2010) Tufa-forming biofilms of German karstwater streams: Microorganisms, exopolymers, hydrochemistry and calcification. *Geological Society, London, Special Publications*, 336(1): 83–118.

Berglind L., Holtan H., Skulberg O.M. (1983) Case studies on off-flavours in some Norwegian lakes. *Water Science and Technology*, 15: 199–209.

Brookes J.D., Ganf G.G. (2001) Variations in the buoyancy response of *Microcystis aeruginosa* to nitrogen, phosphorus and light. *Journal of Plankton Research*, 23: 1399–1411.

Bourke A.T.C., Hawes R.B., Neilson A., Stallman N.D. (1983) An outbreak of hepato-enteritis (the Palm Island mystery disease) possibly caused by algal intoxication. *Toxicon* (Suppl.), 3: 45–48.

Brando V.E., Dekker A.G. (2003) Satellite hyperspectral remote sensing for estimating estuarine and coastal water quality. *IEEE Transactions on Geoscience and Remote Sensing*, 41, 1378–1387.

Bresciani M., Adamo M., de Carolis G., Matta E., Pasquariello G., Vaičiūtė D., Giardino C. (2014) Monitoring blooms and surface accumulation of cyanobacteria in the Curonian Lagoon by combining MERIS and ASAR data. *Remote Sensing of Environment*, 146: 124–135.

Bresciani M., Bolpagni R., Laini A., Matta E., Bartoli M., Giardino C. (2013) Multitemporal analysis of algal blooms with MERIS images in a deep meromictic lake. *European Journal of Remote Sensing*, 46: 445–458.

Bulgakov N.G., Levich A.P. (1999) The nitrogen: phosphorus ratio as a factor regulating phytoplankton community structure. *Archiv für Hydrobiologie*, 146: 3–22.

Camacho A., Garcia-Pichel F., Vicente E., Castenholz R.W. (1996) Adaptation to sulfide and to the underwater light field in three cyanobacterial isolates from Lake Arcas (Spain). *FEMS microbiology ecology*, 21(4): 293–301.

Campbell G., Phinn S. (2010) An assessment of the accuracy and precision of water quality parameters retrieved with the Matrix Inversion Method. *Limnology and Oceanography*: *Methods*, 8, 16–29.

Carmichael W.W., Beasley V., Bunner D.L., Eloff J.N., Falconer I., Gorham P., Harada K.I., Krishnamurthy T.L., Yu M.J., Moore R.E., Rinehart K.L., Runnegar M., Skulberg O.M., Watanabe M. (1988) Naming of cyclic heptapeptide toxins of cyanobacteria (blue-green algae). *Toxicon*, 26: 971–973.

Carmichael W.W. (2001) Health effects of toxin-producing cyanobacteria: "The CyanoHABs". *Human and Ecological Risk Assessment*, 7(5): 1393–1407.

Carmichael W.W. (2008) A world overview – One-hundred-twenty-seven years of research on toxic cyanobacteria –Where do we go from here? In: Hudnell, H.K. (eds.) Cyanobacterial harmful algal blooms: state of the science and research needs. *Advances in Experimental Medicine & Biology*, 619: 105–125. Springer. pp. 500.

Casmatta D.A., Johansen J.R., Vis M.L. Broadwater S.T. (2005) Molecular and morphological characterization of ten polar and near-polar strains within the Oscillatoriales (Cyanobacteria). *Journal of Phycology*, 41: 421–438.

CGER (2010) Lake Kasumigaura Database. National Institute for Environmental Studies: Tsukuba, Japan.

Chen Y.W., Gao X.Y., Chen W.M., Qin B.Q. (1999) Growth characters and pure culture of *Microcystis* from Taihu Lake. *Journal of Lake Sciences*, 11(4): 351–356. (in Chinese).

Chomko R.M., Gordon H.R. (1998) Atmospheric correction of ocean color imagery: Use of the junge power-law aerosol size distribution with variable refractive index to handle aerosol absorption. *Applied Optics*, 27: 5560–5572.

Chorus I., Niesel V., Fastner J., Wiedner C., Nixdorf B., Lindenschmidt K.E. (2001) Environmental factors of MC levels in waterbodies. In: Chorus I (eds.) *Cyanotoxins: Occurrence, Causes, Consequences*. Springer, Berlin, pp. 159–177.

Codd G.A., Lindsay J., Young F.M., Morrison L.F., Metcalf J.S. (2005) Harmful cyanobacteria: from mass mortalities to management measures. In: Huisman J., Matthijs H.C.P., Visser P.M. (eds.) *Harmful cyanobacteria, Aquatic ecology series*. Springer, Dordrecht, pp. 1–24, 242.

Dall'Olmo G., Gitelson A.A. (2005) Effect of bio-optical parameter variability on the remote estimation of chlorophyll-*a* concentration in turbid productive waters: Experimental results. *Applied Optics*, 44: 412–422.

Dall'Olmo G., Gitelson A.A., Rundquist D.C. (2003) Towards a unified approach for remote estimation of chlorophyll-*a* in both terrestrial vegetation and turbid productive waters. *Geophysical Research Letters*, 30 (18): 1938.

Dekker A.G., Malthus T.J., Goddijn L.M. (1992) Monitoring cyanobacteria in eutrophic waters using airborne imaging spectroscopy and multispectral remote sensing systems. *Proceedings of 6th Australasian remote sensing conference*, New Zealand. 1. pp. 204–214.

Dekker A.G., Peters S.W.M. (1993) The use of the Thematic Mapper for the analysis of eutrophic lakes: A case study in the Netherlands. *International Journal of Remote Sensing*, 14(5): 799–821.

Dekker A.G., Zamurović-Nenad Ž., Hoogenboom H.J., Peters, S.W.M. (1996) Remote sensing, ecological water quality modelling and *in situ* measurements: a case study in shallow lakes. *Hydrological Sciences Journal*, 41(4): 531–547.

Devred E., Turpie K. R., Moses W., Klemas V.V., Moisan T., Babin M., Toro-Farmer G., Forget M.H., Jo Y.H. (2013) Future retrievals of water column bio-optical properties using the hyperspectral infrared imager (HyspIRI). *Remote Sensing*, 5: 6812–6837.

Dittmann E., Neilan B., Erhard M., Döhren H.V., Börner T. (1997) Insertional mutagenesis of a peptide synthetase gene that is responsible for hepatotoxin production in the cyanobacterium *Microcystis aeruginosa* PCC 7806. *Molecular Microbiology*, 26(4): 779–787.

Dittmann E., Fewer D.P., Neilan B.A. (2013) Cyanobacterial toxins: biosynthetic routes and evolutionary roots. *FEMS Microbiology Reviews*, 37(1): 23–43.

Doeffer R., Schiller H. (2007) The MERIS case 2 water algorithm. *International Journal of Remote Sensing*, 28: 517–535.

Dong Y.X. (2003) The relationship between distribution of algae and eutrophication of Erhai Lake. In: Bai J.K., Sang Y.M., Kui L.X. (ed) *Dali Erhai Lake scientific reseach*. The Ethnic Publishing House, Beijing, pp. 398–401. (in Chinese).

Donlon C., Berruti B., Buongiorno A., Ferreira M.H., Féménias P., Frerick J., Goryl P., Klein U., Laur H., Mavrocordatos C., Nieke J., Rebhan H., Seitz B., Stroede J., Sciarra R. (2012) The global monitoring for environment and security (GMES) sentinel-3 mission. *Remote Sensing of Environment*, 120: 37–57.

Downing T.G., Meyer C., Gehringer M.M., van de Venter M. (2005) Microcystin content of *Microcystis aeruginosa* is modulated by nitrogen uptake rate relative to specific growth rate or carbon fixation rate. *Environmental Toxicology*, 20: 257–262.

Doxaran D., Froidefond J.M., Castaing P. (2002) A reflectance band ratio used to estimate suspended matter concentrations in sediment-dominant coastal waters. *International Journal of Remote Sensing*, 23: 5079–5085.

Du B.H. (1992) Study on eutrophication of Erhai Lake. *Journal of Lake Sciences*, 4(2): 86–92. (in Chinese).

El-Alem A., Cholmani K., Laurion I., Eo-Adlouni S. (2012) Comparative analysis of four models to estimate chlorophyll-*a* concentration in case-2 waters using MODerate rresolution imaging spectroradiometer (MODIS) imagery. *Remote Sensing*, 4: 2373–2400.

Falconer I.R., Beresford A.M., Runnegar M.T. (1983) Evidence of liver damage by toxin from a bloom of the blue-green alga, *Microcystis aeruginosa*. *Medical Journal of Australia*, 1: 511–514.

Flores E., Herrero A. (2005) Nitrogen assimilation and nitrogen control in cyanobacteria. *Biochemical Society Transactions*, 33: 164–167.

Forsberg C., Ryding, S.O. (1980) Eutrophication parameters and trophic state indices in 30 Swedish waste-receiving lakes. *Archiv für Hydrobiologie*, 89: 189–207.

Fukushima T., Kawamura S., Seki T., Onda Y., Imai A., Matsushige K. (2005) Why has Lake Kasumigaura become turbid? In Verhandlungen. *Verhandlungen Internationale Vereinigung für Theoretische und Angewandte Limnologie*, 29: 732–737.

Fukushima T., Park J., Imai A., Matsushige K. (1996) Dissolved organic carbon in a eutrophic lakes; dynamics, biodegradability and origin. *Aquatic Sciences*, 58: 139–157.

Fukushima T., Kamiya K., Onda Y., Imai A., Matsushige K. (2010) Long-term changes in lake sediments and their infl uences on lake water quality in Japanese shallow lakes. *Fundamental and Applied Limnology/Archiv für Hydrobiologie*, 177(3): 177–188.

Galat D.L., Verdin J.P. (1989) Patchiness, collapse and succession of a cyanobacterial bloom evaluated by synoptic sampling and remote sensing. *Journal of Plankton Reseach*, 11: 925–948.

Ganf G.G., Heaney S.I., Corry J. (1991) Light absorption and pigment content in natural populations and cultures of a non-gas vacuolate cyanobacterium *Oscillatoria bourrellyi* (= *Tychomema bourrellyi*). *Journal of Plankton Research*, 13(5): 1101–1121.

Gao L., Zhou J.M., Yang H., Chen J. (2005) Phosphorus fractions in sediment profiles and their potential contributions to eutrophication in Dianchi Lake. *Environmental Geology*, 48(7): 835–844.

Geitler L. (1932) Cyanophyceae. In: Rabenhorst L. (eds.) *Kryptogamen Flora von Deutschland, Osterreich und der Schweiz 14*. Akademische Verlagsgesellschaft, Leipzig, pp. 130–159. (in German).

Giardino C., Brando V.E., Dekker A.G., Strömbeck N., Candiani G. (2007) Assessment of water quality in Lake Garda (Italy) using Hyperion. *Remote Sensing of Environment*, 109: 183–195.

Gilerson A.A., Gitelson A.A., Zhou J., Gurlin D., Moses W., Ioannou I., Ahmed S.A. (2010) Algorithms for remote estimation of chlorophyll-*a* in coastal and inland waters using red and near infrared bands. *Optical Express*, 18: 24109–24125.

Gin K.Y.H., Koh S.T., Lin I.I. (2003) Spectral irradiance profile of suspended marine clay for the estimation of suspended sediment concentration in tropical waters. *International Journal of Remote Sensing*, 24: 3235–3245.

Gin K.Y.H., Oh S.T., Lin I.I. (2002) Study of the effect of suspended marine clay on the reflectance spectra of phytoplankton. *International Journal of Remote Sensing*, 23: 2163–2178.

Ginn H.P., Pearson L.A., Neilan B.A. (2010) NtcA from *Microcystis aeruginosa* PCC 7806 is autoregulatory and binds to the microcystin promoter. *Applied and Environmental Microbiology*, 76: 4362−4368.

Gitelson A.A., Keydan G., Shishkin V. (1985) Inland waters quality assessment from satellite data in visible range of the spectrum. *Soviet Journal of Remote Sensing*, 6: 28−36.

Gitelson A.A. (1992) The peak near 700 nm on reflectance spectra of algae and water: Relationships of its magnitude and position with chlorophyll concentration. *International Journal of Remote Sensing*, 13: 3367−3373.

Gitelson A.A., Dall'Olmo G., Moses W., Rundquist D.C., Barrow T., Fisher T.R., Gurlin D., Holz J. (2008) A simple semi-analytical model for remote estimation of chlorophyll-*a* in turbid waters: Validation. *Remote Sensing of Environment*, 12: 3582−3593.

Gitelson A.A., Gurlin D., Moses W.J., Barrow T. (2009) A bio-optical algorithm for the remote estimation of the chlorophyll-*a* concentration in case 2 waters. *Environmental Research Letters* 4(4): 045003. (DOI: 10.1088/1748-9326/4/4/045003).

Gobler C.J., Davis T.W., Coyne K.J., Boyer G.L. (2007) Interactive influences of nutrient loading, zooplankton grazing, and microcystin synthetase gene expression on cyanobacterial bloom dynamics in a eutrophic New York lake. *Harmful Algae* 6(1): 119−133.

Gons H.J. (1999) Optical teledetection of chlorophyll a in turbid inland waters. *Environmental Science & Technology*, 33: 1127–1132.

Goodin D.G., Han L., Fraser R.N., Rundquist D.C., Stebbins W.A., Schalles J.F. (1993) Analysis of suspended solids in water using remotely sensed high resolution derivative spectra. *Photogrammetric Engineering and Remote Sensing*, 59: 505–510.

Gordon H.R., Morel A. (1983). Remote assessment of ocean color for interpretation of satellite visible imagery: A review. New York: Springer-Verlag. pp. 1–106.

Granéli E., Carlsson P., Olsson P., Sundström B., Granéli W., Lindahl O. (1989) From anoxia to fish poisoning: The last ten years of phytoplankton blooms in Swedish marine waters. In: Cosper E.M., Bricelj V.M., Carpenter E.J. (ed) *Novel phytoplankton blooms: causes and impacts of recurrent brown tides and other unusual blooms*. Springer, Berlin, pp. 407–427.

Guindon S., Gascuel O. (2003) A simple, fast, and accurate algorithm to estimate large phylogenies by maximum likelihood. *Systems Biology*, 52: 696–704.

Gupta S., Giddings M., Sheffer M. (2001) Cyanobacterial toxins in drinking water: A Canadian perspective. In: Chorus I. (eds.) *Cyanotoxins: Occurrence, Causes, Consequences*. Springer, Berlin, pp. 208–212.

Gurlin D., Gitelson A.A., Moses, W.J. (2011) Remote estimation of Chl-*a* concentration in turbid productive waters — Return to a simple two-band NIR-red model? *Remote Sensing of Environment*, 115: 3479–3490.

Hall T.A. (1999) BioEdit: A user-friendly biological sequence alignment editor and analysis program for Windows 95/98/NT. *Nucleic Acids Symposium Series*, 41: 95–98.

Hallegraeff G.M. (2003) Harmful algal blooms: A global overview. In: Hallegraeff G.M., Anderson D.M., Cembella A.D. (eds.) *Manual on harmful marine microalgae*, vol 11, 2nd edn. IOC-UNESCO. Paris, pp. 25–49.

Han L., Rundquist D.C., Liu L.L., Fraser R.N., Schalles J.F. (1994). The spectral responses of algal chlorophyll in water with varying levels of suspended sediment. *International Journal of Remote Sensing*, 15: 3707–3718.

Hašler P, Dvořák P., Johansen J.R, Kitner M., Ondřej V., Poulíčková A. (2012) Morphological and molecular study of epipelic filamentous genera *Phormidium*, *Microcoleus* and *Geitlerinema* (Oscillatoriales, Cyanophyta/ Cyanobacteria). *Fottea*, *Olomouc*, 12(2): 341–356.

Hastie C.J., Borthwick E.B., Morrison L.F., Codd G.A., Cohen P.T.W. (2005) Inhibition of several protein phosphatases by a non-covalently interacting microcystin and a novel cyanobacterial peptide, nostocyclin. *Biochimica et Biophysica Acta*, 1726: 187–193.

Hilborn E.D., Carmichael W.W., Soares R.M., Yuan M., Servaites J.C., Barton H.A., Azevedo S.M.F.O. (2007) Serologic evaluation of human microcystin exposure. *Environmental Toxicology*, 22(5): 459–463.

Hoffmann L., Komárek J. Kaštovský J. (2005) System of cyanoprokaryotes (cyanobacteria) – state in 2004. *Algological Studies*, 117: 95–115.

Hoge F.E., Lyon, P.E. (1996) Satellite retrieval of inherent optical properties by linear matrix inversion of oceanic radiance models: An analysis of model and radiance measurement errors. *Journal of Geophysical Research*, 101: 16631–16648.

Honkanen R.E., Dukelow M., Zwiller J., Moore R.E., Khatra B.S., Boynton A.L. (1991) Cyanobacterial nodularin is a potent inhibitor of type 1 and type 2A protein phosphatases. *Molecular Pharmacology*, 40: 577–583.

Hoogenboom H.J., Dekker A.G., De Haan, J.F. (1998). Retrieval of chlorophyll and suspended matter in inland waters from CASI data by matrix inversion. *Canadian Journal of Remote Sensing*, 24: 144–152.

Hu M.M., Li Y.H., Wang Y.C., Zhou H.D., Liu Y.D., Zhao G.F. (2013) Phytoplankton and bacterioplankton abundances and community dynamics in Lake Erhai. *Water Science and Technology*, 68(2): 348–356.

Hu H.J., Wei, Y.X. (2006) The freshwater algae of China: systematics, taxonomy, and ecology. Science Press, Beijing, pp. 125–126. (in Chinese).

Imai A., Matsushige K., Nagai T. (2003) Triharomethane formation potential of dissolved organic matter in a shallow eutrophic lake. *Water Research*, 37: 4284–4294.

IOCCG (2000) Remote sensing of ocean colour in coastal, and other optically-complex waters. In: Stuart V. (eds.), *Reports of the International Ocean-Colour Coordinating Group*. IOCCG, Dartmouth, Canada, pp. 1–139.

Jacobson L., Halmann M. (1982) Polyphosphate metabolism in the blue-green alga *Microcystis aeruginosa*. *Journal of Plankton Research*, 4: 481–488.

Jiang Y., Ji B., Wong R.N.S., Wong M.H. (2008) Statistical study on the effects of environmental factors on the growth and microcystins production of bloom-forming cyanobacteriums *Microcystis aeruginosa*. *Harmful Algae* 7(2): 127–136.

Jiang Y.G., Yu G.L., Chai W.B., Song G.F., Li R.H. (2013) Congruence between *mcy* based genetic type and microcystin composition within the populations of toxic *Microcystis* in a plateau lake, China. *Environmental Microbiology Reports*, 5(5): 637–647.

Jochimsen E.M., Carmichael W.W., An J., Cardo D.M., Cookson S.T., Holmes C.E.M., Antunes C.M.B., Melo F.D.A., Lyra T.M., Barreto V.S.T., Azevedo S.M.F.O., Jarvis W.R. (1998) Liver failure and death after exposure to microcystins at a hemodialysis center in Brazil. *New England Journal of Medicine*, 338(13): 873–878.

Joo H.H., Hidaka T., Tsuno H. (2009) Quantification of toxic *Microcystis* and evaluation of its dominance ratio in blooms using real-time PCR. *Environmental Science & Technology*, 43(3): 812–818.

Jüttner F., Watson S.B. (2007) Biochemical and ecological control of geosmin and 2-methylisoborneol in source waters. *Applied and Environmental Microbiology*, 73(14): 4395-4406.

Kaebernick M., Neilan B., Börner T., Dittmann E. (2000) Light and the transcriptional response of the microcystin biosynthesis gene cluster. *Applied and Environmental Microbiology*, 66: 3387–3392.

Kahru M., Leppänen J.M., Rud O. (1993) Cyanobacterial blooms cause heating of the sea surface. *Marine Ecology Progress Series*, 101: 1−7.

Kahru M., Leppänen J.M., Rud O., Savchuk, O.P. (2000) Canobacterial boolms in the Gulf of Finland triggered by saltwater inflow into the Baltic Sea. *Marine Ecology Process Series*, 207: 13–18.

Kameyama K., Sugiura N., Isoda H., Maekawa T. (2002) Effects of nitrate and phosphate concentration on production of microcystins by *Microcystis viridis* NIES-102. *Aquatic Ecosystem Health & Management*, 5(4): 443–449.

Kasai F., Kawachi M., Erata M., Mori F., Yumoto K., Sato M., Ishimoto, M. (2009) NIES-Collection, List of Strains, 8th edn. *The Japanese Journal of Phycology* (Suppl.), 57(1): 216–217.

Kaya K., Sano T. (2005) Bioactive compounds of freshwater cyanobacteria. In: Kasai F., Kaya K., Watanabe M.M. (eds.), *Algal culture collections and the environment*. Tokai University Press, Hadano, pp. 121–176.

Khorram S., Cheshire H., Geraci A., Rosa G. (1991) Water quality mapping of Augusta Bay, Italy from Landsat TM data. *International Journal of Remote Sensing*, 12(4): 803-808.

Kishino M., Ishizaka J., Saitoh S. I., Senga Y., Utashima M. (1997) Verification plan of ocean color and temperature scanner atmospheric correction and phytoplankton pigment by moored optical buoy system. *Journal of Geophysical Research*, 102: 17197–17207.

Komárek J., Albertano P. (1994) Cell structure of a planktic cyanoprokaryote, *Tychonema bourrellyi*. *Algological Studies*, 75, 157–166.

Komárek J., Anagnostidis K. (2005) Cyanoprokaryota–2. Teil: Oscillatoriales. Elsevier GmbH, Heifelberg, pp. 70.

Kong F.X., Gao G. (2005) Hypothesis on cyanobacteria bloom-forming mechanism in large shallow eutrophic lakes. *Acta Ecological Sinica*, 25(3): 589–595. (in Chinese).

Kotak B.G., Lam A.K.Y., Prepas E.E., Hrudey S.E. (2000) Role of chemical and physical variables in regulating microcystin-LR concentration in phytoplankton of eutrophic lakes. *Canadian Journal of Fisheries and Aquatic Sciences*, 57: 1584–1593.

Kuchinke C.P., Gordon H.R., Franz B.A. (2009a) Spectral optimization for constituent retrieval in case 2 waters I: Implementation and performance. *Remote Sensing of Environment*, 113: 571–587.

Kuchinke C.P., Gordon H.R., Harding L.W. Jr., Voss K.J. (2009b) Spectral optimization for constituent retrieval in case 2 waters II: Validation study in the Chesapeake Bay. *Remote Sensing of Environment*, 113: 610–621.

Kurmayer R., Dittmann E., Fastner J., Chorus I. (2002) Diversity of microcystin gene within a population of the toxic cyanobacterium *Microcystis* spp. in Lake Wannsee (Berlin, Germany). *Microbial Ecology*, 43: 107–118.

Kurmayer R., Kutzenberger T. (2003) Application of real-time PCR for quantification of microcystin genotypes in a population of the toxic cyanobacterium *Microcystis* sp. *Applied and Environmental Microbiology*, 69: 6723–6730.

Kutser T. (2004) Quantitative detection of chlorophyll in cyanobacterial blooms by satellite remote sensing. *Limnology and Oceanography*, 49(6): 2179–2189.

Kutser T., Piersion, D.C., Kallio K.Y., Reinart A., Sobek S. (2005) Mapping lake CDOM by satellite remote sensing. *Remote Sensing of Environment*, 94: 535–540.

Le C.F., Li Y.M., Zha Y. Sun D.Y., Huang C.C., Lu H. (2009) A four-band semi-analytical model for estimating chlorophyll a in highly turbid lakes: The case of Taihu Lake, China. *Remote Sensing of Environment*, 113: 1175–1182.

Lehman E.M., McDonald K.E., Lehman J.T. (2009) Whole lake selective withdrawal experiment to control harmful cyanobacteria in an urban impoundment. *Water Research*, 43: 1187–1198.

Li E.H., Wang X.L., Cai X.B., Wang X.Y., Zhao S.T. (2011a) Features of aquatic vegetation and the influence factors in Erhai lakeshore wetland. *Joural of Lake Sciences*, 23(5): 738–746. (in Chinese).

Li H.Y., Xie P., Li G.Y., Hao L., Xiong Q. (2009) In vivo study on the effects of microcystin extracts on the expression profiles of proto-oncogenes (*c-fos, c-jun* and *c-myc*) in liver, kidney and testis of male Wistar rats injected i.v. with toxins. *Toxicon*, 53: 169–175.

Li Y.H., Wang Z., Hu M.M., Chang F.Y., Liu Y.D., Li G.B., Li D.H., Shen Y.W. (2011b) Diversity and successional dynamics of picocyanobacterial community in lake Erhai (China) as inferred from 16s rRNA gene sequences. *Fresenius Environmental Bulletin*, 20(9): 2284–2294.

Li Y.Y. (1992) Cyanophyta of the Xizang Plateau. In: The Comprehensive Scientific Expedition to the Qinghai-Xizang Plateau, Li Y.Y., Wei Y.X., Shi Z.X., Hu H.J. (eds.) *The algae of the Xizang Plateau*. Science Press, Beijing, pp. 77, 419.

Lin S., Shen J.Z, Liu Y., Liu Q., Li R.H. (2011) Molecular evaluation on the distribution, diversity and toxicity of *Microcystis* (Cyanobacteria) species from Lake Ulungur: A mesotrophic and brackish desert lake in Xinjiang, China. *Environmental Monitoring and Assessment*, 175: 139–150.

Lin S., Wu Z.X., Yu G.L., Zhu M.L., Yu B.S., Li R.H. (2010) Genetic diversity and molecular phylogeny of *Planktothrix* (Oscillatoriales, cyanobacteria) strains from China. *Harmful Algae*, 9: 87–97.

Lindell T., Person D., Premazzi G., Zilioli E. (1999) Manual for monitoring European lakes using remote sensing techniques, Part III, Remote sensing of Lakes. EUR 18665 EN, Official Publications of the European Communities, Luxembourg, pp. 1–16l.

Liu Y., Islam M.A., Gao J. (2003) Quantification of shallow water quality parameters by means of remote sensing. *Progress in Physical Geography*, 27(1): 24–43.

Long B.M., Jones G.J., Orr P.T. (2001) Cellular microcystin content in N-limited *Microcystis aeruginosa* can be predicted from growth rate. *Applied and Environmental Microbiology*, 67: 278–283.

Lukac M., Aegerter R. (1993) Influence of trace metals on growth and toxin production of *Microcystis aeruginosa*. *Toxicon*, 31: 293–305.

Lund J.W.G. (1955) Contribution to our knowledge of British algae, VIV. Three new species from the English Lake District. *Hydrobiologia*, 7: 219–229.

Lunetta R.S., Schaeffer B.A., Stumpf R.P., Keith D., Jacobs S.A., Murph, M.S. (2015) Evaluation of cyanobacteria cell count detection derived from MERIS imagery across the eastern USA. *Remote Sensing of Environment*, 157: 24–34.

Lv X.J., Zhu J., Meng L. (2010) Pilot study on diversity of cyanobacteria bloom in Lake Erhai. *Environmental Science Survey*, 29(3): 32–35. (in Chinese).

Ma R.H., Kong W.J., Duan H.T., Zhang S.X. (2009) Quantitative estimation of phycocyanin concentration using MODIS imagery during the period of cyanobacterial blooming in Taihu Lake. *China Environmental Science*, 29(3): 254–260. (in Chinese).

MacKintosh C., Beattie K.A., Klumpp S., Cohen P., Codd G.A. (1990) Cyanobacterial microcystin-LR is a potent and specific inhibitor of protein phosphatases 1 and 2A from both mammals and higher plants. *FEBS Letters*, 264(2): 187–192.

Marahiel M.A. (1992) Multidomain enzymes involved in peptide synthesis. *FEBS Letters*, 307, 40–43.

Matsumoto A., Tsuchiya Y. (1988) Earthy-musty odor-producing cyanophytes isolated from five water areas in Tokyo. *Water Science and Technology*, 20(8–9): 179–183.

Matsushita B., Fukushima T. (2009) Methods for retrieving hydrologically significant surface parameters from remote sensing: A review for applications to East Asia region. *Hydrological Processes*, 23, 524–533.

Meissner S., Fastner J., Dittmann E. (2013) Microcystin production revisited: Conjugate formation makes a major contribution. *Environmental Microbiology*, 15(6): 1810–1820.

Metcalf J.S., Codd G.A. (2012) Cyanotoxins. In: Whitton B.A. (eds.) *Ecology of Cyanobacteria II*: *Their Diversity in Space and Time*. Springer, Netherlands, pp. 651–675.

Mikalsen B., Boison G., Skulberg O.M., Fastner J., Davies W., Gabrielsen T.M., Rudi K., Jakobsen K.S. (2003) Natural variation in the microcystin synthetase operon *mcyABC* and impact on microcystin production in *Microcystis* strains. *Journal of Bacteriology*, 185: 2774–2785.

Mitchell B.G. (1990) Algorithms for determining the absorption coefficient of aquatic particulates using the quantitative filter technique (QFT). *Proceedings SPIE* 1302, Ocean Optics X, 137, (doi:10.1117/12.21440).

Mobley C.D. (1999) Estimation of the remote-sensing reflectance from above-surface measurements. *Applied Optics*, 38: 7442–7455.

Mobley C.D., Sundman L.K., Davis C.O.E.A. (2005) Interpretation of hyperspectral remote-sensing imagery by spectrum matching and look-up tables. *Applied Optics*, 44: 3576–3592.

Moisander P.H., Ochiai M., Lincoff A. (2009) Nutrient limitation of *Microcystis aeruginosa* in northern California Klamath River reservoirs. *Harmful Algae*, 8: 889–897.

Morel A., Gordon H.R. (1980) Report of the working group on water color. *Boundary Layer Meteorology*, 18: 343–355.

Morel A., Prieur L. (1977) Analysis of variations in ocean color. *Limnology and Oceanography*, 22, 709–722.

Moses W.J., Gitelson A.A., Berdnikov S., Povazhnyy V. (2009) Satellite estimation of chlorophyll-*a* concentration using the red and NIR bands of MERIS — The Azov sea case study. *IEEE Geoscience and Remote Sening Letters*, 6: 845–849.

Moses W.J., Gitelson A.A., Perk R.L., Gurlin, D., Rundquist D.C., Leavitt B.C., Barrow T.M., Brakhage P. (2012) Estimation of chlorophyll-*a* concentration in turbid productive waters using airborne hyperspectral data. *Water Research*, 46: 993–1004.

Nagai T., Imai A., Matsushige K., Fukushima T. (2006) Effect of iron complexation with dissolved organic matter on the growth of cyanobacteria in a eutrophic lake. *Aquatic Microbial Ecology*, 44: 231–239.

Neilan B.A., Jacobs D., Del Dot T., Blackall L.L., Hawkins P.R., Cox P.T., Goodman A.E. (1997) rRNA sequences and evolutionary relationships among toxic and non-toxic cyanobacteria of the genus *Microcystis*. *International Journal of Systematic Bacteriology*, 47(3): 693–697.

Neilan B.A., Pearson L.A., Muenchhoff J., Moffitt M.C., Dittmann E. (2012) Environmental conditions that influence toxin biosynthesis in cyanobacteria. *Environmental Microbiology*, 15(5): 1239–1253.

Nichol J.E. (1993) Remote sensing of water quality in the Singapole–Johor–Riau growth triangle. *Remote Sensing of Environment*, 43: 139–148

Nübel U., Garcia-Pichel F., Muyzer G. (1997) PCR Primers to amplify 16S rRNA genes from cyanobacteria. *Applied and Environmental Microbiology*, 63: 3327–3332.

Odermatt D., Giardino C., Heege T. (2010) Chlorophyll retrieval with MERIS case-2-regional in perialpine lakes. *Remote Sensing of Environment*, 114: 607–617.

Ojala A. (1993) The influence of light quality on growth and phycobiliprotein/ chlorophyll a fluorescence quotients of some species of freshwater algae in culture. *Phycologia*, 32(1): 22–28.

Oliver R.L., Hamilton D.P., Brookes J.D., Ganf G.G. (2012) Physiology, blooms and prediction of planktonic cyanobacteria. In: Whitton B.A. (eds.) *Ecology of Cyanobacteria II*: *Their Diversity in Space and Time*. Springer Netherlands, pp. 155–194.

O'Reilly J.E., Maritorena S., Mitchell B.G., Siegel D.A., Carder K.L., Garver, S., Kahru M., McClain C. (1998) Ocean color chlorophyll algorithms for SeaWiFS. *Journal of Geophysical Research: Oceans*, 103: 24937−24953.

O'Reilly J.E., Maritorena S., Siegel D.A., O'Brien M.C. Toole D., Chavez F.P., Strutton P., Cota G.F., Hooker S.B., McClain C.R., Carder K.L., Muller-Karger F., Harding L., Magnuson A., Phinney D., Moore G.F., Aiken J., Arrigo K.R., Letelier R., Culver M. (2000) Ocean chlorophyll a algorithms for SeaWiFS, OC2, and OC4: Version 4. In: O'Reilly, J.E., and 24 Coauthors, *SeaWiFS Postlaunch Calibration and Validation Analyses, Part 3*. In: Hooker S.B., Firestone E.R. (eds.) *SeaWiFS Postlaunch Technical Report Series.* NASA Goddard Space Flight Center, Greenbelt, Maryland, 11: 9–19.

Otten T.G., Xu H., Qin B.Q., Zhu G., Paerl H.W. (2012) Spatiotemporal patterns and ecophysiology of toxigenic *Microcystis* blooms in Lake Taihu, China: implications for water quality management. *Environmental Science & Technology*, 46(6): 3480–3488.

Oyama Y., Matsushita B., Fukushima T., Matsushige K., Imai A. (2009) Application of spectral decomposition algorithm for mapping water quality in a turbid lake (Lake Kasumigaura, Japan) from Landsat TM data. *ISPRS Journal of Photogrammetry and Remote Sensing*, 64(1): 73–85.

Oyama Y., Matsushita B., Fukushima T., Nagai T., Imai, A. (2007) A new algorithm for estimating chlorophyll-*a* concentration from multi-spectral satellite data in Case II waters: A simulation based on a controlled laboratory experiment. *International Journal of Remote Sensing*, 28: 1437–1453.

Paerl H.W., Fulton R.S., Moisander P.H., Dyble J. (2001) Harmful freshwater algal blooms, with an emphasis on cyanobacterial. *Scientific World Journal*, 1: 76–113.

Paerl H.W., Huisman J. (2008) Blooms like it hot. *Science*, 320: 57–58.

Posada D., Crandall K.A. (1998) Modeltest: testing the model of DNA substitution. *Bioinformatics*, 14(9): 817–818.

Rapala J., Sivonen K., Luukkainen R., Niemelä S.I. (1993) Anatoxin-a concentration in *Anabaena* and *Aphanizomenon* under different environmental conditions and comparison of growth by toxic and nontoxic *Anabaena*-strains – a laboratory study. *Journal of Applied Phycology*, 5: 581–591.

Revaclier R. (1978) Examens biologiques des eaux du Léman, étude du phytoplancton. Rapports de la commission internationale pour la protection des eaux du Léman contre la pollution, 99–166.

Reynolds C.S., Jaworski G.H.M., Cmiech HA., Leedale G.F. (1981) On the annual cycle of the blue-green alga *Microcystis aeruginosa* Kütz emend Elenkin. *Proceedings of the Royal Society of London B: Biological Sciences*, 293(1068): 419–477.

Rinehart K.L., Namikoshi M., Choi B.W. (1994) Structure and biosynthesis of toxins from blue-green algae (cyanobacteria). *Journal of Applied Phycology*, 6: 159–176.

Runnegar M.T., Kong S., Berndt N. (1993) Protein phosphatase inhibition and in vivo hepatotoxicity of microcystins. *American Journal of Physiology*, 265: G224–G230.

Santini F., Alberotanza L., Cavalli R.M., Pignatti S. (2010) A two-step optimization procedure for assessing water constituent concentrations by hyperspectral remote sensing techniques: An application to the highly turbid Venice lagoon waters. *Remote Sensing of Environment*, 114: 887–898.

Schopf J.W. (2000) The fossil record: Tracing the roots of the cyanobacterial lineage. In Whitton B.A. & Potts M. (eds.) *The Ecology of Cyanobacteria*. Dordrecht, the Netherlands: Kluwer Academic Publishers, pp. 13–35.

Schopf J.W., Kudryavtsev A.B., Czaja A.D., Tripathi A.B. (2007) Evidence of Archean life: Stromatolites and microfossils. *Precambrian Research*, 158: 141–155.

Schopf J.W., Packer B.M. (1987) Early Archean (3.3-billion to 3.5-billion-year-old) microfossils from Warrawoona Group, Australia. *Science*, 237: 70–73.

SCOR-UNESCO (1966) Determination of photosynthetic pigment in seawater. Monographs on oceanographic methodology. Paris, France. pp. 1–18.

Scott J.T., McCarthy M.J., Otten T.G., Steffen M.M., Baker B.C., Grantz E.M., Wilhelm S.W., Paerl H.W. (2013) Comment: An alternative interpretation of the relationship between TN:TP and microcystins in Canadian lakes. *Canadian Journal of Fisheries and Aquatic Sciences*, 70(8): 1265–1268.

Šejnohová L., Maršálek B. (2012) *Microcystis*. In: Whitton B.A. (eds.) *Ecology of Cyanobacteria II*: *Their Diversity in Space and Time*. Springer, Netherlands, pp. 195–228.

Shao J.H., Peng L., Luo S., Yu G.L., Gu J.D., Lin S., Li R.H. (2013) First report on the allelopathic effect of *Tychonema bourrellyi* (Cyanobacteria) against *Microcystis aeruginosa* (Cyanobacteria). *Journal of Applied Phycology*, 25: 1567–1573.

Shao J.H., Wu X.Q., Li R.H. (2009) Physiological responses of *Microcystis aeruginosa* PCC7806 to nonanoic acid stress. *Environmental Toxicology*, 24: 610–617.

Shao J.H., Xu Y., Wang Z.J., Jiang Y.G., Yu G.L., Peng X. Li R.H. (2011) Elucidating the toxicity targets of β-ionone on photosynthetic system of *Microcystis aeruginosa* NIES-843 (Cyanobacteria). *Aquatic Toxicology*, 104: 48–55.

Simis S.G.H., Peters S.W.M., Gons H.J. (2005) Remote sensing of the cyanobacterial pigment phycocyanin in turbid inland water. *Limnology and Oceanography*, 50: 237−245.

Sirenko A. (1972) Physiological fundamentals of reproduction of the blue-green algae in reservoirs. *Naukova Dumka, Kiev*, pp. 403. (in Russian).

Sivonen K. (1990) Effects of light, temperature, nitrate, orthophosphate, and bacteria on growth of and hepatotoxin production by *Oscillatoria agardhii* strains. *Applied and Environmental Microbiology*, 56: 2658–2666.

Sivonen K. (1996) Cyanobacterial toxins and toxin production. *Phycologia* (Suppl.), 35(6): 12–24.

Skulberg O.M., Skulgerg R. (1991) A comparative investigation and taxonomic relationship of *Tychonema tenuis* and *Tychonema bourrellyi*. *Algological studies*, 64: 271–279.

Smith V.H. (1983) Low nitrogen to phosphorus ratios favor dominance by blue-green algae in lake phytoplankton. *Science*, 22: 669–671.

Smith V.H., Tilman G.D., Nekola J.C. (1999) Eutrophication: Impacts of excess nutrient inputs on freshwater, marine, and terrestrial ecosystems. *Environmental Pollution*, 100: 179–196.

Sommer U. (1985) Comparison between steady-state and non-steady state competition: Experiments with natural phytoplankton. *Limnology and Oceanography*, 30(2): 335–346.

Song L.R., Sano T., Li R.H., Watanabe M.H., Liu Y.D., Kaya K. (1998) Microcystin production of *Microcystis viridis* (cyanobacteria) under different culture conditions. *Phycological Rresearch* (suppl.), 46: 19–23.

Song L.R., Lei L.M., He Z.R., Liu Y.D. (1999) Growth and toxin analysis in two toxic cyanobacteria *Microcystis aeruginosa* and *Microcystis virdis* isolated from Dianchi Lake. *Acta Hydrobiological Sinica*, 23(5): 402–408. (in Chinese).

Sournia A., Chretiennot-Dinet M.J., Ricard M. (1991) Marine phytoplankton: How many species in the world ocean? *Journal of Plankton Reseach*, 13: 1093–1099.

Suda S., Watanabe M.M., Otsuka S., Mahakahant A., Yongmanitchai W., Nopartnaraporn N., Liu Y.D., Day J.G. (2002) Taxonomic revision of water-bloom-forming species of oscillatorioid cyanobacteria. *International Journal of Systematic and Evolutionary Microbiology*, 52: 1577–1595.

Tamura K., Stecher G., Peterson D., Filipski A. Kumar S. (2013) MEGA6: Molecular Evolutionary Genetics Analysis Version 6.0. *Molecular Biology and Evolution*, 30: 2725–2729.

Tandeau de Marsac N., Lee H.M., Hisbergues M., Castets A.M., Bédu S. (2001) Control of nitrogen and carbon metabolism in cyanobacteria. *Journal of Applied Phycology*, 13: 287–394.

Tillett D., Dittmann E., Erhard M., von Döhren H., Börner T., Neilan B.A. (2000) Structural organization of microcystin biosynthesis in *Microcystis aeruginosa* PCC7806: An integrated peptide-polyketide synthetase system. *Chemistry & Biology*, 7: 753–764.

Vaitomaa J., Rantala A., Halinen K., Rouhiainen L., Tallberg P., Mokelke L., Sivonen K. (2003) Quantitative real-time PCR for determination of microcystin synthetase E copy numbers for *Microcystis* and *Anabaena* in lakes. *Applied and Environmental Microbiology*, 69(12): 7289–7297.

Van der Woerd H.J., Pasterkamp R. (2008) HYDROPT: A fast and flexible method to retrieve chlorophyll-*a* from multispectral satellite observations of optically complex coastal waters. *Remote Sensing of Environment*, 112: 1795–1807.

Via-Ordorika L., Fastner J., Kurmayer R., Hisbergues M., Dittmann E., Komarek J., Erhard M., Chorus I. (2004) Distribution of microcystin producing and non-microcystin-producing *Microcystis* sp. in European freshwater bodies: Detection of microcystins and microcystin genes in individual colonies. *Systematic and Applied Microbiology*, 27: 592–602.

Wang M., Shi W., Tang J. (2011a) Water property monitoring and assessment for China's inland Lake Taihu from MODIS-Aqua measurements. *Remote Sensing of Environment*, 115(3): 841–854.

Wang Q., Xie P., Chen J., Liang G.D. (2008) Distribution of microcystins in various organs (heart, liver, intestine, gonad, brain, kidney and lung) of Wistar rat via intravenous injection. *Toxicon*, 52: 721–727.

Wang S.M., Dou H.S. (1998) A directory of lakes in China. Science Press, Beijing, pp 580. (in Chinese).

Wang S.Y., Liu X.B., Liu C. (2010) Analysis on spatial variation of nitrogen in top layer water of Erhai Lake. *Water Resources Protection*, 26(6): 37–41.

Wang Z., Wang Y.C., Hu M.M., Li Y.H., Liu Y.D., Shen Y.W., Li G.B., Wang G.H. (2011b) Succession of the phytoplankton community in response to environmental factors in north Lake Erhai during 2009–2010. *Fresenius Environmental Bulletin*, 20(9): 2221–2231.

Wang Z.J., Xu Y., Shao J.H., Wang J., Li R.H. (2011c) Genes ssociated with 2-methylisoborneol biosynthesis in cyanobacteria: Isolation, characterization, and expression in response to light. *Plos One*, 6(4): e18665.

Watanabe M.F., Oishi S. (1985) Effects of environmental factors on toxicity of a cyanobacterium (*Microcystis aeruginosa*) under culture conditions. *Applied and Environmental Microbiology*, 49: 1342–1344.

Watanabe M.F., Tsuji K., Watanabe Y., Harada K.I., Suzuki M. (1992) Release of heptapeptide toxin (microcystin) during the decomposition process of *Microcystis aeruginosa*. *Natural Toxins*, 1: 48–53.

Wei Z.H., Zhu M.L., Yu G.L., Li R.H. (2012) Occurrence of planktonic cyanobaterium *Tychonema bourrellyi* in Erhai Lake and its taxonomic studies. *Acta Hydrobiologica Sinica*, 36(6): 1171–1175. (in Chinese).

WHO (World Health Organization) (2006) Guidelines for drinking water quality, First Adendum to third ed., Recommendations, vol. 1, Geneva, Switzerland, pp. 195.

Wu S.K., Xie P., Liang G.D., Wang S.B.. Liang X.M. (2006) Relationships between microcystins and environmental parameters in 30 subtropical shallow lakes along the Yangtze River, China. *Freshwater Biololgy*, 51: 2309–2319.

Wu W.J., Li G.B., Li D.H., Liu Y.D. (2010) Temperature may be the dominating factor on the alternant succession of *Aphanizomenon flos-aquae* and *Microcystis aeruginosa* in Dianchi lake. *Fresenius Environmental Bulletin*, 19: 846–853.

Wu X.Q., Xiao B.D., Li R.H., Wang C.B., Huang J.T., Wang Z. (2011) Mechanisms and factors affecting sorption of microcystins onto natural sediments. *Environmental Science & Technology*, 45(7): 2641–2647.

Wu Y.S., Yu G.L., Li R.H., Song L.R., Jiang H.X., Riding R., Liu L.J., Liu D.Y., Zhao R. (2014) Cyanobacterial fossils from 252 Ma old microbialites and their environmental significance. *Scientific Reports*, 4: 3820.

Xie L.Q., Xie P., Li S.X., Tang H.J., Liu H. (2003) The low TN/TP ratio, a cause or a result of *Microcystis* blooms? *Water Research*, 37: 2073–2080.

Xu Y., Wang G.X., Yang W.B., Li R.H. (2010) Dynamics of the water bloom-forming *Microcystis* and its relationship with physicochemical factors in Lake Xuanwu (China). *Environmental Science and Pollution Research*, 17: 1581–1590.

Xu Y., Wu Z.X., Yu B.S., Yu G.L., Peng X., Wang G.X., Li R.H. (2008) *Microcystis wesenbergii* (Komárek) Komárek (Cyanobacteria) representing a main waterbloom forming species but non-microcystin-producer in China. *Environmental Pollution*, 2156: 162-167

Xu H., Paerl H.W., Qin B.Q., Zhu G.W., Gao G. (2010) Nitrogen and phosphorus inputs control phytoplankton growth in eutrophic Lake Taihu, China. *Limnology and Oceanography*, 55(1): 420–432.

Yang M., Yu J.W., Li Z.L., Guo Z.H., Burch M., Lin T.F. (2008) Taihu Lake not to blame for Wuxi's woes. *Science*, 319: 158.

Yang W., Matsushita B., Chen J., Fukushima T. (2011a) Estimating constituent concentrations in case II waters from MERIS satellite data by semi-analytical model optimizing and look-up tables. *Remote Sensing of Environment*, 115: 1247–1259.

Yang W., Matsushita, B., Chen J., Fukushima T. (2011b) A relaxed matrix inversion method for retrieving water constituent concentrations in case II waters: The case of Lake Kasumigaura, Japan. *IEEE Transactions on Geoscience and Remote Sensing*, 49: 3381–3392.

Yang W., Matsushita B., Chen J., Fukushima T., Ma R. (2010) An enhanced three-band index for estimating chlorophyll-*a* in turbid case-II waters: Case studies of Lake Kasumigaura, Japan, and Lake Dianchi, China. *IEEE Geoscience and Remote Sening Letters*, 7(4): 655–659.

Yoshida M., Yoshida T., Yukari T., Hosoda N., Hiroishi S. (2007) Dynamics of microcystin-producing and non-microcystin-producing *Microcystis* populations is correlated with nitrate concentration in a Japanese lake. *FEMS Microbiology Letters*, 266(1): 49–53.

Yu G.L., Zhu M.L., Chen Y.X., Pan Q.Q., Chai W.B., Li R.H. (2015) Polyphasic characterization of four species of *Pseudanabaena* (Oscillatoriales, Cyanobacteria) from China and insights into polyphyletic divergence within the *Pseudanabaena* genus. *Phytotaxa,* 192(1): 1–12.

Yuan L., Zhu W., Xiao L., Yang L.Y. (2009) Phosphorus cycling between the colonial cyanobacterium *Microcystis aeruginosa* and attached bacteria, *Pseudomonas*. *Aquatic Ecology*, 43(4): 859–866.

Zhang Y.L., Gin B.Q, Chen W.M., Zhu G.W. (2005) A preliminary study of chromophoric dissolved organic matter (CDOM) in Lake Taihu, a shallow subtropical lake in China. *Acta Hydrochimica et Hydrobiologica*, 33: 315–323.

Zhao Y.Y., Xie P., Zhang X.Z. (2009) Oxidative stress response after prolonged exposure of domestic rabbit to a lower dosage of extracted microcystins. *Environmental Toxicology and Pharmacology,* 27: 195–199.

Zheng G., Fu B., Duan Y., Wang, Q., Matsuo, M., Takano B. (2004) Iron speciation related to colors of Jurassic sedimentary rocks in Turban Basin, Northwestern China. *Journal of Radioanalytical and Nuclear Chemistry,* 26: 421–427.

Zhou Q.C., Chen W., Shan K., Zheng L.L., Song L.R. (2014) Influence of sunlight on the proliferation of cyanobacterial blooms and its potential applications in Lake Taihu, China. *Journal of Environmental Sciences*, 26(3): 626–635.

Glossary

Abbreviations	Definition and dimension in SI units	Introduced in Section
a_{ph}	absorption coefficients of phytoplankton (m^{-1})	4.2.2
$Cal(\lambda)$	spectral reflectance calibration factor	4.2.2
CCA	Canonical Correspondence Analysis	3.2.8, 3.3.7
CDOM	colored dissolved organic matter	1.6, 4.
Chl-*a*	Chlorophyll-*a* (mg m^{-3})	1, 2, 3, 4, 5
Ct	mean cycle threshold	2.2.4, 3.2.5
DO	issolved oxygen (mg L^{-1})	2.2.2, 2.4, 3.2.1
DOC	dissolved organic carbon (g m^{-3})	4.2.1
DOM	dissolved organic matter (g m^{-3})	1.6.1
DTN	dissolved total nitrogen (mg L^{-1})	2.2.2, 3.2.1
$E_d(\lambda)$	downward irradiance	4.2.2
GC-MS	gas chromatography–mass spectrometry	3.2.7, 5
HCBs	harmful cyanobacteria blooms	1.1, 1.2, 1.3, 1.5, 5.1
HPLC	high performance liquid chromatography	1.4.2, 2.2.3, 3.3.5, 5.1
IOPs	Inherent Optical Properties	1.6, 4.1
ISS	Inorganic suspended solids (g m^{-3})	4.2
LC-MS	liquid chromatography–mass spectrometry	1.4.2
$L_u(\lambda)$	water-leaving radiance	4.2.2
$L_{sky}(\lambda)$	downward radiance of skylight	4.2.2
LUT	look-up-table	1.6.3, 4.2, 4.3
MC	microcystin (μg L^{-1})	1, 2, 3, 5
MCI	maximum chlorophyll index	5.2
mcy	microcystin biosynthesis genes	1, 2, 3, 5
MERIS	Medium Resolution Imaging Spectrometer	1.5, 1.6, 4.2, 4.4

Abbreviations	Definition and dimension in SI units	Introduced in Section
ML	Maximum likelihood	3.2.6
2-MIB	2-methylisoborneol	1.1
m/z	Mass to charge ratio	3.3.4
MNB	mean normalized bias (%)	4.2.5, 4.3
MODIS	Moderate Resolution Imaging Spectroradiometer	1.6, 1.4
NAP	non-algal particles	1.6, 4
NH_4-N	ammonia nitrogen (mg L^{-1})	1.3, 2.2, 2.3, 3.2, 3.7
NIR	near-infrared	1.6, 4
NJ	Neighbor-joining	3.2.6
NMAE	normalized mean absolute (%)	4.2.5, 4.3
NO_3-N	nitrate nitrogen (mg L^{-1})	1.3, 1.4, 2.2, 2.3, 3.2.1
N/P	ratio of nitrogen and phosphorus	1.3, 1.4, 2.1, 2.4
NRMS	normalized root mean square error (%)	4.2.5, 4.3
OSS	Organic suspended solids (g m^{-3})	4.2.2
PE	phycoerythrin	3.3.3
PC	phycocyanin	1.1, 3.3.3
qPCR	real-time quantitative polymerase chain reaction	1.4, 1.5, 1.8, 2.2, 3.2
RMSE	root- mean-square error (mg m^{-3}, g m^{-3} or m^{-1})	4.2.5, 4.3
$R_{rs}(\lambda)$	above-water remote-sensing reflectance (sr^{-1})	4.2.2
SAMO-LUT	Semi-analytical model-optimizing and look-up-table	1.6, 4, 5
SD	transparency (m)	2.2.2, 2.4, 3.2.1
SeaWiFS	Sea-viewing Wide Field-of-view Sensor	1.6.1, 4.4
SIOPs	Specific Inherent Optical Properties	4
TEM	transmission electron microscopy	1.8, 3.1, 3.2.3, 3.3.1
TN/TP	ratio of total nitrogen and phosphorus	1.3.3, 1.8, 2, 5
TSS	Total suspended solids (g m^{-3})	4.2.2
WQPs	water quality parameters	1.6, 2.2.1, 3.2.1, 3.3.7
WT	water temperature(℃)	1.4, 2.2.2, 3.2.1